Kinematic Coupling between the Foot and Lower Limb during Gait

Michael Bernhard Pohl

Submitted in accordance with the requirements of

Doctor of Philosophy

The University of Leeds

The Centre for Sport and Exercise Sciences

January, 2006

The candidate confirms that the work submitted is his own and that appropriate credit has been given where reference has been made to the work of others.

Acknowledgements

This work could not have been completed without the guidance of my supervisory team. My thanks go out to Dr John Buckley, Dr Neil Messenger and Professor Susan Ward for their supporting roles in ensuring that I have reached this stage.

The research presented in chapter 5 was conducted in collaboration with Dr Jim Woodburn (University of Leeds) and Dr Mark Cornwall (Arizona State University) at the Academic Unit of Arthritis Research, University of Leeds. My contribution to the work was the development of the research hypothesis, experimental planning, interpretation of results in addition to assisting in the data collection.

The data collection in chapters 8 and 9 was collected with the aid of undergraduate project students. I would like to thank Tom Chesters, Richard Metcalfe, Elliot Messenger and David Snape for their assistance.

Special Thanks

There have been many people who have assisted me in the completion of this thesis who I would like to offer my gratitude including my family, friends and the staff/students at the Centre for Sport & Exercise Sciences. However, I would like recognise a few individuals who made a major contribution to my efforts. I would especially like to thank John Buckley who as well as playing the lead supervisory role, has significantly contributed to my professional development as an academic researcher. A very special thank you goes to my sister Charlotte Pohl, who in addition to providing proofreading, offered tremendous support whenever the going got tough. A big thanks goes to Holly Adamthwaite who gave up her time for numerous pilot tests. Finally, I would like to thank my parents for helping me to get to where I find myself in life now.

Abstract

Introduction: Abnormal kinematic coupling between the foot and lower limb has been associated with chronic overuse injuries of the lower extremity during running. However, the normal coupling relationship between the two segments remains unclear. The equivocal findings in the literature may be due to previous studies concentrating on determining coupling at discrete instances only, along with the failure to include the midtarsal joint in coupling analyses. By including motion across the midtarsal joint and measures of continuous coupling, this research aimed to gain a more complete understanding of the relationship between foot and lower limb kinematics during gait.

Methods: Following the development of a multi-segment foot model, *in-vitro* and *in-vivo* studies were conducted to assess the validity and reliability of determining foot and lower limb segmental kinematics during gait. Three experiments were then undertaken to assess the rigidity of the kinematic coupling between the forefoot, rearfoot and shank by manipulating step width, running speed, foot strike pattern and mode of gait (run versus walk). Kinematic coupling was assessed by determining how well matched the angular displacements of two adjacent segments (e.g rearfoot eversion/inversion with shank internal/external rotation) were in both spatial and temporal terms using both discrete point and cross correlation analyses.

Results: Although the *in-vitro* study suggested care should be taken when interpreting data obtained from skin mounted markers the modelling and analysis approach used *in-vivo* was found to have good within- and between-day reliability. In all conditions it was evident that following touchdown, the shank internally rotated, the rearfoot everted and the forefoot dorsiflexed and abducted. This was followed by the reversal of the segmental angular displacements starting with that of the shank, followed by the rearfoot and then the forefoot. During running, coupling between rearfoot eversion/inversion and shank internal/external rotation was consistently high ($r \geq 0.92$) regardless of step width, speed or foot strike pattern. In walking, however, this coupling value was low ($r = 0.49$). Rearfoot eversion/inversion was also highly coupled with both forefoot dorsiflexion/plantarflexion and abduction/adduction in running and walking. However, there was little evidence of any coupling between rearfoot eversion/inversion and forefoot eversion/inversion.

Conclusion: The consistently high kinematic coupling between the rearfoot and shank during running suggests a robust coupling mechanism that is able to withstand changes in the loading of the subtalar joint. However, lower coupling between these two segments in walking, implies that the relationship is not entirely rigid and some degree of elasticity exists at the subtalar joint. Strong coupling of forefoot sagittal and transverse plane motions with rearfoot frontal plane motion during running and walking suggests the two segments are linked via the action of the midtarsal joint. From the timings of discrete kinematic events it appeared that shank external rotation was driving rearfoot inversion and that this in turn was causing the forefoot to plantarflex and abduct. This implies that a kinetic chain exists with proximal segments driving motion of the distal segments during propulsion.

Implications: If the proximal segments drive the motion of the foot then injuries associated with excessive or prolonged pronation should not only be treated using orthoses, but also by using interventions to modify the kinematics of the joints proximal to the ankle-joint-complex. Future work should determine the effects of muscle stiffness on subtalar joint kinematics since this may have important implications in terms of lower extremity injuries.

TABLE OF CONTENTS

CONTENT **PAGES**

CONTENT PAGES

LIST OF TABLES AND FIGURES

CONTENT **PAGES**

Chapter 1 - Introduction

1.1 Introduction

The coupling between movements of the foot and tibia during gait has been suggested to be a possible injury mechanism. This coupling mechanism is a result of the function of the subtalar joint which is thought to act like a mitered hinge, whereby pronation and supination of the foot is transferred into internal and external rotation of the tibia respectively (Inman et al., 1981) and it has been proposed that excessive or prolonged pronation may cause excessive or prolonged internal rotation of the tibia (Powers et al., 2002; Stergiou and Bates, 1997; Tiberio, 1987). As a consequence this may alter the normal kinematics further up the kinetic chain and increase the risk of obtaining an overuse injury of the lower extremity.

Studies investigating foot function during gait have typically approximated foot pronation and supination using calcaneal eversion and inversion, as this component is the simplest to measure (Edington et al., 1990). However, there is a growing consensus in the literature that the joints of the midfoot contribute significantly to overall foot motion during walking (Carson et al., 2001; Hunt et al., 2001; Leardini et al., 1999; Woodburn et al., 2004). Despite this, there have been few investigations into the influence of the midfoot on the subtalar coupling mechanism during gait.

Traditionally studies looking at the kinematic coupling between the foot and lower leg have used measures that only provide information about the segments at discrete points in time during the stance phase. Parameters such as peak absolute angles, angular excursions and/or the timings of specific events have all been used to assess

the degree of kinematic coupling between segments/joints (McClay and Manal, 1998; Nigg et al., 1993; Reischl et al., 1999). Though some insight has been gained into the coupling relationship with the use of the above mentioned methods, none of these approaches had provided information concerning kinematic coupling over the whole stance phase. For a more complete understanding of the coupling relationship between two segments it is necessary to include measures that assess the continuous kinematic coupling over the entire stance phase (Stergiou and Bates, 1997).

Some investigations into the kinematic coupling have involved manipulating the kinematic behaviour of one segment and then observing the alterations in the adjacent segment's kinematics. This has been performed using experimental manipulations such as the use of orthotics or modification of shoe design (Stacoff et al., 2001; Williams et al., 2003). However, the kinematic changes of the rearfoot and shank resulting from these manipulations were small and non-systematic and therefore, provided little information regarding the coupling relationship. The experimental manipulations undertaken within the present thesis involved the alteration of gait characteristics. It was hoped that such manipulations would induced significant alterations in rearfoot kinematics, and by observing any alterations in the shank and forefoot segments, the complex coupling mechanisms between the three segments would be better understood.

1.2 Thesis Objectives

The aim of this thesis was to investigate the association between midtarsal joint motion and the kinematic coupling at the subtalar joint during gait. More specifically,

to determine whether forefoot motion was coupled to rearfoot motion and thus had an effect on the amount of tibial rotation occurring. The overall objective of the thesis was to gain a more complete picture of how the foot is kinematically coupled with the lower limb during gait. It was believed that this would lead to a greater understanding of how abnormal kinematic coupling may serve as an injury mechanism for the lower extremity during running.

1.2.1 Specific Aims of the Thesis

- Review the current literature and provide an overview of the biomechanics of the foot and lower limb during gait and its association with injuries of the lower extremity.
- Review the current literature with regard to the current understanding of the kinematic coupling between the foot and lower limb.
- Test the validity of using external markers to measure subtalar joint kinematics.
- Develop a repeatable method to determine forefoot, rearfoot and shank 3-D angular kinematics.
- Investigate whether forefoot, rearfoot and shank kinematic coupling is altered by step width during running.
- Investigate whether forefoot, rearfoot and shank kinematic coupling differs between walking and running.
- Investigate whether forefoot, rearfoot and shank kinematic coupling differs between running speeds.
- Investigate whether forefoot, rearfoot and shank kinematic coupling is altered by foot strike pattern during running.

- Determine the robustness of the kinematic coupling between rearfoot frontal plane motion and transverse plane rotation of the shank.
- Determine the robustness of the kinematic coupling between rearfoot frontal plane motion and forefoot planar rotations.
- Observe if midtarsal joint function has any influence on kinematic coupling at the subtalar joint.

1.2.2 Structure of the Thesis

The general aim of this thesis was to investigate the kinematic coupling between the foot and lower limb due to its association with chronic overuse injuries of the lower extremity. Chapter 2 provides the reader with a comprehensive background about the anatomy and normal biomechanics of the foot and lower limb. Chapter 3 continues to review the literature, this time focusing on the kinematic coupling between the foot and lower limb. Chapter 4, the general methods section describes the laboratory setup, equipment, data processing techniques and the biomechanical model of the foot used during the collection of data for the gait studies. Two pilot studies are included in this chapter, the first of which describes the residual analysis process from which the cut-off frequency was determined for the filtering of the kinematic data. The second pilot study assesses the accuracy and validity of the data capture/processing equipment in obtaining true angular displacement measurements. Chapter 5 is a preliminary investigation into the feasibility of using external skin markers to model subtalar joint kinematics. It was also deemed necessary to include a section dealing with the reliability of the results which is provided in chapter 6. The following three chapters (chapters 7-9) describe how different gait manipulations implemented to alter rearfoot kinematics affected the coupling between the foot and lower limb. Chapter 7

examines the influence of running with a different step width on the kinematic coupling between the forefoot, rearfoot and shank. Chapter 8 looks at the affect of mode of gait and running speed on kinematic coupling. Finally, chapter 9 investigates how varying foot-strike pattern affected the kinematic coupling. The conclusions of chapters 7-9 are collated in a general discussion in chapter 10, where the questions postulated by the aims of the thesis are addressed. A summary of how the main findings have contributed to wider knowledge is presented and future avenues for further research are discussed.

Chapter 2 - Anatomy and Function of the Foot and Ankle during Gait

2.1 Introduction

As the final linkage in the lever system of the leg, the foot has to transmit the forces of stance and locomotion to the ground in a way that is related to the terrain (Klenerman, 1991). The foot and ankle must perform many other functions during gait including:

- Absorbing shock to the body as the foot impacts on the ground
- Converting transverse torque from the lower extremity
- Providing a rigid lever for effective push-off
- Providing a structural supporting platform for the body

Due to its multifactorial functions the foot by nature is a very complex structure. The normal mechanics of the foot and ankle are the combined effects of muscle, tendon, ligament and bone function (Donatelli, 1996).

2.2 Skeletal Structure of the Foot and Ankle

The foot is made up of 26 bones (7 tarsals, 5 metatarsals and 14 phalanges) with the distal ends of the tibia and fibula forming part of the ankle joint. For the purpose of this thesis, the foot can be divided into three sections: the rearfoot, the midfoot and the forefoot (Figure 2.1). Although three distinct functional sections are presented, it must be stressed that the entire foot works together to form a very complex and intricate structure.

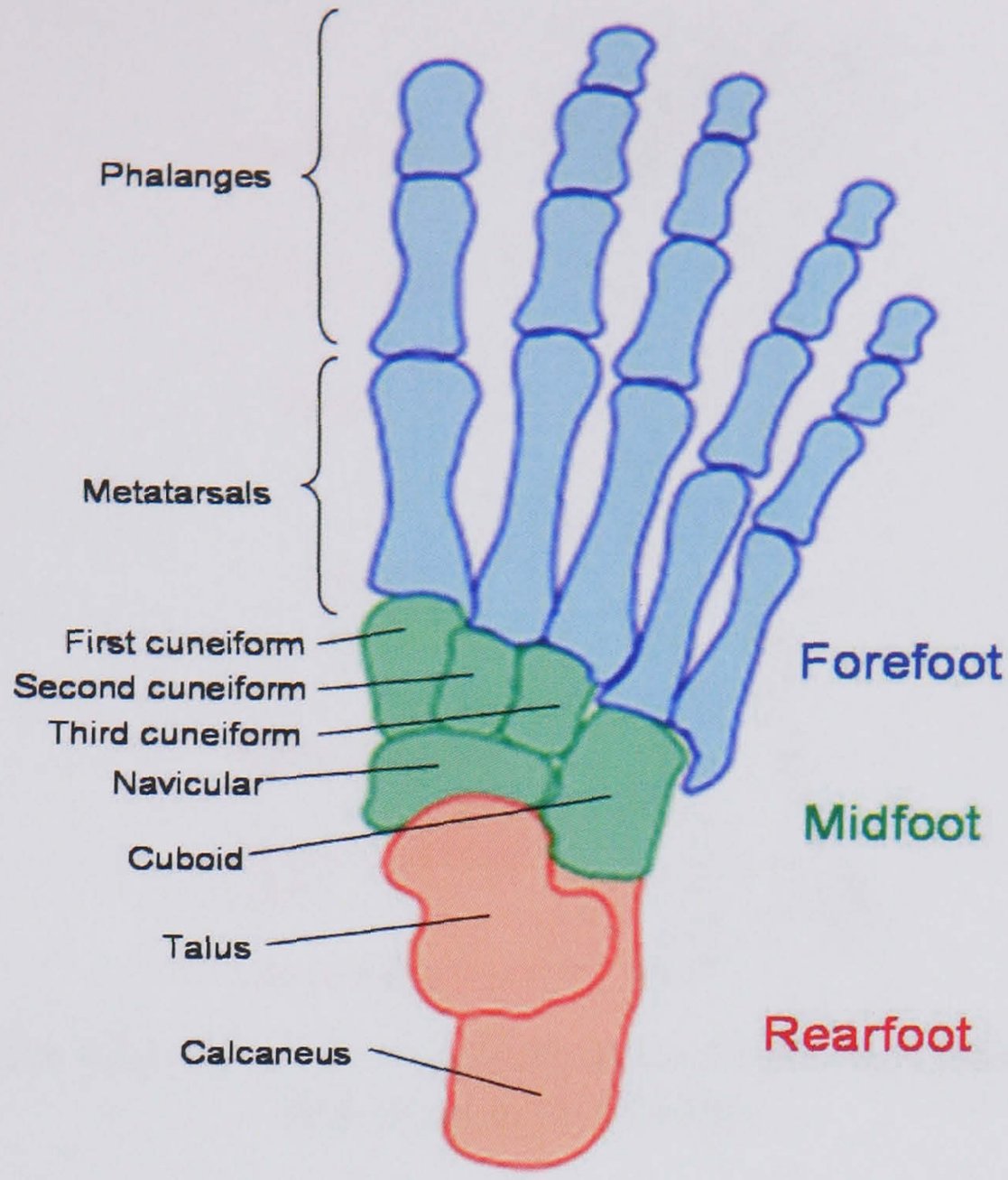

Figure 2.1. Dorsal view of the right bones of the foot. The three functional sections of the foot are presented.

2.2.1 The Lower Leg (Shank)

Since the purpose of this thesis is to examine the motion of the foot relative to the lower leg, a description of the bones of the lower leg is required. For a description of the anatomical terms used within the thesis refer to Appendix A. There are two bones in the lower leg (shank), the tibia and the fibula, which lie side by side and articulate with each other at the superior and inferior (inferior tibiofibular joint) ends (Figure 2.2). Both bones articulate with the talus at the distal end to form the ankle, or talocrural joint. The medial surface of the tibia is prolonged downward as the medial malleolus. Similarly, the fibula, which lies on the lateral side of the tibia, projects downwards to form the lateral malleolus (Bryan, 1996). Many tendons run behind the malleoi and insert into the bones of the foot.

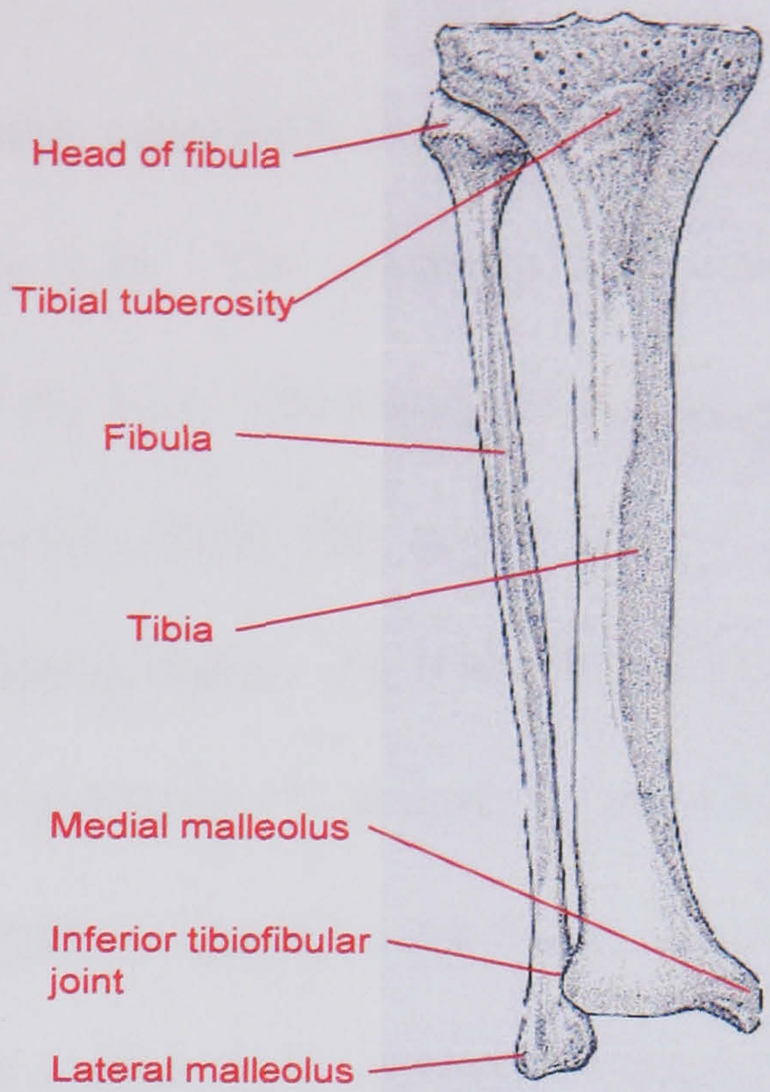

Figure 2.2. Anterior view of the bones of the right lower leg (shank). Adapted from Solomon et al. (2003).

2.2.2 The Rearfoot

The rearfoot consists of the talus and the calcaneus (Figure 2.3). The talus forms the connecting link between the leg and foot and forms the talocrural joint with the tibia and fibula. It has articular facets on the superior (trochlear) surface and medial and lateral sides for the tibia and fibula, on the inferior surface for the calcaneus, and on the anterior surface (head) for the navicular (Logan et al., 2004). The calcaneus is the most posterior foot bone and lies below and slightly on the lateral side of the talus. The large posterior section forms the heel of the foot and provides a lever for the muscles of the calf which act via the insertion of the Achilles tendon. The anterior surface articulates with the cuboid (calcaneocuboid joint) and on the medial surface a shelf of bone projects medially to support the head of the talus (Bryan, 1996). The superior surface has three facets which all articulate with the talus to form the subtalar joint.

2.2.3 The Midfoot

The navicular, cuboid and three cuneiform (medial, intermediate and lateral) bones make up the midfoot (Figure 2.3). The navicular is a curved, boat shaped bone situated on the medial side of the foot. The proximal surface articulates with the head of the talus (talonavicular joint) while the distal surface has three facets which articulate with the three cuneiform bones. The cuboid is a square-shaped bone which lies on the lateral side of the navicular. It articulates proximally with the calcaneus, distally with the fourth and fifth metatarsals and medially with the lateral cuneiform and navicular. On the plantar surface there is a deep oblique groove for the tendon of the peroneus longus muscle (Logan et al., 2004). The three cuneiform bones lie side by side and articulate proximally with the navicular, and distally with the first three metatarsals.

2.2.4 The Forefoot

The forefoot segment is constituted of the five metatarsal bones and 14 phalanges (Figure 2.3). The metatarsals are numbered from 1 (most medial) through to 5 (most lateral) and are located distal to the cuneiform and navicular. The bases (proximal end) articulate with each other and with the cuneiforms or cuboid (tarsometatarsal joints), while the heads (distal end) articulate with the proximal phalanges of their own digits (metatarsophalangeal joints). The phalanges are the most distal bones of the foot and form the toes. Each toe has three phalanges (proximal, middle and distal) with the exception of the hallux (1^{st} metatarsal) or 'big toe' which does not have a middle phalanx.

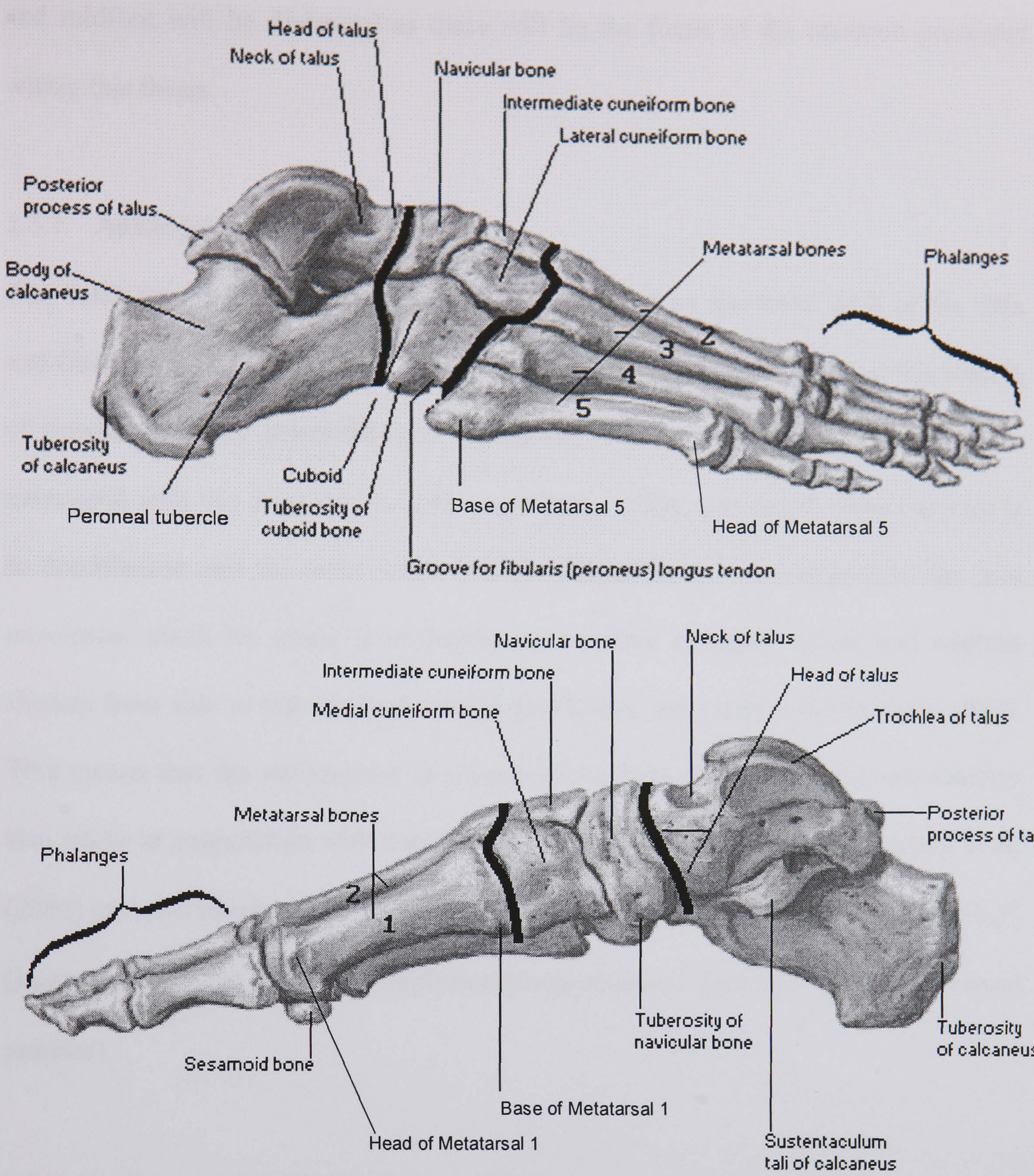

Figure 2.3. Lateral (top) and medial view of the bony structures of the right foot. Adapted from Donatelli (1996).

2.3 Joints of the Foot and Ankle

The numerous bones of the foot articulate with each other to form 23 compound joints. Rather than elaborate on each of these joints, the primary joints of the rearfoot

and midfoot will be discussed as these will be the focus of the research presented within this thesis.

2.3.1 Ankle joint (Talocrural joint)

The ankle (or talocrural joint) is a hinge joint formed by the distal ends of the tibia and fibula with the trochlea of the talus. The primary motion occurring at this joint is of dorsiflexion and plantarflexion. However, two axes of movement have been associated with this joint (Hicks, 1953; Lundberg, 1989); one exists when the joint is in dorsiflexion and the other when it is in plantarflexion. Consequently, the foot movement about the ankle is analogous to a poorly mounted wheel and swerves slightly from side to side as dorsi- and plantarflexion takes place (Klenerman, 1991). This means that the movements of inversion/eversion and internal/external rotation also occur in conjunction with movements in the sagittal plane. Indeed, Arndt et al. (2004) reported maximum rotations over the stance phase for the ankle joint to be 6.3° (inversion/eversion), 18.7° (dorsiflexion/plantarflexion) and 5.0° (internal/external rotation).

2.3.2 Subtalar Joint (Talocalcaneal Joint)

The subtalar (or talocalcaneal) joint is generally described as a hinge joint formed between the talus and calcaneus (Donatelli, 1996; Lundberg, 1989) and is responsible for the conversion of the rotatory forces of the lower extremity and the absorption of shock upon impact with the ground. Movement in this joint occurs about an oblique axis which extends anteromedially from the neck of the talus to the posterolateral portion of the calcaneus. Using 46 cadaver feet, Inman (1976) established that the mean orientation of the axis was 42° (SD ± 9°) from the horizontal and 23° (SD ±

11°) from the midline (Figure 2.4). However, a large variation in the axis orientation was found with values ranging from 20.5 to 68.5° from the horizontal and 4 to 47° from the midline.

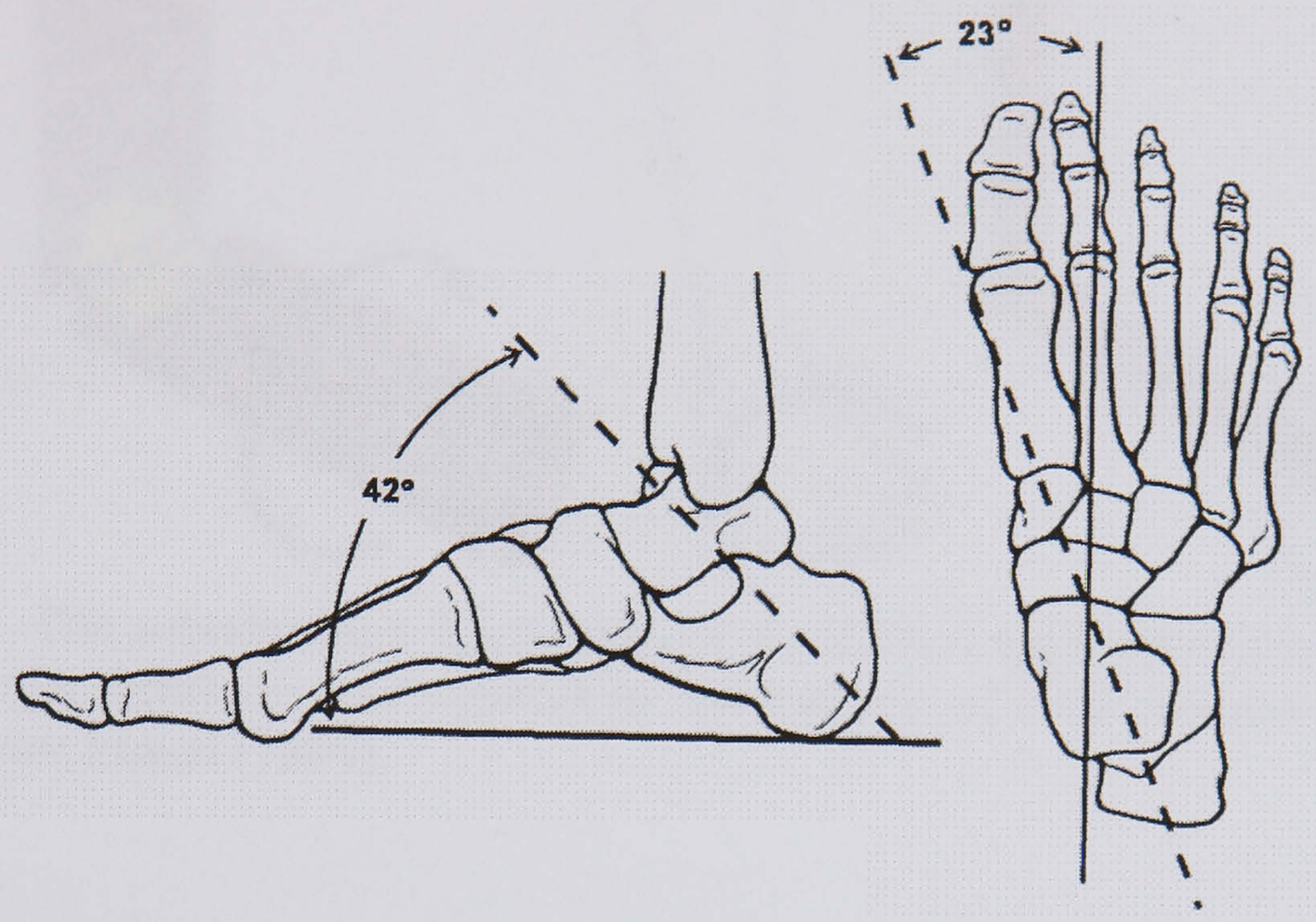

Figure 2.4. Subtalar joint axis orientation with respect to the horizontal (left) and the midline (right). Adapted from Manter (1941).

Due to the subtalar joint axis being oblique to the three cardinal planes of the body movements at the joint are considered "triplanar" (Edington et al., 1990). Thus dorsiflexion, abduction and eversion occur collectively in a movement know as subtalar pronation while plantarflexion, adduction and inversion are reflective of subtalar supination. Another important consequence of the oblique orientation of the subtalar joint axis is that it functions as a torque converter of the lower leg (Donatelli, 1996) during the stance phase of gait (closed kinetic chain). Hence subtalar joint pronation and supination cause internal and external rotation of the lower leg and vice versa. Inman (1976) compared this behaviour to the action of a mitered hinge (Figure 2.5). The kinematic link between pronation/supination and shank rotation has been a focus of research in the aetiology of chronic overuse injuries of the lower extremity (Hintermann and Nigg, 1998) and is dealt with in more detail in chapter 3.

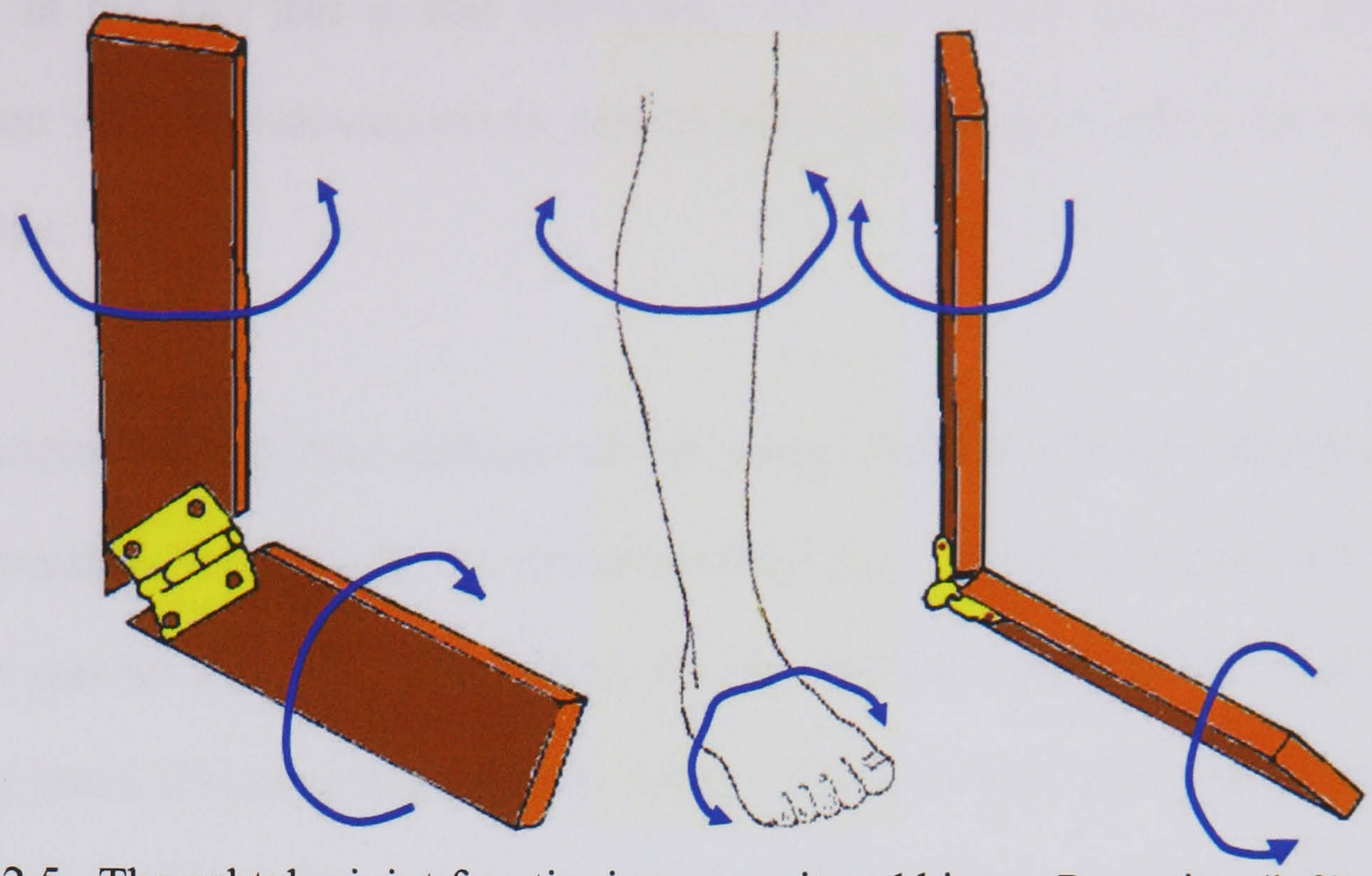

Figure 2.5. The subtalar joint functioning as a mitered hinge. Pronation (left) and supination (far right) are accompanied by internal and external rotation of the shank. Adapted from Inman (1981).

Despite widespread acceptance of the mitered hinge theory in orthopaedic literature (Edington et al., 1990), recent work has started to question its validity. For instance Lundberg (1989) found the orientation of the axis to be approximately 32° from both the horizontal and midline. He also reported that the axis orientation was variable within subjects as it was dependant upon the input movement performed at the ankle-joint-complex. For example, the joint axis deviation from the midline was 37° during external shank rotation but only 23° during internal rotation. This finding is in agreement with studies conducted *in-vitro* (Engsberg, 1987; van Langelaan, 1983).

2.3.3 Midtarsal Joint (Chopart's Joint)

The midtarsal (or Chopart's) joint is the collective term for two joints: the talonavicular joint and the calcaneocuboid joint (Bryan, 1996). The talonavicular joint has been described as being a ball and socket joint and is the most mobile joint in the tarsal region (Lundberg, 1989; van Langelaan, 1983). This joint is unusual,

however, in the fact that it also articulates with the cuboid and thus works in conjunction with the calcaneocuboid joint to allow movement between the rearfoot and forefoot.

After studying the articular surfaces of the joints, Elftman (1960) postulated that during pronation the axes of the calcaneocuboid joint and the talonavicular joint would be parallel and thus allow a more flexible midfoot that was more capable of absorbing shock (Figure 2.6). However, during supination these axes were thought to be not parallel which would serve to 'lock' the midtarsal joint and create a rigid stable midfoot for propulsion. In addition, a stable cuboid might act as a fulcrum for the peroneus longus muscle which would pull around the cuboid and plantarflex the first metatarsal during push-off (Donatelli, 1996). Elftman (1960) also hypothesised that the action of both the calcaneocuboid joint and midtarsal joint could be collectively represented by the midtarsal joint axis.

Manter (1941) and Hicks (1953) described two axes of motion at the midtarsal joint: one was longitudinal and the other oblique. The longitudinal axis slopes upward and medial with the primary movements occurring being inversion and eversion. It is possible that this axis is similar to that proposed by Elftman (1960) for the midtarsal joint. The second axis reported by Manter (1941) and Hicks (1953) is said to be oblique. Rotation about this axis was a combination of dorsiflexion occurring with abduction or plantarflexion in conjunction with adduction. It was believed that increased rotation about the oblique axis was linked to hyperpronation. Therefore, the stability of the midtarsal joint about both axes is reduced for every degree of pronation (Donatelli, 1996).

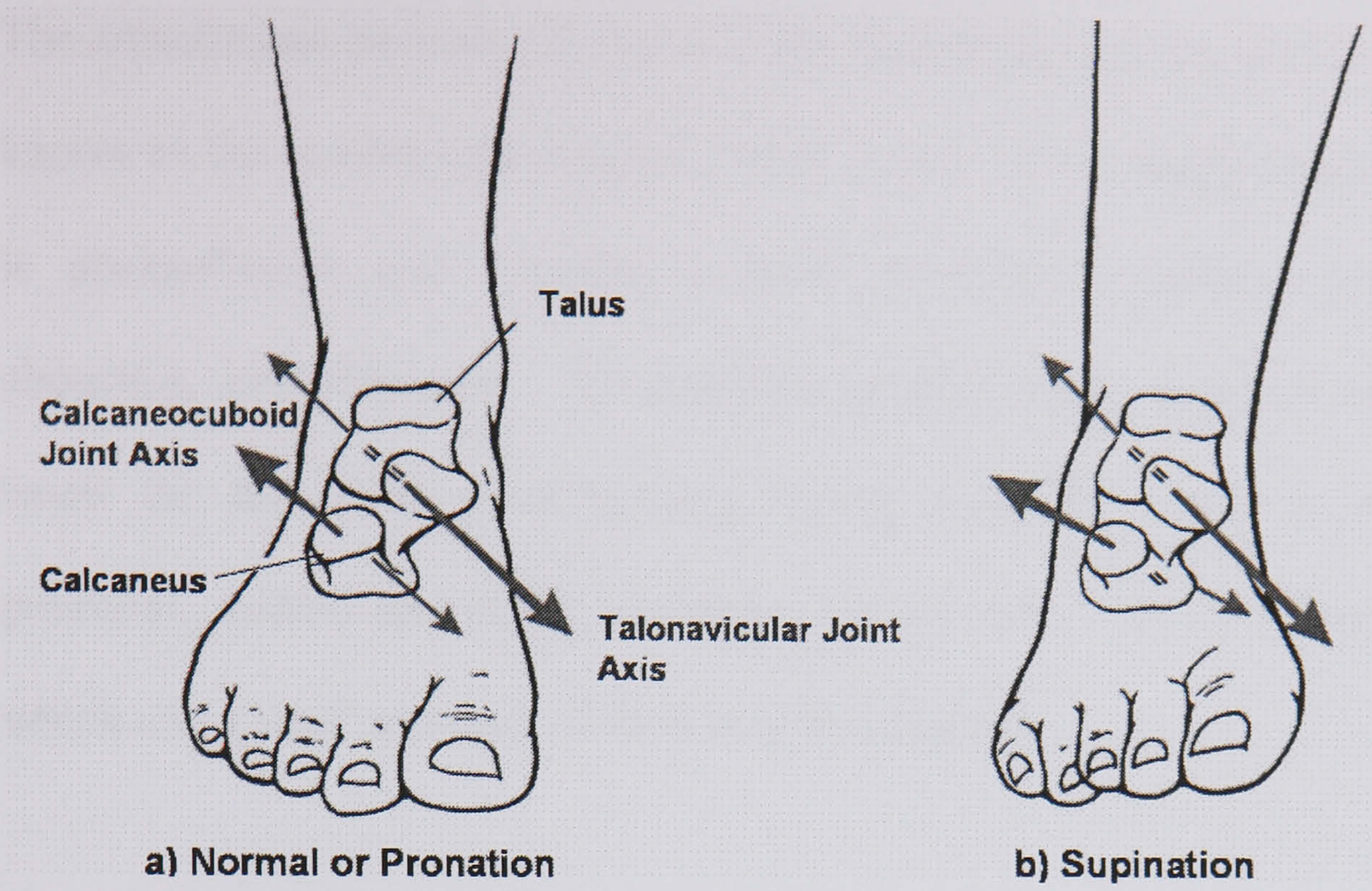

Figure 2.6. Representation of how Elftman suggested the axis of the talonavicular joint and the calcaneocuboid joint may interact to produce: a) a flexible midfoot during normal standing or pronation, or b) a rigid 'locked' midfoot during supination. Adapted from Waller and Maddalo (1995).

2.3.4 Tarsometatarsal Joints

The tarsometatarsal joints are formed by the articulations between the bases of the metatarsals with the three cuneiforms and the cuboid. These joints allow for flexion and extension of the metatarsal bones and are primarily a continuation of the midtarsal joint, compensating for extreme rearfoot motion (Root et al., 1977). The opposing motions of the first and fifth metatarsals can result in a pronation or supination twist of the forefoot. A pronation twist results from plantarflexion of the first metatarsal and dorsiflexion of the fifth metatarsal, whereas a supination twist is a combination of dorsiflexion of the first metatarsal and plantarflexion of the fifth metatarsal (Hicks, 1953).

2.3.5 Metatarsophalangeal and Interphalangeal Joints

The articulations between the heads of the metatarsals and the proximal phalanges are known as the metatarsophalangeal (MTP) joints. The primary motion at these joints is plantarflexion and dorsiflexion with secondary transverse plane motions of abduction and adduction. To distribute weight evenly between all the metatarsal heads the foot must yield laterally during push-off (Inman et al., 1981). The proximal, middle and distal phalanges are separated by the interphalangeal joints which allow small amounts of flexion and extension.

2.3.6 The Medial Longitudinal Arch

The medial longitudinal arch is formed by the calcaneus, talus, navicular, the three cuneiform bones and metatarsals 1-3 (Bryan, 1996). In a standing position, lowering of the arch is produced by internal rotation of the tibia, pronation of the subtalar joint and a lowering of the first metatarsal to be more parallel with the ground (described as first ray extension by Hicks (1954). In contrast, raising of the arch is achieved by external rotation of the tibia, supination of the subtalar joint and plantarflexion of the first metatarsal (first ray flexion). Hence, subtalar joint pronation and supination are strongly associated with the lowering and raising of the medial arch (McPoil and Knecht, 1985). It is therefore common for clinicians to define a pronated/supinated foot type based on the height and structure of the medial longitudinal arch.

The rising of the medial longitudinal arch can also be attributed to another factor known as the 'windlass mechanism' (Hicks, 1954). A thick, fibrous band known as the plantar aponeurosis joins the calcaneus and the base of the proximal phalanx of all the toes, with the base of the big toe (hallux) being the strongest. When the hallux is

dorsiflexed at the MTP joint it acts as a lever that winds the aponeurosis around the posterior surface of the metatarsal head. This increases the tension in the aponeurosis which then serves to shorten the distance between the hallux and the calcaneus by pulling them together. Since the plantar aponeurosis originates predominantly from the medial aspect of the calcaneus, the windlass mechanism promotes not only the raising of the arch, but also inversion of the calcaneus and subtalar joint supination (Donatelli, 1996).

2.4 Muscles of the Foot and Ankle

Two groups of muscles are associated with the foot and ankle: extrinsic and intrinsic (Luttgens et al., 1992).

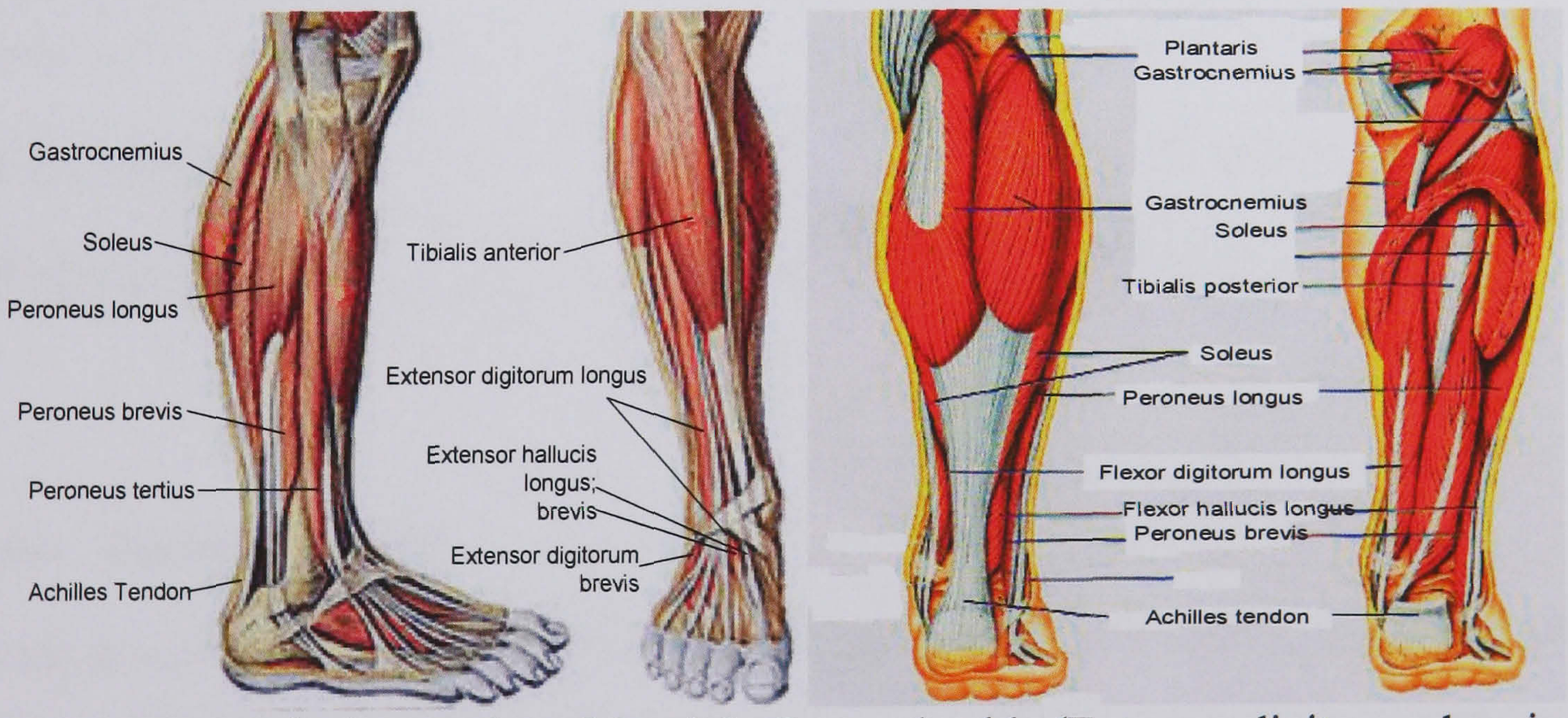

Figure 2.7. Extrinsic muscles of the right foot and ankle (Extensor digitorum brevis is an intrinsic muscle. Adapted from Solomon (2003).

2.4.1 Extrinsic Muscles

Extrinsic muscles have distal tendon attachments on the foot with proximal attachments that are located on bones outside of the foot (Figure 2.7). The primary actions of these muscles are summarised in Table 2.1 (Hall, 1999). In general, the

muscles acting to dorsiflex the ankle-joint-complex (tibialis anterior, extensor digitorum longus, peroneus tertius and extensor hallucis longus) are more active during the swing phase of gait (see section 2.5.1 for description of the gait cycle) and the initial part of the stance phase as the foot is eccentrically lowered to be flat on the floor (Perry and Lafortune, 1995). Contrastingly, the muscles associated with plantarflexion are more active from midstance through propulsion until toe-off.

Table 2.1. Extrinsic muscles of the foot and ankle and their primary function.

Muscle	Primary Action
Tibialis anterior	Dorsiflexion, inversion
Extensor digitorum longus	Dorsiflexion, eversion
Peroneus tertius	Dorsiflexion, eversion
Extensor hallucis longus	Dorsiflexion, inversion, hallux dorsiflexion
Gastrocnemius	Plantarflexion
Soleus	Plantarflexion
Plantaris	Assists with plantarflexion
Peroneus longus	Plantarflexion, eversion
Peroneus brevis	Plantarflexion, eversion
Flexor digitorum longus	Plantarflexion, inversion, toe plantarflexion
Flexor hallucis longus	Plantarflexion, inversion, toe plantarflexion
Tibialis posterior	Plantarflexion, inversion

2.4.2 Intrinsic Muscles

Aside from the extensor digitorum brevis, all the intrinsic muscles are located on the plantar surface of the foot. The muscles on the plantar aspect are usually described as being arranged in layers (Figure 2.8). The intrinsic muscles act as a functional unit and have a significant role in stabilising the foot during propulsion (Luttgens et al., 1992), acting to dorsiflex, plantarflex, abduct and adduct the toes (Mann and Inman, 1964).

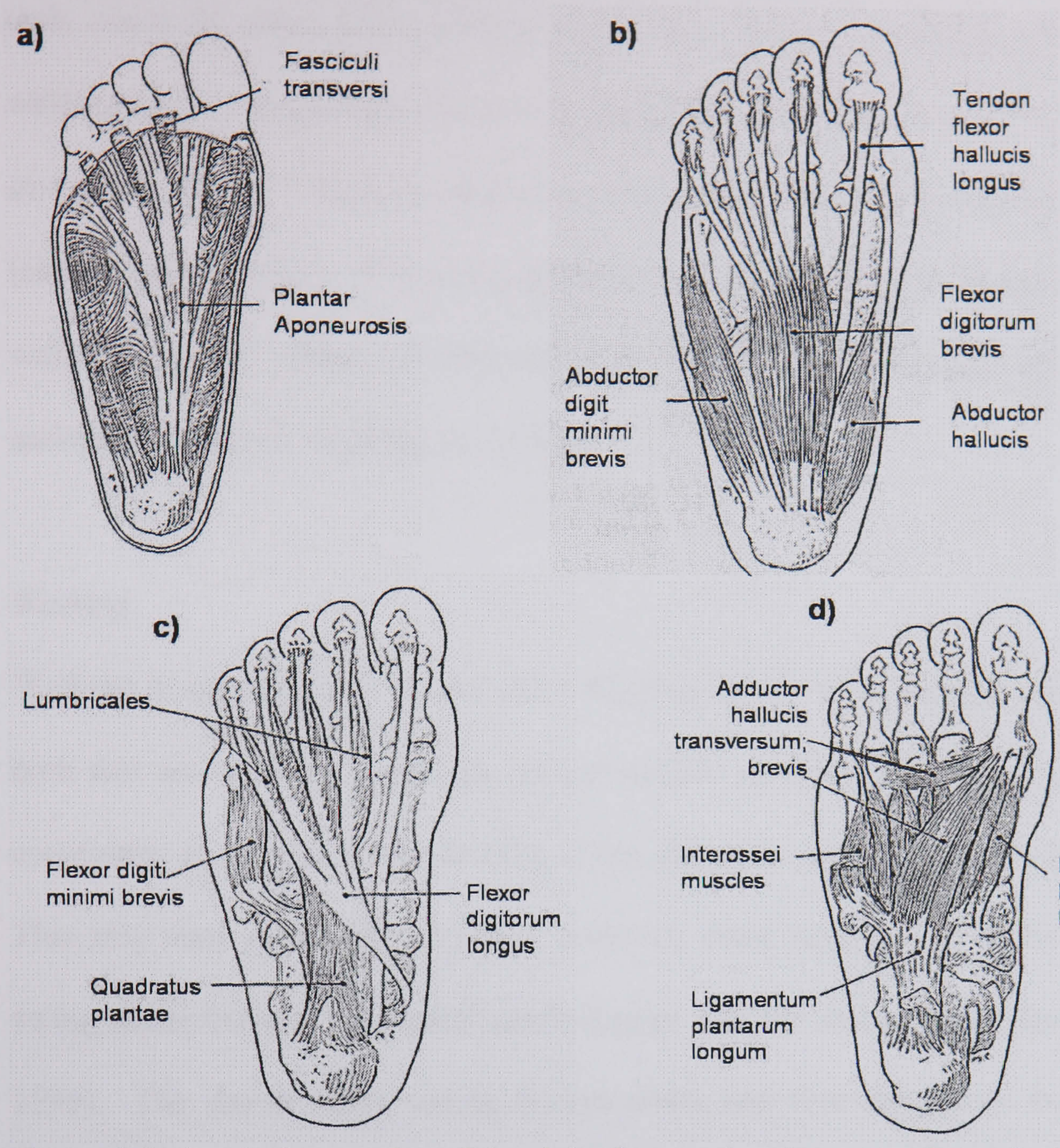

Figure 2.8. Intrinsic muscles of the right foot on the plantar surface: a) plantar aponeurosis; b) superficial layer; c) middle layer; d) deep layer. Adapted from Luttgens at al. (1992).

2.5 Biomechanics of the Foot and Lower Limb during Gait

2.5.1 The Gait Cycle

Before one can begin to understand the kinematic coupling relationship between the foot and lower limb during gait, an understanding of the general gait cycle is required. The gait cycle is defined as the time interval between two successive occurrences of one of the repetitive events of walking or running (Whittle, 1996). The most convenient event to use is the instant at which one foot contacts the ground. Therefore the gait cycle begins when one foot comes into contact with the ground and

ends when the same foot contacts the ground again (Novacheck, 1998). In both walking and running there are two primary phases of gait, stance and swing. The stance phase occurs when the foot is in contact with the ground and is weight bearing (closed kinetic chain). The swing phase is the period when the foot is not in contact with the ground. There are differences in the gait cycle dependant on the mode of ambulation used i.e. walking or running.

Walking

Walking is characterised by two short duration double limb support phases in which both feet are in contact with the ground (makes up 10% of the gait cycle). Stance constitutes up to approximately 60% of the gait cycle with swing 40% (Perry, 1992). This may vary with walking speed, however, since increases in speed result in the swing phase becoming proportionately longer, and the stance phase shorter (Whittle, 1996). The stance phase can be broken down into five sub-phases beginning with initial contact of the foot (Figure 2.9). During walking this is usually with the heel and is frequently called 'heel strike/ contact.' Following heel strike, the leg accepts the weight as the foot comes down to make full contact with ground and is known as 'foot flat'. The first period of double support is associated with the first two sub-phases of stance since both feet are still in contact with the ground. The body then pivots over the load bearing foot and the centre of gravity passes directly over the foot, a sub-phase known as 'midstance'. The body continues to progress forwards and the heel of the foot begins to leave the ground ('heel-off') as the opposing leg is also starting to make contact. The final event in the stance phase is 'toe-off' which occurs when the toes of the support foot are just leaving the ground. The second period of double stance occurs between 'heel-off' and 'toe-off'. The swing phase can be sub-

divided into three components. The first is the 'acceleration' (pre-swing) sub-phase, which makes up approximately one third of the swing phase, beginning with 'toe-off' and ending when the foot is opposite the new stance foot. This is followed by 'midswing' which continues until the tibia of the swinging limb is vertical and in front of the stance leg. The final division of the swing phase is 'deceleration' (terminal swing) which ends when the swinging foot strikes the floor.

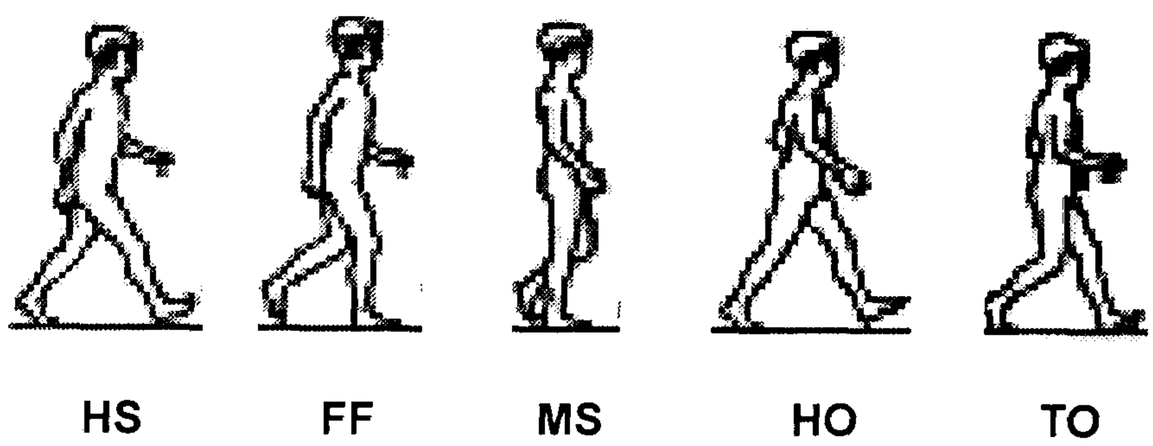

Figure 2.9. Stance phase of walking gait. HS= heel contact; FF= foot flat; MS=midstance; HO= heel-off; TO= toe-off. Adapted from Novacheck (1998).

Running

In contrast to walking, running has no double support phases but instead has two flight phases where both feet are not in contact with the ground (Donatelli, 1996). During average jogging speeds (approximately $3.2ms^{-1}$), ground contact represents 39% for stance and 61% for swing, though as the runner moves faster, less time is spent in stance (Novacheck, 1998). Periods of acceleration and deceleration of the centre of mass occur during running and are referred to as 'absorption' and 'generation.' Absorption is the period where the centre of mass of the body falls from its peak vertical displacement during the flight phase. Absorption continues through heel-strike until the centre of mass reaches its lowest vertical displacement and starts to be propelled upward in the period known as generation. Generation then continues until the centre of mass reaches maximum vertical displacement during the flight phase again. Due to these periods (absorption and generation) not coinciding with

heel-strike and toe-off, the stance phase of running can be divided into two sub-phases. During the first half of stance the lower extremity is serving to absorb energy from the impact with the ground (absorption) and will be referred to as the cushioning phase. The second half of stance is about generating power to propel the body's centre of mass upwards (generation) and will be referred to as the propulsion phase.

Most pathological problems involving the lower extremities become apparent in the stance phase since the joints/ soft tissues are undergoing greater stress due to the weight-bearing load placed on them (Mann, 1995). The constraints provided by the closed kinetic chain play a large role in the patterns of gait and the biomechanical relationship between the various joints of the lower extremity becomes much more critical. The centre of mass is transferring forces through the lower limb from a proximal direction whereas the ground exerts force from the distal aspect. For this reason the stance phase of gait has received the most attention in attempts to understand the aetiology of chronic overuse injury to the lower extremity, and will therefore be the focus within the context of this thesis.

2.5.2 Association between Pronation and Overuse Injuries

Today, running is perhaps the most common form of exercise in the world with approximately 32 million Americans including it as part of their leisure activities (Duffey et al., 2000). Many people include this pastime as part of their everyday lives in a bid to stay healthy. As many as 37-56% of those runners, however, will sustain an overuse injury during the year (van Mechelen, 1992). The risk of sustaining an overuse injury is multi-factorial and may depend on a number of variables such as the intensity, duration and frequency of training (Lysholm and Wiklander, 1987; Messier

et al., 1991), shoes (Robbins and Gouw, 1990; van Gheluwe et al., 1999) and running surface (O'Connor and Hamill, 2002; Stergiou and Bates, 1997). However, anatomical factors involving abnormal biomechanics or malalignments of the lower extremity have frequently been associated as being risk factors linked to chronic overuse injuries (Krivickas, 1997; Lysholm and Wiklander, 1987; McClay and Manal, 1998a; Messier et al., 1991; Murphy, 2003).

One such biomechanical anomaly that has been associated with overuse injuries is that of hyperpronation of the foot (Hintermann and Nigg, 1998). Although the relationship between pronation and injury is not well understood, a number of studies have found excessive pronation to be linked with a variety of ailments of the lower extremity including knee pain (Duffey et al., 2000; Williams et al., 2001), 'shin splints' (Messier and Pittala, 1988; Yates and White, 2004) and plantar fascitis (Kibler et al., 1991). However, excessive pronation is not always predictive of overuse injuries (Messier et al., 1991; Powers et al., 2002; Wen et al., 1997).

2.5.3 Measurement of Pronation during Gait

The confounding findings concerning the link between pronation and overuse injuries in the literature may be in part attributable to whether pronation is assessed with static measurements (Wen et al., 1997; Yates and White, 2004) or by using dynamic measurements during gait (Duffey et al., 2000; Powers et al., 2002). It is therefore necessary to describe how pronation is measured during gait.

The orientation of the subtalar joint axis makes the measurement of rotation at the joint using conventional planar analysis (cardinal planes) difficult, since it consists of

dorsiflexion/plantarflexion, eversion/inverison and abduction/adduction. The component of subtalar joint motion that is most independent of motion at other joints and the simplest to measure is calcaneal inversion and eversion (Edington et al., 1990). Static rearfoot angles typically involve the measurement of the angle of rearfoot relative to the lower leg in the frontal plane during quiet standing (Wen et al., 1997; Yates and White, 2004). This is represented by the angle (ß) between a longitudinal line bisecting the rearfoot and a longitudinal line bisecting the distal third of the lower limb (Razeghi and Batt, 2002) (Figure 2.10). The assessment of pronation during running has traditionally been carried out by using the same angle to quantify the magnitude of subtalar joint pronation. This was typically performed by using 2-D filming techniques to monitor the movement of four external markers: two on the longitudinal line of the heel and two on the longitudinal line of the lower leg. Thus the rearfoot eversion angle during running could then be calculated in every frame of the stance phase.

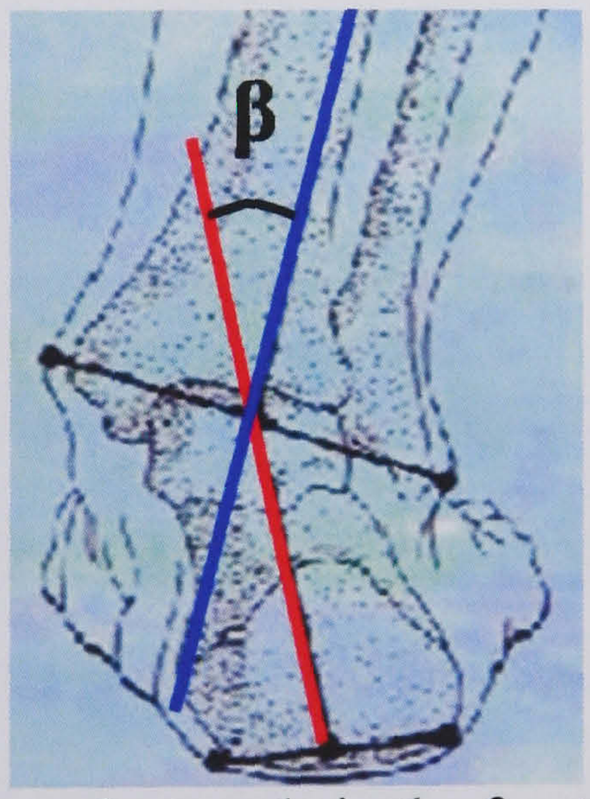

Figure 2.10. Measurement of rearfoot angle in the frontal plane. The blue line represents the longitudinal line of the distal third of the lower limb, with the red line the longitudinal line of the rearfoot. The value, β, represents the rearfoot eversion angle. Adapted from Mann (1995).

Measuring the angle of the rearfoot relative to the lower leg has been suggested to provide information about motion at the subtalar joint. It is perhaps not surprising that conflicting reports exist in the literature concerning the effects of excessive pronation when it is evident that static rearfoot angles have been reported to be poorly correlated with the dynamic rearfoot angle (Kernozek and Greer, 1993). It would be ideal if clinicians could use static foot measurements to predict dynamic foot behaviour since this would save the time consuming process of a comprehensive gait analysis procedure. However, this is not the case, and it is of more importance to investigate the behaviour of the foot during running since this is when injury problems of the lower extremity become apparent. Dynamic measurements of rearfoot motion will therefore be used within the context of this thesis.

2.5.4 3-D or 2-D Analysis of Rearfoot Motion

Until recently, the majority of rearfoot running studies had been conducted using a simple two-dimensional (2-D) analysis (Hamill et al., 1992; Stacoff et al., 2001; Stergiou and Bates, 1997; van Gheluwe et al., 1999). This method usually entailed the placement of a single camera to film the posterior aspect of the frontal plane motion of the foot and lower leg as the subject performed over-ground or treadmill running. Most of these studies were collected using film which required manual digitisation to obtain the marker co-ordinate data. Using 3-D analyses, two or more cameras must be used to film the markers during running, which meant even more time spent digitising. In addition, extra processing was entailed in a 3-D study since a direct linear transformation (DLT) is required to calculate marker co-ordinate data from two or more cameras. Therefore, 3-D studies were scarce due to the increased time spent processing data. However, three-dimensional rearfoot analyses have been

shown to yield different results to that of 2-D analyses (Areblad et al., 1990; Cornwall and McPoil, 1995; McClay and Manal, 1998b).

Cornwall and McPoil (1995) found that rearfoot motion measured with either a 2-D or 3-D analysis was essentially similar between 8 and 60% of the stance phase of walking. However, there were discrepancies in the rearfoot angle at heel-strike between the two conditions and they did not compare the influence of the two analysis methods on rearfoot motion during the last 40% of the stance phase. McClay and Manal (1998b) provided supporting evidence that the rearfoot angle at heel-strike was indeed different between 2-D and 3-D analyses. They also found that the rearfoot angle at toe-off was influenced by the type of analysis, therefore, making a 3-D analysis essential for any investigation of rearfoot kinematics over the entire stance phase.

Areblad et al. (1990) postulated that 2-D analyses of rearfoot motion were hampered by projection errors, which depended on the alignment of the rearfoot and lower leg with the film plane, in this case, the frontal plane. Indeed, they found that the peak rearfoot angle and the angle at heel-strike were very sensitive to the alignment angle between the foot and camera view axis. Indeed, a slight change in this alignment angle of 2.7° resulted in a 1° alteration in the two afore mentioned rearfoot angles. This has important implications for between-subject rearfoot kinematic comparisons since subjects may run with varying degrees of 'toe-out' (foot abduction relative to the laboratory). McClay and Manal (1998b) showed that the 'toe-out' angle ranged from -13.3° (toe-in) to 31.9° (toe-out) in a small sample of 18 runners. Interestingly, they found that runners who had the most pronounced 'toe-out' running styles also

exhibited the greatest rearfoot kinematic differences between the 2-D and 3-D analyses.

2.5.5 Pronation during Running

This thesis has already highlighted that the stance phase of running can be divided approximately into two halves known as the cushioning and propulsion phases respectively (section 3.1.2). Following initial contact with the ground, the foot begins to pronate, which has the effect of 'unlocking' the midtarsal joint (see section 2.3.3) allowing the foot to become a more flexible structure (Elftman, 1960). This in turn enables to foot to better accommodate the underlying surface (James and Jones, 1990) and attenuate the impact loads experienced (Pratt, 1989). However, during the propulsion phase of stance, the foot supinates which supposedly 'locks' the midtarsal joint, changing the foot into a rigid lever for effective push-off. Excessive pronation may present an elevated risk of injury to the lower extremity due to increased or prolonged flexibility of the foot failing to provide the support needed to stabilise the foot during push-off. This means that increased forces may be applied to the supporting structures of the foot due to the additional effort required by the intrinsic and extrinsic musculature of the foot to compensate for this lack of support (James and Jones, 1990).

2.5.6 Kinematic Coupling between the Foot and Leg as an Injury Mechanism

Another proposed injury mechanism is linked to the kinematic relationship between motion of the foot and that of the lower leg. Due to the mitered hinge action of the subtalar joint, pronation serves to induce internal rotation of the shank, while supination is accompanied by external rotation of the shank (Inman et al., 1981).

Hence, abnormal movements of the foot such as excessive pronation may have a knock on effect on the kinematics of the shank. For this reason the kinematic coupling relationship between pronation and supination of the foot with internal and external rotation of the shank has often been linked with chronic overuse injuries of the lower extremity (Dierks et al., 2004; Powers et al., 2002; Stergiou and Bates, 1997; Tiberio, 1987). If excessive pronation occurs during running then this would result in excessive internal rotation of the shank which must then be absorbed at the knee (James and Jones, 1990) or hip (Tiberio, 1987). This may then alter the normal alignment between the hip, knee and ankle-joint-complex and thus induce abnormal motion at the patellofemoral joint (Kernozek and Greer, 1993).

A mechanical dilemma is evident when prolonged internal shank rotation occurs as a result of prolonged pronation. During running it has been postulated that both subtalar joint pronation and knee flexion induce shank internal rotation, whereas subtalar supination and knee extension induce shank external rotation (Hamill et al., 1992; Tiberio, 1987). However, if pronation was prolonged then an antagonistic relationship would become evident at the knee since opposing torques would be acting at the proximal and distal ends of the tibia, thus increasing stresses placed on the joints and soft tissue (Stergiou et al., 1999).

In short, a number of potential injury mechanisms exist as a consequence of the kinematic coupling between the foot and lower leg. For this reason, the kinematic coupling relationship between pronation and supination of the foot with internal and external rotation of the shank has been the focus of much research with regard to the aetiology of chronic overuse injuries of the lower extremity (Dierks et al., 2004;

Powers et al., 2002; Stergiou and Bates, 1997; Tiberio, 1987). Thus the next chapter of the literature review will address the issues surrounding the measurement and current understanding of kinematic coupling between the foot and lower limb.

Chapter 3 - Kinematic Coupling between the Foot and Lower Limb during the Stance Phase of Gait

3.1 Definition of Kinematic Coupling

When the movements of two or more body segments are co-ordinated within an overall movement pattern it can be said that they are coupled. The segments may be linked via the body segment's kinematics such as linear/angular displacement, velocity of acceleration. Within the context of this thesis, kinematic coupling will be defined as the angular displacement of one segment being related to the angular displacement of the other segment in question (both spatially and temporally). Since the aim of this thesis was to assess the kinematic coupling between the foot and lower limb, coupling will refer to the kinematic link between the two segments whereby foot pronation and supination are accompanied by shank internal and external rotation respectively. Segments can be kinematically coupled even though they are not necessarily mechanically interdependant. Mechanical coupling refers to when a body segment's movement behaviour is coupled to another segment due to a mechanical link between the two segments. This mechanical link may be rigid in nature or contain some elastic element. A rigid link would mean that the movement of one segment would instantly affect the movement of other segment. However, if there is some element of elasticity in the mechanical coupling, then there may be a delay between the motion of one segment being transferred to the other. Kinematic coupling between the foot and lower limb is mechanical in nature since the two segments are linked directly by the bones in the ankle-joint-complex. However, it is possible that this mechanical link is influenced by the numerous ligaments and muscles that cross the joints between the foot and lower limb.

3.2 Measures of Kinematic Coupling

3.2.1 Discrete Measures of Kinematic Coupling

Absolute Angles

Perhaps the most basic measure used for assessing the kinematic coupling between the rearfoot and shank is the comparison of peak values for both rearfoot eversion and shank internal rotation (McClay and Manal, 1997; Powers et al., 2002; Reischl et al., 1999; Woodburn et al., 2002). If there is a strong kinematic coupling relationship between the rearfoot and shank via the action of a 'mitered hinge' subtalar joint, then any increases or decreases in peak rearfoot eversion should be reflected by respective changes in peak shank internal rotation. McClay and Manal (1997) compared the kinematic coupling in subjects who ran with normal rearfoot with those who excessively pronate. They found that peak rearfoot eversion was significantly greater in the hyperpronator group (21.2°) compared to the normal subjects (11.2°) but there was no difference in terms of peak shank internal rotation between the groups. On a similar note, Reischl et al. (1999) reported that peak foot pronation was not a statistically significant predictor of the magnitude of peak shank internal rotation.

Measures of peak joint angles are dependant on accurate/reliable placement of markers. Slight variations in the position of the markers can result in a shift in the absolute value of inter-segment angles (Carson et al., 2001), an anomaly that would alter the peak values obtained. It has been proposed that these offsets could be reduced by subtracting a neutral position for joints during a static reference trial (Leardini et al., 1999). However, failure to place subjects in the same neutral reference position for the static trial could also influence the peak values obtained

during running. Pierrynowski et al. (1996) showed that untrained physiotherapy students could only be expected to place the rearfoot within 2° of the subtalar neutral position 48% of the time. This ability of foot care specialist to obtain the same level of accuracy was higher with a confidence of 73%, which still leaves much room for improvement.

Angular Excursions

Another method of measuring the kinematic coupling between the rearfoot and shank is the use of angular excursion values (McClay and Manal, 1998; Nawoczenski et al., 1998; Nigg et al., 1998). Using this technique, rearfoot eversion excursion is defined as the eversion range of motion from heel-strike (touchdown) to peak eversion. Shank internal rotation excursion is found between heel-strike and peak shank internal rotation. Excursion values have the advantage of not being influenced by offsets caused by the experimental setup (marker placement, reference position). This was highlighted by Ferber et al. (2002) who demonstrated that angular excursion value measures were more reliable between-day as compared to absolute peak angle measures. They reported between-day intraclass coefficient correlations (ICC) of 0.93 and 0.91 for excursion values of rearfoot eversion and shank internal rotation respectively. However, the equivalent ICCs were only 0.63 and 0.68 for absolute peak values of rearfoot eversion and shank internal rotation.

According to the mitered hinge theory of the subtalar joint, it would be expected that the magnitude of the rearfoot eversion excursion would predict the magnitude of shank internal rotation excursion. In a study comparing runners with low or high arches, rearfoot eversion excursion and shank internal rotation were suggested to be

unrelated (Nawoczenski et al., 1998). This investigation found that although rearfoot eversion excursion was similar for the two different arch groups, shank internal rotation excursion was significantly greater (4°) in high arch group. However, McClay and Manal (1998) found that rearfoot eversion excursions were not different between hyperpronators and normals with values of 12.8 and 12.7 respectively. Additionally, no changes in shank internal rotation excursion were observed between the two groups (Pronators = 9.8°, normals = 8.9°) so no conclusions could be drawn about whether the excursion angles of both segments were related. Hence, the relationship between rearfoot eversion and shank internal rotation in terms of both peak and excursion values is not clear and questions the validity of the mitered hinge model suggested by Inman (1981).

Transfer

It was mentioned in section 2.3.2 that Lundberg (1989) questioned whether the subtalar joint was oriented at approximately 45° in the sagittal plane (Inman et al., 1981). Lundberg (1989) found the value to be more along the lines of 32° using roentgen stereophotogrammetry (x-ray) and bone mounted markers. Since this was conducted in a static situation, however, it is not certain how representative the findings were of subtalar joint mechanics during running. It is difficult to measure the orientation of the subtalar joint axis directly without the use of invasive techniques, which usually entails the use of bone mounted markers. However, a number of studies have examined the relative amounts of rearfoot eversion and shank internal rotation that occur during the stance phase of running (McClay and Manal, 1997; Nawoczenski et al., 1998; Nigg et al., 1993). In these studies, a transfer coefficient was defined to describe the transfer of eversion excursion (peak eversion minus

eversion at touchdown) of the rearfoot into shank internal rotation excursion (peak shank internal rotation minus the angle at touchdown) through the ankle joint complex (Nigg et al., 1993). If the subtalar joint axis was oriented at approximately 45° in the sagittal plane, it would be midway between the frontal and transverse planes of the body implying that there should be equal amounts of rearfoot eversion and shank internal rotation occurring during pronation (McClay and Manal, 1997). This would of course result in a transfer ration of 1.0. In a study of 30 runners, Nigg et al. (1993) found that the mean transfer coefficient was 1.32 indicating that more rearfoot eversion was occurring relative to shank internal rotation. McClay and Manal (1997) came to a similar conclusion when they reported a transfer coefficient of 1.38. The dominance of rearfoot eversion motion over shank internal rotation suggests a subtalar joint axis that allows more frontal plane motion than transverse plane motion to occur. This would suggest that the subtalar joint axis would be inclined closer to the horizontal than the 42° suggested by Inman (1981) thus supporting the findings of Lundberg (1989).

The transfer coefficient has been cited as a potential predictor of the anatomical sites where injuries are more likely to occur (McClay and Manal, 1997; Nawoczenski et al., 1998; Williams et al., 2001). It was found that runners who hyperpronate have a lower coefficient (1.23) compared to normal subjects (1.53), and was postulated that the increased relative motion of shank internal rotation might place the former group at greater risk for knee problems (McClay and Manal, 1997). Williams et al. (2001) found that runners with high medial foot arches also had lower transfer coefficient values compared to low arched runners. The subjects in the high arch group also had a higher prevalence of knee injuries. Both these studies suggest that ratios favouring a

larger excursion of shank internal rotation may be linked with an increased risk of obtaining an overuse knee injury.

Timing

Timing has also been long associated with studies investigating joint coupling (Hamill et al., 1992; Stergiou et al., 1999). As mentioned in section 3.3.1, a disruption in the timing between rearfoot frontal plane and knee sagittal plane motion may pose an increased risk of suffering an overuse injury. Hamill et al. (1992) investigated the effect of running in shoes with varying midsole hardness on the timing of peak rearfoot eversion and peak knee flexion. The time to peak knee flexion was unaffected by midsole hardness, occurring between 44.2 and 45.9% of the stance phase. On the other hand, peak rearfoot eversion was found to occur significantly earlier (38.7% stance) when running with the softest midsole compared to the harder midsoles (42.8-43.8% stance). Hence, the rearfoot began to invert while the knee was still flexing, resulting in an antagonistic relationship at the knee. This is due to the foot imposing an external torque on the shank while the flexing knee forces the shank to internally rotate. A major assumption of this injury mechanism is that internal and external rotation of the shank occurs in conjunction with rearfoot eversion and inversion respectively.

Studies investigating the timing relationship between the foot and shank are scarce. McClay and Manal (1998) reported that the time to both peak rearfoot eversion and shank internal rotation was similar for both pronators and people with normal rearfoot motion during running. They also found that peak rearfoot eversion and shank internal rotation occurred at similar times, 0.92 and 0.10s after touchdown

respectively. In contrast, Reischl et al. (1999) indicated that the timing of peak pronation was not predictive of the timing of peak shank internal rotation during walking. In fact, the timing of peak shank internal rotation occurred earlier (15.2%) in the stance phase with respect to peak pronation (26.8%). Therefore, the timing of events between foot and shank kinematics warrants further investigation since the evidence so far has been inconclusive.

Comparing only the timing of specific discrete events within the stance phase (e.g. time to peak eversion) shares a common weakness with the use of discrete angles (e.g peak eversion or eversion excursion) or joint excursion ratios to assess coupling. This is that all these measures assess the kinematic relationship between two segments based only on instantaneous events in the stance phase. In fact non of the measures provide any information regarding the latter stages of the stance phase, since peak rearfoot eversion and peak shank internal rotation occur during the first half of stance. Nor do they enlighten the investigator into the continuous joint coupling relationship throughout the entire stance phase.

3.2.2 Continuous Measures of Kinematic Coupling

For a more complete picture of the kinematic coupling it is necessary to assess not only at a single time point, but the angular motions over the entirety of the stance phase. This was the aim of Stergiou and Bates (1997) when they set out to measure the kinematic coupling between the actions of the rearfoot and knee during running. In addition to measuring the timing of discrete events, they introduced a curve correlation (cross-correlation) technique to quantify the relationship between the two joints across the entirety of the stance phase. Using this method, studies have been

conducted to measure alterations in continuous coupling between rearfoot frontal plane (subtalar joint motion) and sagittal plane knee motion induced by alterations in stride length and obstacle clearance during running (Stergiou et al., 1999; Stergiou et al., 2003). It was reported that under- or over-striding reduced the curve correlation coefficient ($r = 0.57$ and 0.61 respectively) compared to when subjects ran with their normal self-selected stride length ($r = 0.71$) (Stergiou et al., 2003). Similarly, running over obstacles of increasing height was shown to lower the curve correlation coefficient compared to normal unimpeded running (Stergiou et al., 1999). Therefore, it appeared that alterations in stride length and running over obstacles served to lower the temporal coupling between the rearfoot and knee across the stance phase.

It was mentioned earlier (section 2.5.6) that asynchronous timing between rearfoot frontal plane and knee sagittal plane motion may present an elevated risk of injury. This was based on the assumption that shank internal rotation accompanied the movements of both rearfoot eversion and knee flexion, with shank external rotation occurring in conjunction with rearfoot inversion and knee extension. However, since the afore mentioned studies comparing rearfoot and knee kinematics were only conducted using a 2-D analysis, the assumption that shank internal/external rotation occurs in synchrony with rearfoot eversion/inversion was never confirmed. It would thus, be of considerable use to establish the continuous kinematic coupling relationship between the rearfoot and shank.

3.2.3 Variability in Kinematic Coupling

Recent studies have investigated the role of variability in coupling as a potential injury risk (Dierks et al., 2004; Hamill et al., 1999; Heiderscheit et al., 2002). One of

the first studies was conducted by Hamill et al. (1999) who incorporated a method known as the continuous relative phase (CRP). Here, phase plots of the normalised angular velocity versus the normalised angular displacement are plotted for each segment of interest (proximal and distal). Then the phase angle for each specific data point was calculated in each of the phase plots. Finally the CRP was defined as the difference between the two phase angles at each specific point (distal segment angle subtracted from the proximal segment angle). Hamill et al. (1999) found that patients with patellofemoral pain (PFP) showed less variation in CRP (rearfoot eversion/inversion vs tibial internal/external rotation) across the stance phase, especially at the events of touchdown and toe-off. This suggested that the coupling between the two segmental motions was less variable in individuals with a lower extremity pathology. However, a number of limitations have been associated with the use of CRP approach. For example, it has been argued that in order to decrease the possibility of one segment dominating the CRP (due to greater ROM), it is necessary to normalise the angular displacement/velocity data (Hamill et al., 1999). On the other hand, Kurz and Stergiou (2002) demonstrated that normalisation tended to modify the CRP curve configuration both graphically and numerically. Due to the disagreement between authors to use one method or the other, it remains difficult to make comparisons with the literature. Another limitation is that a CRP analysis is based on the assumption that the data is sinusoidal in nature, which may not be the case. Finally, since the CRP angle is essentially a function of both the position and velocity of one segment relative to both the position and velocity of the other segment, it is difficult to interpret this result in terms of a mechanical cause of injury (DeLeo et al., 2004).

Another method that has been used to asses joint coupling variability is a technique using vector coding angles (Dierks et al., 2004; Heiderscheit et al., 2002). First an angle-angle diagram for the two segments (distal versus proximal) of interest was constructed and then the angle of the resultant trajectory between two successive data points was calculated for all successive points (at each instant in time). Essentially this technique is similar to the transfer ratio described earlier (section 3.3.2) since this technique divides rearfoot frontal plane excursion by the shank transverse plane excursion. However, instead of using excursion values between two discrete points of interest (e.g. touchdown and peak absolute angle) it is more analogous to a continuous transfer ratio since it is calculated at every instant in the stance phase (DeLeo et al., 2004). Hence, this technique can be used to determine the relative amounts of angular displacement that the two segments are undergoing relative to one another.

3.3 Manipulation of Segmental Kinematics to Investigate Coupling

Much of the literature investigating the kinematic coupling relationship between the rearfoot and shank has come from experiments that either a) compare coupling between subgroups of subjects (McClay and Manal, 1997; Nawoczenski et al., 1998; Williams et al., 2001), or b) study the effect of adding orthotics/altering shoe construction on coupling (Stacoff et al., 2001; Stacoff et al., 2000b; Williams et al., 2003). The problem with comparing subgroups is that this usually entails comparing subjects where one or more of the groups may represent extremes of the population, for example, people who hyperpronate or have contrasting arch heights. These populations contain people whose kinematic coupling properties do not represent the norm, thus this may confound any conclusions concerning normal kinematic coupling

patterns. In addition, quite often any differences found in terms of segmental kinematics or coupling are small and unsystematic. Studies altering shoe construction or using orthotics within a repeated measures design attempted to alter the kinematics of one segment and observe the knock on effect on the adjacent segments. However, frequently the experimental manipulations were not successful in inducing substantial kinematic alterations in the segments, hence it was difficult to conclude much about the coupling relationship between them. There is, consequently, a need for studies which use experimental manipulation that substantially alter the kinematics of one of the segments of interest. Observing the effect the altered kinematics of the selected segment has on the adjacent segment kinematics would provide more understanding about the coupling relationship at the joint.

3.3.1 Barefoot and Shod Running

There are confounding reports in the literature regarding the kinematic differences between barefoot and shod running (De Wit et al., 2000; Stacoff et al., 2000a). In a biomechanical analysis of the stance phase, De Wit at al. (2000) reported that a significantly smaller eversion excursion between touchdown and peak impact force was evident in barefoot running compared to shod running. However, rearfoot eversion during barefoot running was measured using skin mounted markers, whereas rearfoot motion during shod running was assessed using markers mounted on the shoe itself. This creates uncertainty in terms of the validity of the findings since it has previously been demonstrated that the calcaneus may move within the heel of a running shoe (Stacoff et al., 1992; van Gheluwe et al., 1995). Stacoff et al. (1992) attempted to quantify the effect of calcaneal slippage within the heel of a shoe during running by cutting windows in the heel counter of a running shoe so that markers

could still be mounted on the calcanues. They found that rearfoot eversion excursions measured using markers on the calcaneus (touchdown to max absolute angle) were 13.7° and 12.1° during barefoot and shod running respectively. In the same study it was demonstrated that the rearfoot kinematic curve patterns (frontal plane) were different between barefoot and shod conditions towards the end of the stance phase. This discrepancy, however, may have been caused by the planar errors associated with the 2-D analysis (section 3.2.3) conducted within the study.

Stacoff et al. (2000a) compared the 3-D tibiocalcaneal kinematics between barefoot and shod running using markers mounted directly onto the bones. They reported that differences between the two conditions (barefoot versus shod) were typically less than 1° in terms of both rearfoot eversion (peak absolute angle and eversion excursion) and tibial internal rotation (peak and excursion angles). Similarly, the angle-angle diagrams of rearfoot frontal plane versus tibial transverse plane motions showed similar patterns for both barefoot and shod conditions, thus indicating good kinematic agreement across the entire stance phase. Given the difficulties in placing external markers on the forefoot whilst the foot is shod, it seems feasible to conduct kinematic analyses of foot and lower limb coupling using a barefoot running protocol. The main goal of the thesis is to gain greater understanding into the coupling mechanisms between the foot and lower limb. However, caution must be taken when interpreting the findings within this thesis to represent the situation during shod running.

3.3.2 Step Width

One experimental manipulation that has been proven to significantly alter rearfoot kinematics is the variation of step width during running (Williams and Ziff, 1991). In

this study, a midline was drawn down the centre of the treadmill and subjects were asked to run with three different step widths: crossing over the midline (cross-over); a mid position where the medial border of the foot landed on the midline (mid); and a wide position (wide). It was found that as step width was altered from a wide, to a mid and then to a cross-over condition, both peak rearfoot eversion and eversion excursion increased in a stepwise manner. The difference between the wide and cross-over conditions in terms of the peak and excursion angles was approximately 5°. It was postulated that the increased rearfoot eversion during cross-over running may have been due to the heel being in more inverted position at heel-strike meaning that the heel had to undergo more eversion in order for the foot to be flat on the floor (Williams and Ziff, 1991). In contrast, during wide-base running the heel was in a less inverted position at heel-strike, thus reducing the amount of eversion required to place the foot flat on the floot. It is possible that changes in step width serve to alter rearfoot frontal plane kinematics by inducing changes in the mediolateral component of the ground reaction forces (GRF). During cross-over running the foot and leg are moving in a more medial manner across the body prior to heel-strike, indicating that the centre of gravity (CG) is displacing medially. During stance, this medial displacement of the CG must be reversed which requires an increased lateral GRF. McClay and Cavanagh (1994) reported that during cross-over running a single subject demonstrated a predominantly laterally directed mediolateral GRF, with the lateral impulse making up 97.5% of the total mediolateral impulse. The action of this increased lateral GRF together with the more inverted heel at heel-strike would serve to increase the eversion moment present at the ankle-joint-complex. In wide-base running, medial impulse dominated with 81.5% of the total mediolateral impulse in the same subject (McClay and Cavanagh, 1994). Therefore, together with the less

inverted heel position at heel strike this might reduce the eversion moment occurring at the ankle-joint-complex. In conclusion, although it is known that changes in step width can alter rearfoot frontal plane kinematics during running, it is not known what influence this would have on transverse plane shank kinematics.

3.3.3 Walking versus Running

Typically studies conducted using walking have demonstrated lower values in terms of rearfoot peak and excursion angles compared to studies looking at running. Peak rearfoot eversion was found to vary from 3.8 to 7.3°, and eversion excursion values ranged from 5.2 to 6.9° during walking (Cornwall and McPoil, 2002; Moseley et al., 1996; Woodburn et al., 2002). On the other hand, studies conducted using running report peak rearfoot eversion to be between 11.2 and 12.7 and excursion values that range from 12.7 to 16.4° (McClay and Manal, 1998; Stacoff et al., 2001). A reason for this difference in eversion magnitude between walking and running could be due to higher impact forces having to be absorbed by the foot during running. During walking, vertical peak ground reaction force (GRF) has been found to be approximately 1.0-1.2 BW (body weight) (Chao et al., 1983). In running (jogging) this peak value has been reported to be higher and generally around 2.0–3.0 BW and increases with speed (Cavanagh and Lafortune, 1980). Given that it is widely believed that one of the principal roles of the subtalar joint is to absorb shock during the early part of the stance phase, then it follows that an increased amount of rearfoot eversion would be required to absorb the higher impact forces associated with running. It could be postulated that the increased rearfoot motion during running might also result in increased transverse shank rotation via subtalar joint coupling.

However, a study investigating this relationship in both walking and running has yet to be conducted.

There also appear to be differences in terms of the temporal coupling relationship between the rearfoot and shank in walking and running. During running, both Nigg et al. (1993) and McClay and Manal (1998) have shown that the general pattern of motion was that of rearfoot eversion accompanied by shank internal rotation during the first half of stance, with these motions simply being reversed during the latter half of stance. The evidence indicating there is a similar kinematic coupling relationship during walking is less compelling. While studies tend to agree that the shank internally rotates until approximately 14-21% stance followed by external rotation (Hunt et al., 2001; Leardini et al., 1999), there is no clear consensus on the pattern of rearfoot frontal plane motion. For instance, some research has found that the rearfoot everts until 25-35% stance followed by inversion (Hunt et al., 2001; Liu et al., 1997), while other studies suggest that the rearfoot continues to evert until after 50% stance (Cornwall and McPoil, 2002; Woodburn et al., 2002). These studies suggest that the mechanical coupling between the foot and shank is different during walking and running and thus the coupling relationship is not simply a consequence of the subtalar joint functioning as a mitered hinge. A study confirming this would be of benefit to the scientific literature.

3.3.4 Running Speed

An increase in the velocity of running has been associated with alterations in rearfoot kinematics (Andrew, 1990; Stergiou et al., 1999). Andrew (1990) reported that significantly greater ranges of eversion excursion were evident as running speed was

increased from 3.6 to 4.4 and then to 6.0ms^{-1}. He also found that the time to peak rearfoot eversion occurred earlier at higher running speeds. Stergiou (1999) showed that running speed affects the continuous coupling between rearfoot frontal plane and knee sagittal plane motion across the stance phase. A slower speed resulted in a lower curve correlation value indicating less temporal coupling between the actions of the two joints. This suggests that kinematic coupling rearfoot and shank may also be affected by changes in running speed since the rearfoot and knee are supposedly connected via transverse rotation of the shank (Tiberio, 1987).

3.3.5 Foot Strike Pattern

In a similar manner to step width, mode of gait and running speed, Stacoff et al. (1989) showed that rearfoot kinematics can also be influenced by the position of the foot at touchdown during running. They reported that when using a forefoot touchdown rearfoot eversion excursion was lower in comparison to when a rearfoot touchdown was used. The excursion values were only measured during the first 25% of stance, but it has been stated that peak rearfoot eversion may not be reached until approximately 40% of the stance phase (Hamill et al., 1992).

Foot strike pattern may alter rearfoot kinematics via the interaction between the midtarsal and subtalar joints. It was speculated earlier in this thesis (see section 2.5.5) that subtalar joint pronation allows the midfoot (midtarsal joint) to become more mobile, and subtalar supination serves to lock the midtarsal joint creating a rigid lever out of the foot. If this relationship is robust, then it would be expected that it is reversible. That is a rigid midfoot would be expected to limit subtalar joint pronation, whereas a flexible midfoot would allow more subtalar pronation. During rearfoot

strike running, the midtarsal joint would be flexible at touch-down as subtalar joint pronation occurred during initial loading. However, during a forefoot strike running pattern, the forefoot is the first part of the foot to make contact with the ground. Therefore, at touch-down the foot is in a similar plantarflexed position as it would be during the propulsion phase of stance i.e. the midtarsal joint should be locked so the foot is a rigid lever. If the midtarsal and subtalar joints are indeed interdependent on one another, then it would be expected that the rigid midtarsal joint would serve to decrease the amount of subtalar pronation. It may be that this relationship is not so clear to see in forefoot strike running since after the initial contact of the forefoot, the heel then contacts the ground meaning the foot is no longer in a rigid plantarflexed position. However, by using a condition where the runner keeps their heels off the ground throughout the entire stance phase, it should be possible to simulate the rigid plantarflexed foot position associated with the propulsion phase.

3.4 Including the Midfoot in a Foot-Shank Kinematic Coupling Analysis

It has been stated that motion at the subtalar joint must be transferred via the talus to the tibia. However, the talus also shares an articulation with the navicular (talonavicular joint) and thus the actions of the subtalar and midtarsal joints may be interdependent on one another during gait (Donatelli, 1996). It would therefore, be expected that the distal segments of the foot would show some level of kinematic coupling with the rearfoot. Indeed, during standing movements of the foot and lower leg it has been found that significant amounts of midtarsal joint motion accompany pronation/supination and transverse rotation of the shank (Lundberg, 1989; Nester et al., 2002). A number of studies have now begun to emerge that make use of multi-

segment foot models during walking in a bid to gain a more complete understanding of the foot as a whole (Carson et al., 2001; Hunt et al., 2001; Leardini et al., 1999; Myers et al., 2004; Woodburn et al., 2004).

A five segment foot model was proposed by Leardini et al. (1999) which divided the foot into sections including the shank, rearfoot (calcaneus), midfoot (navicular, cuboid and cuneiforms), 1st metatarsal and the proximal phalanx of the hallux. However, the model involved placing markers on plates which were attached to dorsal aspect of the foot using metallic clamps and tape. Since there are a number of tendons present around the attachment area of the clamps, it is questionable how much motion measured between segments was attributable to motion of the underlying bones as opposed to artefacts due to tendons. It has also been shown that markers mounted on stalks can resonate significantly upon impact with the ground and increase measurement errors (Karlsson and Tranberg, 1999).

A growing number of studies are using a four segment model consisting of the shank, rearfoot (calcaneus), forefoot (metatarsals) and hallux (proximal phalanx) (Carson et al., 2001; Hunt et al., 2001; Myers et al., 2004; Rattanaprasert et al., 1999; Woodburn et al., 2004). In this model, midtarsal joint motion is represented using motion of the forefoot segment relative to the rearfoot. Using such an approach it has even been possible to observe differences between clinical patients when compared to normal controls. For instance, it was reported that patients with tibialis posterior dysfunction had prolonged forefoot dorsiflexion during stance, as well as a significantly more inverted forefoot position after heel-off, when compared to asymptomatic subjects (Rattanaprasert et al., 1999). Similary, Woodburn et al. (2004) found that rheumatoid

arthritis patients had a reduced range of forefoot motion in all three cardinal planes compared to normal healthy subjects. Both the afore mentioned clinical studies also found differences between groups in terms of rearfoot kinematics, signifying the interdependency of the forefoot and rearfoot on each other. To the author's knowledge, however, a comprehensive study determining the kinematic coupling relationship between these two segments has not yet been conducted. Therefore, an investigation into the coupling mechanism present between the forefoot, rearfoot and lower leg is required for a more complete picture of how the foot and leg interact.

3.5 Defining the Problem / Implications for Future Research

The link between foot pronation and shank internal rotation has long been a focus of injury research due to the theory that the two segments are mechanically coupled as a consequence of anatomy at the ankle-joint-complex (Hicks, 1953). It has been suggested that rearfoot frontal plane motion (eversion/inversion) is transferred into transverse tibial rotation (internal/external) via the subtalar joint, which is believed to function as a mitered hinge (Inman et al., 1981). Consequently, abnormal foot movements may alter normal kinematics and kinetics of the lower limb, resulting in increased risk of injury to bone and/or soft tissue structures (James and Jones, 1990; Tiberio, 1987). However, as highlighted by a review of the literature the kinematic relationship between the foot and lower limb remains unclear (DeLeo et al., 2004; Hintermann and Nigg, 1998; Powers et al., 2002), thus warranting further investigation. The equivocal findings of previous research may have been the result several factors including the measures used to assess coupling, the interventions used

to disrupt coupling and the failure to include the distal joints of the foot in the investigations.

Studies have typically examined the mechanical coupling relationship using only kinematic data determined at discrete points in the stance phase, e.g. maximum rearfoot eversion (Nawoczenski et al., 1998; Stacoff et al., 2000a; Williams et al., 2001). In order to gain a more complete understanding of the kinematic coupling between the segments it is necessary to include measures of the continuous coupling throughout the entire stance phase (DeLeo et al., 2004; Hamill et al., 1999). Therefore, kinematic coupling between the foot and lower limb was assessed using both discrete and continuous measures within the context of this thesis.

Experimental manipulations that have been used to investigate the coupling between the foot and lower limb, such as orthotics and shoe alterations (Stacoff et al., 2001; Stacoff et al., 2000b; Williams et al., 2003), may not have induced large enough kinematic alterations in the segments of interest to be able to formulate conclusions regarding the coupling relationship. Gait factors such as step width, mode of gait, running speed and foot-strike pattern, however, have been shown to significantly alter rearfoot frontal plane kinematics. Therefore, the use of manipulating these gait factors to alter rearfoot kinematics is justified. Then by observing the effect that the altered rearfoot kinematics had on the adjacent segments of the forefoot and shank it would be possible to gain further insight into the coupling relationship between the foot and lower leg.

Another confounding factor in studies investigating foot function during gait is the method of using calcaneal eversion and inversion to approximate foot pronation and supination (Edington et al., 1990). However, Lundberg et al. (1989) and Nester et al. (2002) showed that significant amounts of rotation occur at the midtarsal joint, and there is growing evidence that motion at this joint contributes significantly to overall foot motion during walking (Carson et al., 2001; Hunt et al., 2001; Woodburn et al., 2004). Despite this, little is known about how the midtarsal joint influences rearfoot kinematics and thus subtalar joint coupling during gait. It was the primary aim of this thesis to develop further understanding of how motion at the foot is coupled with motion of the lower leg by including the midtarsal joint in the analysis.

The purpose of this thesis was to investigate the association between midtarsal joint motion and the kinematic coupling at the subtalar joint during running. More specifically, to determine whether forefoot motion was coupled to rearfoot motion and thus could influence shank rotation. In order to accomplish this task, it was required that a multi-segment foot model was developed that provided valid kinematic measurements. For this reason, an *in-vitro* study was conducted to assess the validity of the measurement techniques used in the *in-vivo* gait studies. The main focus was to investigate the feasibility of using external skin markers to model the subtalar joint kinematics of the underlying bones. This entailed first determining whether skin mounted markers on the rearfoot and shank produced joint angles similar to the represented underlying bones, the calcaneus and the tibia. Secondly, the validity of using tibiocalcaneal joint rotations to represent the subtalar joint was also tested, since it is often assumed that the talus does not move with respect to the tibia. Along with testing the validity of measurements conducted within the context of the thesis, it was

also deemed necessary to include a section dealing with the reliability of the measurements techniques used. Therefore, the reliability of determining the angular displacements of adjacent segments included in the multi-segment model was assessed.

By conducting experimental manipulations that altered rearfoot motion and then observing the knock-on effect on the adjacent segments of the shank and forefoot, it was possible to deduce how rigidly coupled the segments were at the subtalar and midtarsal joints respectively. The three main gait manipulation studies of the thesis each used a different experimental condition to alter rearfoot kinematics. By then observing how these alterations influenced the adjacent segments, the shank and forefoot, it was possible to examine the degree of kinematic coupling between them. The gait manipulations chosen for variation within this thesis were step width, mode of gait, running speed and foot strike pattern.

Chapter 4 - General Methodology

This chapter describes the general methods that were applied to collect and process the data for the experimental gait studies (chapters 6-9). The methodology concerning the *in-vitro* study examining the validity of measurements conducted using external markers (chapter 5) is contained in the chapter itself, since an entirely different experimental protocol was applied compared to the experimental gait studies. The first section within this chapter (section 4.1) deals with theoretical background concerning both 3-D analyses of human movement and data smoothing (filtering). Section 4.2 then details the exact methodologies that were applied during the data capture and processing of the experimental running/walking studies. Section 4.3 describes the biomechanical model of the foot and lower leg (and calculation of joint angles) that was used in the experimental gait studies of this thesis. The final two sections of this chapter (sections 4.4 and 4.5) present two pilot studies that were conducted to address issues surrounding the general methods utilised within this thesis. The first of these pilot studies (section 4.4) was an investigation to determine the optimum cut-off frequency that was used to smooth the raw kinematic data. The second pilot study (section 4.5) was conducted to determine the accuracy of the measurement/ analysis systems that were used during data capture/ processing, thus validating the results obtained in the experimental chapters.

4.1 Theoretical Background

4.1.1 Three-dimensional Analysis of Human Movement

Bone Position and Orientation Reconstruction from Marker Positions

To quantify three-dimensional angular joint kinematics during gait it is necessary to determine the relative position orientation of adjacent limb segments. In order to

define a segment in three-dimensional space (Global co-ordinate system: GCS) it is necessary to attach an orthogonal right handed Cartesian co-ordinate system (often called the local co-ordinate system: LCS) to the segment of interest. Since the segments are assumed to be a rigid body, if the position and orientation of the LCS is known, then the position of any point on the limb segment is known (Nigg and Herzog, 1999). To define the LCS in the GCS, a minimum of three non-collinear markers must be attached to the segment of interest. One axis is taken as a unit vector in the plane between two of the markers. The second axis is defined using a unit vector orthogonal to the plane. Finally, the third axis is calculated as the cross-product of the first two axes. It should, however, be noted that more than three markers can be used to define the LCS.

Once the LCS has been defined, its position and rotation needs determining with reference to the GCS. This is achieved by determining the cosine of the angle that each unit vector of the LCS (x, y, z) makes with each of the co-ordinate axes of the global system (X, Y, Z). These values are termed direction cosines (Zatsiorsky, 1999) and can be written using a 3 x 3 rotation matrix [R] as follows (equation 4.1):

$$[R]=\begin{bmatrix} \cos_{Xx} & \cos_{Xy} & \cos_{Xz} \\ \cos_{Yx} & \cos_{Yy} & \cos_{Yz} \\ \cos_{Zx} & \cos_{Zy} & \cos_{Zz} \end{bmatrix} \qquad \text{Equation 4.1}$$

where $\cos_{Xy}$ represents the cosine of the angle between the X axis of the global system and the y axis of the local system.

Anatomical and Technical Co-ordinate Systems

The definition of a LCS with respect to the anatomy of the segment is very important. If the joint kinematics are to be described in clinically relevant terms then it necessary

to ensure that each of the segmental axes has some anatomical significance with the underlying bone (e.g. rotation about one of the axes represents sagittal plane motion). Such a co-ordinate system is known as an 'anatomical co-ordinate system.' However, it is not always possible during gait to track markers attached in positions appropriate for the definition of an anatomically significant co-ordinate system. If this is indeed the case then it is necessary to use markers attached to the segment in non-anatomically significant positions (technical markers) and define a local 'technical co-ordinate system.' By performing an anatomical landmark calibration procedure (Cappozzo et al., 1995) it is possible to determine the position of a segmental anatomical landmark in the local technical co-ordinate system. For any position, *P*, of the bone the following relationship holds (equation 4.2):

$$P_G = L_G + [R]P_t \qquad \text{Equation 4.2}$$

where P_G is the position of the anatomical landmark in the GCS, L_G is the location of the origin of the local technical co-ordinate system in the GCS, [R] is the orientation of the local technical co-ordinate system in the GCS, and P_t is the position of the anatomical landmark (any point of the bone) in the local technical co-ordinate system. Following this anatomical landmark calibration procedure, the position of the anatomical landmarks can then be reconstructed in the GCS during gait using the position and orientation local technical co-ordinate system. Thus at any instant in time a number of anatomical landmarks can be reconstructed and used to define the anatomical co-ordinate system of a segment in the GCS. When calculating segmental and joint kinematics it is the local anatomical co-ordinate system that is used.

Clusters of External Markers

The aim of a three dimensional kinematic study of movement is to describe the motion of the underlying bones in a segment. Due to the invasive nature of placing markers directly on the bones external markers are usually placed on the skin of the segment of interest. However, these external markers do not always represent true skeletal locations and these errors can propagate during the calculation of segment and joint kinematics. The differences between external marker positions and the true skeletal locations are referred to as absolute and relative errors (Nigg and Herzog, 1999). Absolute marker error is defined as movement of one specific marker with respect to specific bony landmarks of a segment, whereas relative marker error is defined as the relative movement of two markers with respect to each other. Tranberg and Karlsson (1998) found that markers mounted on the foot and ankle moved between 1.8 and 4.3mm corresponding to the underlying bones. The movement of skin markers relative to the bones has also been demonstrated to influence joint kinematics. For instance, Reinschmidt et al. (1997) found that although external markers and bone mounted markers demonstrated similar tibiocalcaneal rotation curves in terms of shape, the rotations were generally overestimated when using external markers.

One way to minimise the errors caused by skin movement artefacts is to place markers in locations where there is minimal skin displacement relative to the underlying bone during human movement. Markers located directly on the skin above anatomical landmarks such as the greater trochanter, lateral epicondyle of the femur, head of the fibula and lateral malleolus have been reported to undergo large displacements relative to the underlying bony landmark which were roughly

proportional to the angular displacement of the closest joint (Cappozzo et al., 1996). The same authors also found that skin markers located on the lateral portion of the tibia away from the gastrocnemius may exhibit smaller movements. Other investigators have reported that the use of rigid marker attachment frames may serve to improve the representation of bone movement from external markers (Digby et al., 2005; Manal et al., 2000). If the external markers are attached to a rigid shell which is then placed on the segment, the marker cluster will move rigidly together thus eliminating the problem of marker moving relative to one another. However, the rigid plate will still move as one 'unit' relative to the underlying bone and will influence every marker in a uniform way. Consequently, any chance of compensating for the skin movement artefact between bone and skin is lost. In contrast, by using deformable clusters on the skin and in the hypothesis of somewhat uncorrelated local movement of the markers, algorithms may be implemented which compensate for the above mentioned artefacts (Cappozzo et al., 1995). For example, it may be that only one marker in cluster of four is moving in a significantly different manner to the underlying bone. In this case a deformable marker cluster is advantageous since the relative movement between skin markers can be compensated for. This might be performed using a 'least squares' method which can be applied to reduce errors in the position description caused by changes in the relative marker positions due to non-rigid behaviour of the segment (Spoor and Veldpaus, 1980).

Joint kinematics

As mentioned previously, it is possible to describe at any instant of time during movement, the position and orientation in the global co-ordinate system of a local co-ordinate system considered rigid with the bone (Equation 4.1). It was also stated that

it is desirable to use a local co-ordinate system that has some anatomical significance with the underlying bone (anatomical co-ordinate system). If angular joint kinematics are to be investigated then it is necessary to ascertain the orientation of the two adjacent bones, proximal and distal, relative to one another. Thus, the relative orientation between the proximal (R_p) and distal (R_d) anatomical co-ordinate systems needs to be found. This is done by defining the distal co-ordinate system in the proximal co-ordinate system (equation 4.3):

$$R_j = R_p^T R_d \qquad \text{Equation 4.3}$$

where R_j is the joint orientation matrix (orientation matrix of the distal co-ordinate system relative to the proximal co-ordinate system) and R_p^T is the transpose of the proximal orientation matrix (Fioretti et al., 1997). The matrix R_j can be expressed in a similar manner to that of equation 4.1 but this time the proximal co-ordinate system is considered the stationary 'global' co-ordinate system. While the orientation matrix gives a complete description of relative orientation it is not easily interpretable. A number of conventions exist to convert the orientation matrix into more interpretable format. Cardan angles are widely used in biomechanics because they provide a representation of joint orientation analogous to the anatomical representation that both clinicians and researchers use (Fioretti et al., 1997; Nigg and Herzog, 1999). By definition, they are obtained as an ordered sequence of rotations about the three axes of a selected Cartesian co-ordinate system (x,y,z) to obtain the attitude of a second co-ordinate system (X,Y,Z). If the (x,y,z) co-ordinate system is rotated by an angle α about the X (or x) axis then the resulting orientation matrix is (equation 4.4):

$$R_{X,\alpha} = R_{x,\alpha} = R_\alpha = \begin{bmatrix} 1 & 0 & 0 \\ 0 & \cos\alpha & -\sin\alpha \\ 0 & \sin\alpha & \cos\alpha \end{bmatrix} \qquad \text{Equation 4.4}$$

Similarly, if the co-ordinate system is then rotated by an angle β about the Y (or y) axis then the resulting orientation matrix would be as follows (equation 4.5):

$$R_{Y,\beta} = R_{y,\beta} = R_{\beta} = \begin{bmatrix} \cos\beta & 0 & \sin\beta \\ 0 & 1 & 0 \\ -\sin\beta & 0 & \cos\beta \end{bmatrix} \quad \text{Equation 4.5}$$

Finally, the orientation matrix of a rotation of angle γ about the Z (or z) axis is given by (equation 4.6):

$$R_{Z,\gamma} = R_{z,\gamma} = R_{\gamma} = \begin{bmatrix} \cos\gamma & -\sin\gamma & 0 \\ \sin\gamma & \cos\gamma & 0 \\ 0 & 0 & 1 \end{bmatrix} \quad \text{Equation 4.6}$$

Since matrix multiplication is not commutative, the final parametric rotation matrix depends on the order in which axis rotations occur. In other words, Cardan angles are sequence dependant and thought must be paid to the order in which basic rotations are assumed to be performed. The most widely used convention was proposed by Grood and Suntay (1983) and has been recommended as the International Society of Biomechanics (ISB) standard (Wu and Cavanagh, 1995). The first rotation (γ) is about the Z axis (medio-lateral) of the proximal segment (or, equivalently, about the z axis of the distal co-ordinate system). The second rotation (α) is about the x axis (floating axis) of the distal segment in its new orientation following the first rotation. Finally, the third rotation (β) is about the y axis (longitudinal) of the distal segment in the new orientation following the first and second rotations. Hence, the final joint orientation matrix (R_j) is given by the following product of the axis rotation matrices (equation 4.7):

$$R_j = R_{Z,\gamma} R_{x,\alpha} R_{y,\beta} = R_{\gamma} R_{\alpha} R_{\beta} =$$

$$\begin{bmatrix} \cos\gamma\cos\beta - \sin\gamma\sin\alpha\sin\beta & -\sin\gamma\cos\alpha & \cos\alpha\sin\beta + \sin\gamma\sin\alpha\cos\beta \\ \sin\gamma\cos\beta + \cos\gamma\sin\alpha\sin\beta & \cos\gamma\cos\alpha & \sin\gamma\sin\beta - \cos\gamma\sin\alpha\cos\beta \\ -\cos\alpha\sin\beta & \sin\alpha & \cos\alpha\cos\beta \end{bmatrix} \quad \text{Equation 4.7}$$

Therefore, the values of α, β, and γ will give the angular joint displacement for rotations in the frontal, transverse and sagittal planes respectively.

4.1.2 Filtering of Kinematic Data

Raw co-ordinate data may contain noise from sources such as the optoelectronic device. Random errors, or noise, are the components of the signal which are not due to the motion measured. It is therefore desirable to reduce this noise, which is usually of high frequency (Winter, 2005). This removal of the high frequency components from the signal can be achieved using a process known as smoothing, or low pass filtering. Filtering of the data is aimed at selectively rejecting or attenuating certain frequencies of the raw signal. This is often achieved using a low-pass filter with a cut-off frequency, above which the signals are attenuated, thus reducing the noise component of the signal.

However, even though the signal is assumed to occupy the lower end of the frequency spectrum with noise occupying the higher frequency, the two components overlap (Winter, 2005). The cut-off frequency is usually placed within this area of overlap and can result in slight distortion of the signal. Therefore, a compromise has to be made when selecting the appropriate cut-off frequency, since a value set too low will reduce noise drastically but at the expense of increased signal distortion, whereas a value set too high will allow too much noise to pass. There are several ways to choose the optimum cut-off frequency but one of the most common is to perform a residual analysis of the difference between filtered and unfiltered signals over a large range of cut-off frequencies (Winter, 2005).

4.2 Laboratory Setup and Data Collection

4.2.1 Camera Setup

A seven camera ProReflex® (Qualisys Medical AB, Sweden) semi-automatic motion analysis system was used to acquire all 3-D marker data. The cameras were mounted on tripods at various heights and positioned in an 'umbrella' formation (Nigg and Herzog, 1999) around a force platform (Kistler, Switzerland) mounted in the middle of a 14m runway (Figure 4.1). Pilot testing was conducted to determine the optimum location for the cameras by getting subjects to walk/run through the capture volume using the pre-selected experimental marker setup (section 4.3.1).

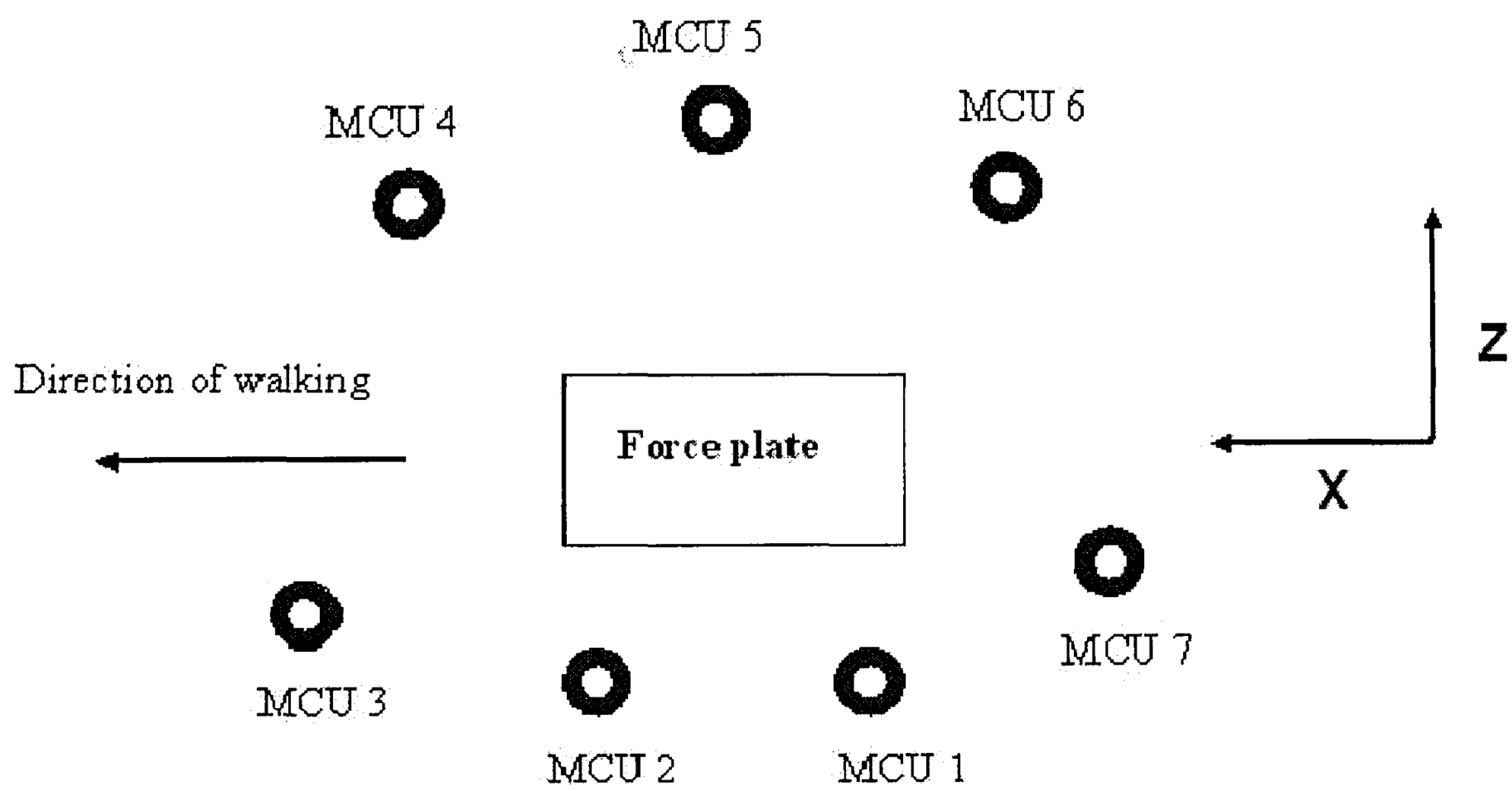

Figure 4.1. Schematic of laboratory setup and global co-ordinate system (GCS).

4.2.2 Calibration of 3-D Camera System

Prior to each testing session, the capture volume was calibrated using the Wand Kit 750mm (Qualisys Medical AB, Sweden) supplied with the cameras. This process involved the placement of the reference object (L frame) in the capture volume to

define the orientation and origin of the global co-ordinate system (GCS). This reference object consisted of an L frame with a long and short arm perpendicular to one another. Four spherical reflective markers were positioned on the frame: one on the corner (origin); one along the short arm (200mm from the origin); two along the long arm (at 550 and 770mm from the origin). The L frame was placed in the centre of the force plate with the long arm facing in the direction of walking/running and was used to define the origin and orientation of the GCS (section 4.3.3). A calibration wand (Qualisys Medical AB, Sweden) consisting of two markers located a fixed known distance from one another (750mm) was then moved through the measurement volume in as many orientations as possible (to assure all axes were properly scaled) for a duration of 30 seconds. This was done by holding the wand in one hand and waving it round-and-round and from side-to-side as the investigator walked through the volumetric space above the force plate. A calibration was deemed successful when both the average residual for every camera and the standard deviation of the wand length were less than 1.0mm. The volume calibrated for data capture was of the following dimensions: height 1.2m; length (direction of gait) 2.2m; width 2.0m.

4.2.3 Data Collection

Retroreflective markers were attached to subjects (section 4.3.1) who then walked/ ran through the data capture volume in the direction of the X axis of the GCS (Figure 4.1). Three-dimensional co-ordinate data for the markers was captured by the ProReflex cameras using a sample frequency of 240Hz. Vertical ground reaction force was collected by the force plate at a sampling frequency of 960Hz and was time synchronised with the marker trajectory data using Qualisys Track Manager (Qualisys Medical AB, Sweden). A static trial was also captured while the subjects assumed a

standardised standing posture (for a duration of three seconds) with the heel centres 0.18m apart and the long axes of the feet (heel to first metatarsal head) at an angle of 11.6° to each another. This position was chosen as it represents the average preferred standing foot position (McIlroy and Maki, 1997).

4.2.4 Data Processing

The x, y, z co-ordinates of each reflective marker were calculated from the two-dimensional camera images using direct linear transformation (Abdel-Aziz and Karara, 1971). In accordance with the requirements of DLT, the camera setup ensured that each marker could be viewed by a least two cameras (but preferably three) at all times during the stance phase of walking (and 20 frames prior to and after the stance phase). A trial was only accepted when the reconstruction residuals of all the marker positions were less than 2mm throughout the capture period defined above. This criteria was established to prevent the erratic 'jumping' of marker position due to dramatic changes in the residual. Careful attention was also applied to the tracking parameters within the software (Qualisys Track Manager, Qualisys Medical AB, Sweden) to reduce the effects of erratic marker movements due to residual changes. In addition, where incomplete marker trajectories were present it was first attempted to alter the tracking parameters within the software to complete the trajectory. Where incomplete paths were still present, they were completed by Qualisys Track Manager using a NURBS interpolation to fill in the missing x, y, z co-ordinate points. This process, however, was never conducted for more than 9 consecutive frames or the trial was discarded. The marker trajectories were individually labelled and exported for the time period spanning from 20 frames prior to touchdown until 20 frames after toe-off. The marker trajectories were then smoothed using a fourth-order Butterworth

filter with a cut-off frequency of 12Hz (cut-off value determined by residual analysis: see section 4.4 for details).

Vertical ground reaction force data was also exported for the same time period as the marker trajectory data. Vertical ground reaction force (F_z) was used to identify the stance phase of the gait cycle. The beginning of the stance phase (touchdown) was defined as the first frame where F_z was consistently greater than 20N with the end of stance (toe-off) being the first frame where F_z dropped consistently below 20N. The value of 20N was considered to be a sufficient threshold in order to determine whether the subject had landed on, or left the plate. To enable a kinematic comparison between experimental conditions and subjects, it was necessary to time-normalise the stance phase. Therefore, the stance phase for every trial was normalised to 100 data points using a cubic spline function. The processed marker trajectory data was used to calculate joint angles which are dealt with in the following section concerning the biomechanical modeling.

4.3 Biomechanical Modelling of the Foot and Lower Limb

4.3.1 Marker Setup

Markers were attached to the skin to represent the motion of the underlying bones. These markers were retroreflective spheres of 7mm diameter and were attached to the skin using double sided sticky tape. In addition, Mtac pre wrap adherent (Mueller Sports, USA) was applied to skin prior to marker application to ensure the markers stayed in place during data capture. Eighteen markers were applied to the foot and lower leg of the right limb (see Figure 4.2 and Table 4.1 for details). Some of these

markers were positioned on the skin approximating an anatomical landmark (anatomical marker) whereas some were placed in a location that had no anatomical relevance (technical marker). Anatomical landmarks were found using palpation and then marked with a pen allowing easier and more accurate placement of the markers. The markers were then used to either define segmental anatomical co-ordinate systems (a) and/or technical co-ordinate systems (t) (Table 4.1).

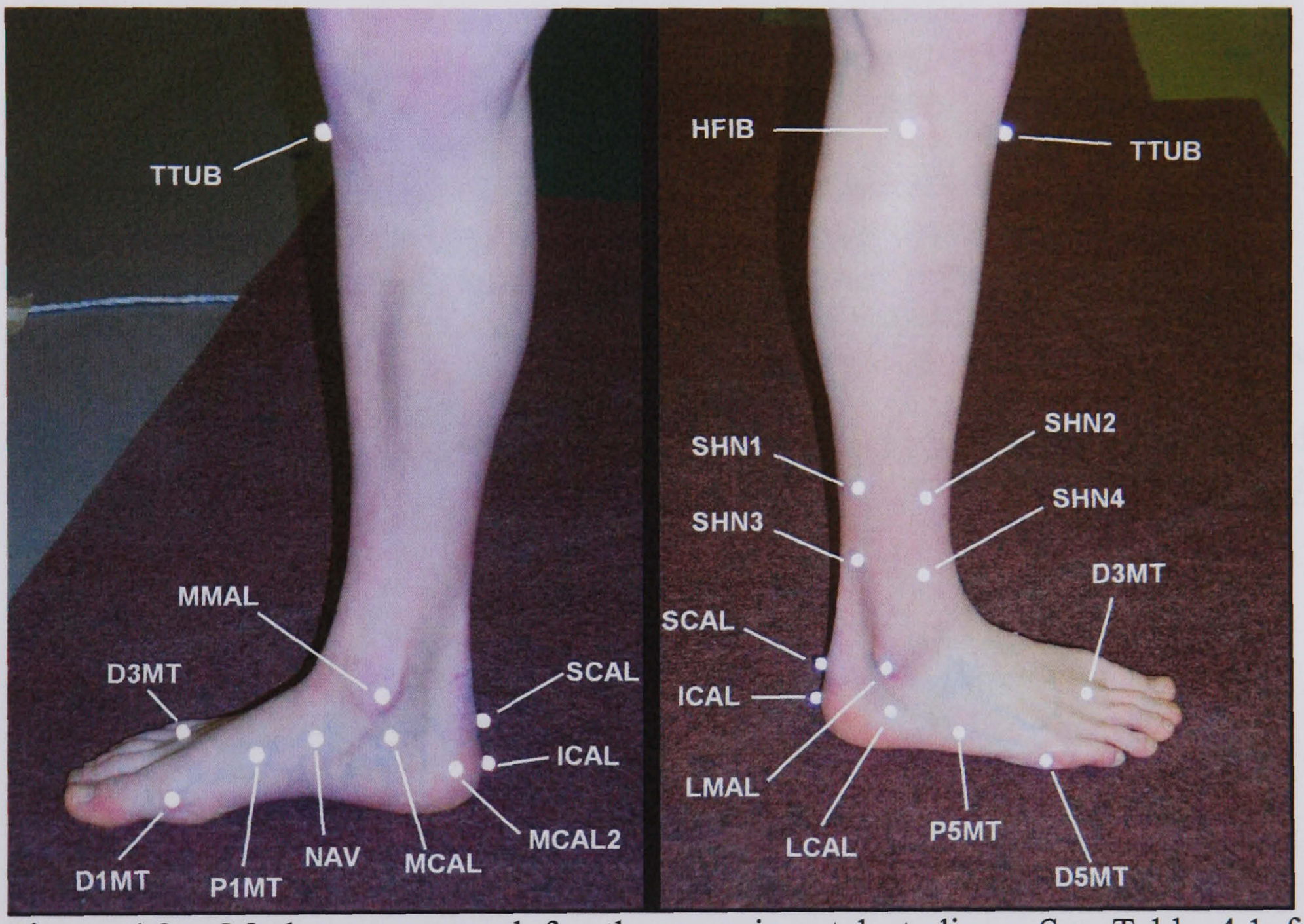

Figure 4.2. Marker setup used for the experimental studies. See Table 4.1 for definition/location of the markers.

Table 4.1. Location of external skin markers. *Markers with an (a) placed next to them were used to define a segmental anatomical co-ordinate system. **Markers with a (t) placed alongside were used to define a segmental technical co-ordinate system. ***Markers with both an (a) and (t) alongside were used in the definition of both anatomical and technical co-ordinate systems.

Marker		**Location**
HFIB	*(a)	Most lateral projection of the Head of Fibula
TTUB	*(a)	Most anterior prominence of the Tibial Tuberosity
SHN1	**(t)	Lateral aspect of the shank
SHN2	**(t)	Lateral aspect of the shank
SHN3	**(t)	Lateral aspect of the shank
SHN4	**(t)	Lateral aspect of the shank
LMAL	*(a)	Most lateral projection of the Lateral Malleolus
MMAL	*(a)	Most medial projection of the Medial Malleolus
SCAL	***(a),(t)	Superior Calcaneal posterior surface (on bisection line)
ICAL	*(a)	Inferior Calcaneal posterior surface (on bisection line)
LCAL	***(a),(t)	Lateral aspect of the Peroneal Tubercle
MCAL2	**(t)	Medial aspect of the calcaneus
MCAL	*(a)	Most medial projection of the Sustentaculum Tali
NAV		Most lateral projection of the Tuberosity of the Navicular
P1MT	*(a)	Most medial projection of the base of the first metatarsal
D1MT	***(a), (t)	Most medial projection of the head of the first metatarsal
D3MT		Midway between the heads of the second/third metatarsal heads
D5MT	***(a),(t)	Most lateral projection of the head of the fifth metatarsal head
P5MT	***(a),(t)	Most lateral projection of the base of the fifth metatarsal head

4.3.2 The Segmental Models

The shank and foot complex was represented by three rigid segments (Figure 4.3):

1) Shank (including tibia and fibula bones),
2) Rearfoot (calcaneus)
3) Forefoot (five metatarsals).

Each segment was assumed to be rigid and was identified using an embedded anatomical cartesian co-ordinate system based on anatomical landmarks (Cappozzo et al., 1995). The anatomical co-ordinate system for each segment was based on markers placed at specific anatomical landmarks during the capture of the static standardised reference trial (section 4.2.3). All the segmental models were created using Visual3D

software (C-motion, USA). Subtalar joint motion was represented by relative motion between the rearfoot and shank in the frontal and transverse plane. The midtarsal joint was modelled as motion of the forefoot relative to the rearfoot.

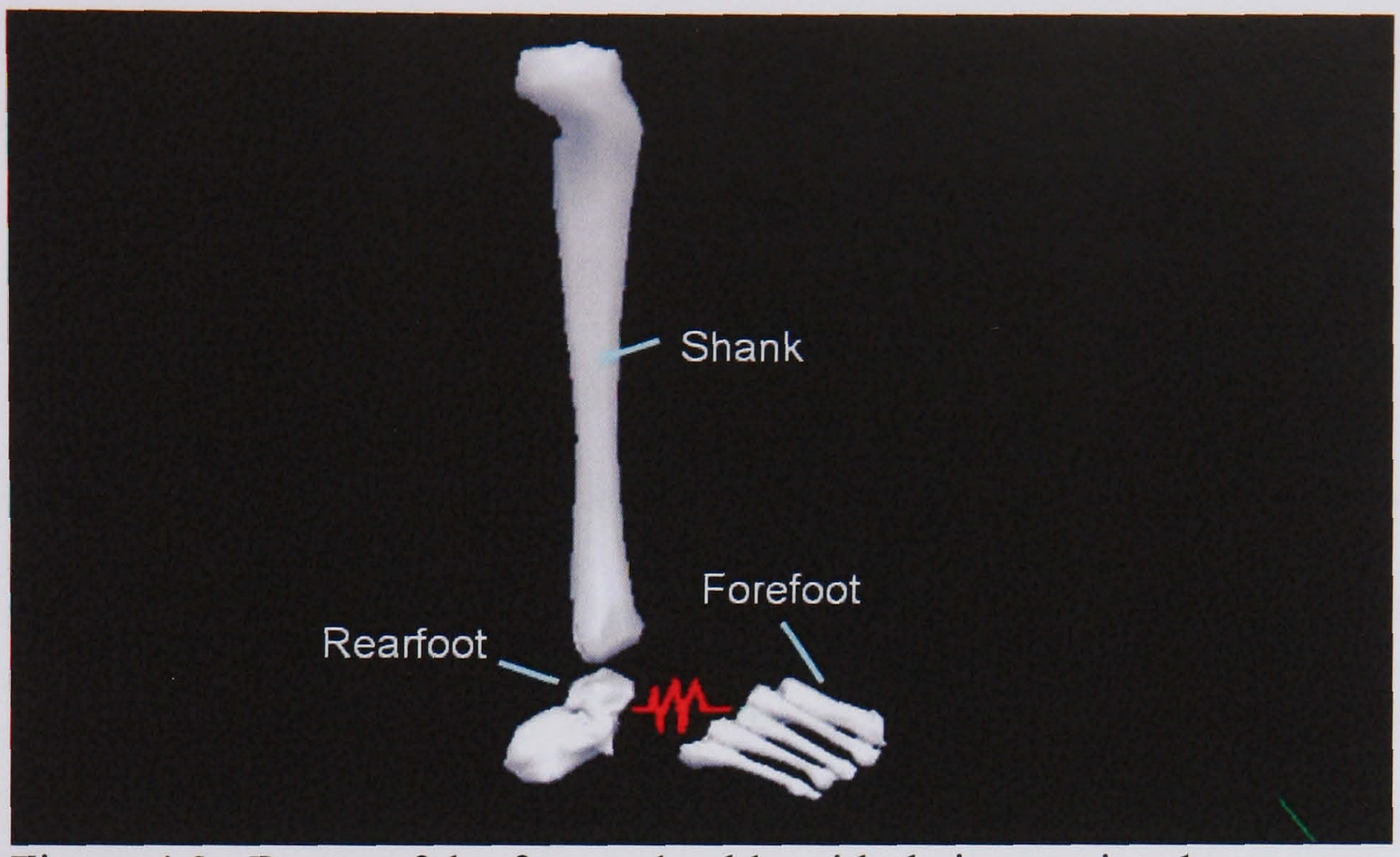

Figure 4.3. Bones of the foot and ankle with their associated segment.

4.3.3 The Global Co-ordinate System

The global (or laboratory) co-ordinate system was defined as a right hand cartesian system. The X axis was chosen to coincide with the direction of progression in which subjects walked/ran through the data capture volume. The Y axis was orthogonal to the floor with its positive direction pointing upwards. The Z axis was the cross-product of X and Y with the positive direction pointing laterally away from the subject line of progression during gait.

4.3.4 Shank Co-ordinate System

The shank segment was assumed to represent the motion of the underlying tibia. The shank anatomical co-ordinate system was defined using skin markers placed on the tibial tuberosity (TTUB), head of fibula (HFIB), medial malleolus (MMAL) and the

lateral malleolus (LMAL) (Figure 4.4). The origin was located at the midpoint between the malleoli. The HFIB, MMAL and LMAL defined the frontal plane from which the antero-posterior axis (x) was orthogonal with its positive direction forwards. A quasi-sagittal plane, orthogonal to the frontal plane, was defined by TTUB and the midpoint between the two malleoli (LMAL, MMAL). The vertical axis (y) was defined by the intersection between the above-mentioned planes with its positive direction proximal (Cappozzo et al., 1995). The medio-lateral axis (z) was the cross-product of x and y with its positive direction lateral (on the right limb). The markers SHN1, SHN2, SHN3 and SHN4 were placed on the distal lateral aspect of the shank so they did not lie on either the tibialis anterior or triceps surae muscle groups. These markers were chosen as technical markers to track the motion of the shank segment during the walking trials rather than use the markers placed on the bony anatomical landmarks (HFIB, TTUB, LMAL, MMAL). This was due to the large skin artifact movement associated with the bony anatomical landmarks of this segment (Cappozzo et al., 1996).

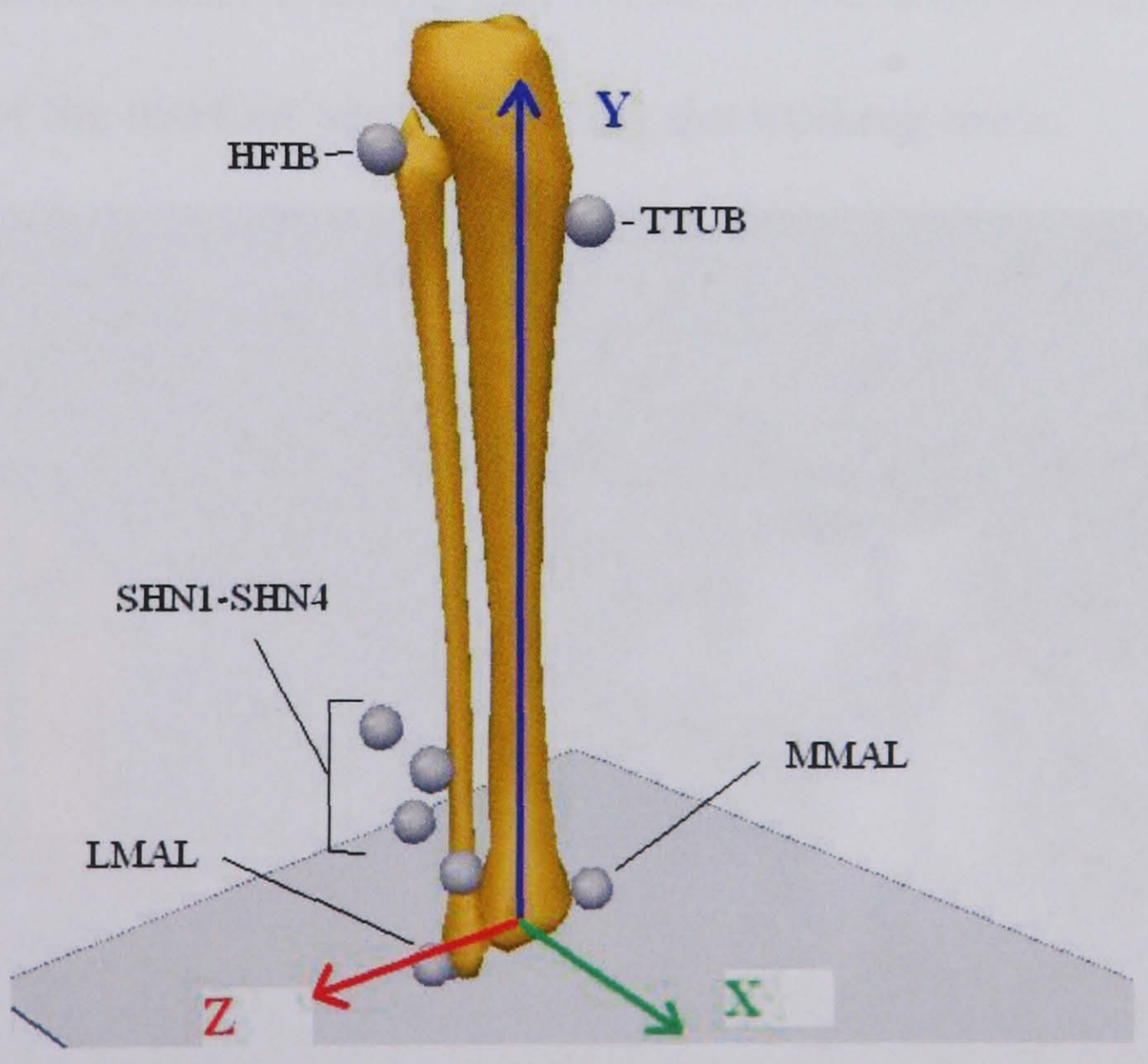

Figure 4.4. Shank anatomical co-ordinate system with associated segmental markers.

4.3.5 Rearfoot Co-ordinate System

This was based on the model by Carson et al. (2001) but was adapted since it was found during pilot testing that markers mounted on a wand attached to the calcaneus underwent too much vibration on impact during running. For this reason the rearfoot anatomical co-ordinate system was defined using skin markers placed directly on the calcaneus. A posterior heel bisection line was made along which markers were placed in a proximal (SCAL) and distal (ICAL) position. Markers were also located on the sustentaculum tali (MCAL) and peroneal tubercle (LCAL). The origin of the axes system was taken as SCAL. The antero-posterior axis (x) joined the origin with the midpoint between MCAL and LCAL with its positive direction anterior (Figure 4.5a). This axis was adjusted to be parallel to the floor to correct for the calcaneal pitch (orientation of the calcaneus in the sagittal plane). The sagittal plane was defined by SCAL, ICAL and the midpoint between MCAL and SCAL (Figure 4.5b). The medio-lateral axis (z) was orthogonal to the sagittal plane with its positive direction lateral. The cross product of z and x gave the vertical axis (y) with its positive direction proximal. The markers LCAL, SCAL and MCAL2 were used as technical markers to track the motion of the rearfoot segment during the walking trials.

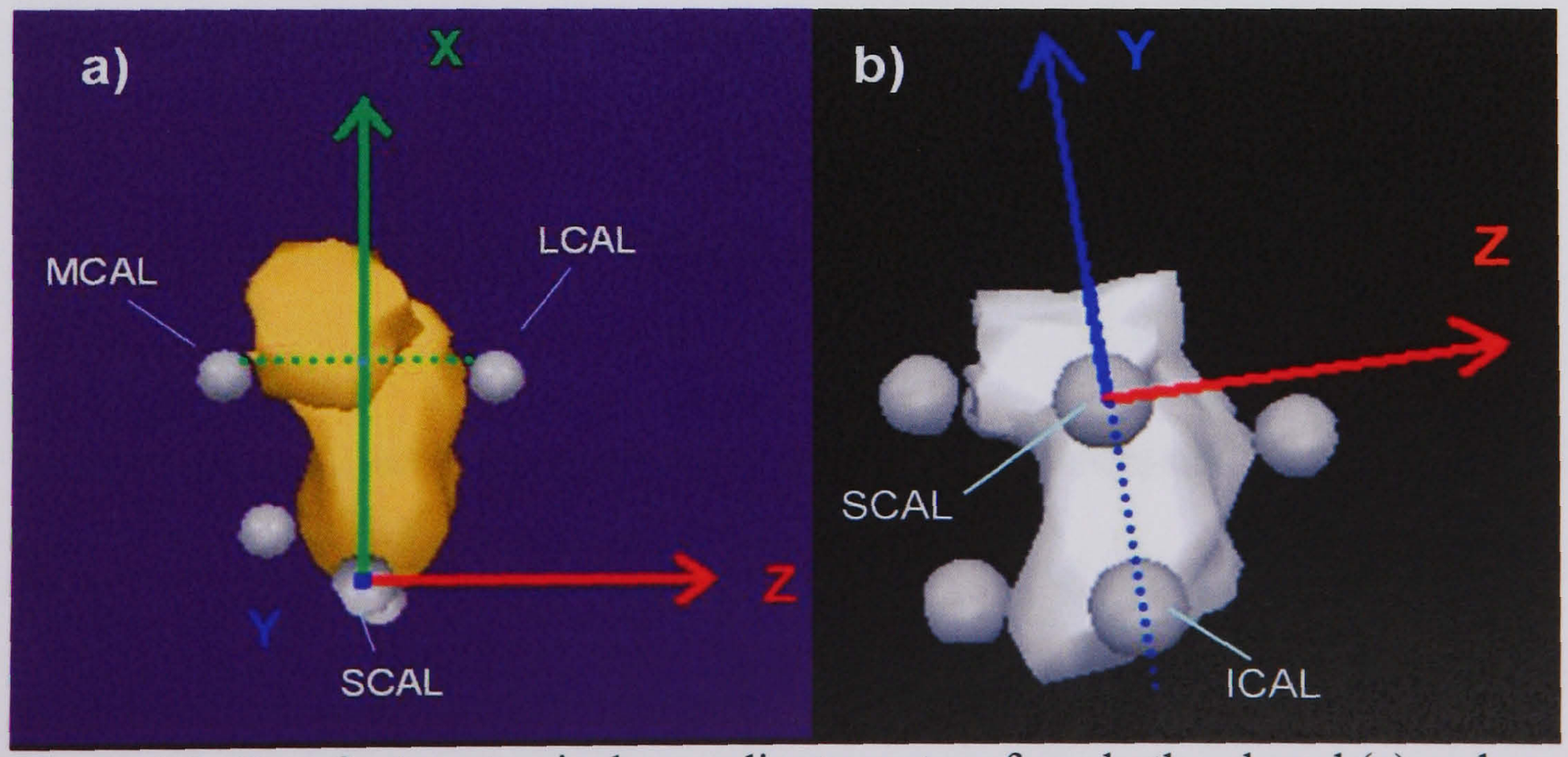

Figure 4.5. Rearfoot anatomical co-ordinate system from both a dorsal (a) and posterior (b) view.

4.3.6 Forefoot Co-ordinate System

The definition of the forefoot anatomical co-ordinate system was determined using markers placed on the base and head of both the first (P1MT and D1MT respectively) and fifth (P5MT and D5MT respectively) metatarsals (Figure 4.6). The origin for this frame was located at the midpoint between P1MT and P5MT. The vertical axis (y) was perpendicular to the floor with its positive direction upwards. The antero-posterior axis (x) ran parallel with the floor from the origin through the midpoint between D1MT and D5MT with its positive direction anterior. The medio-lateral axis (z) was the cross-product of x and y with the lateral direction being positive.

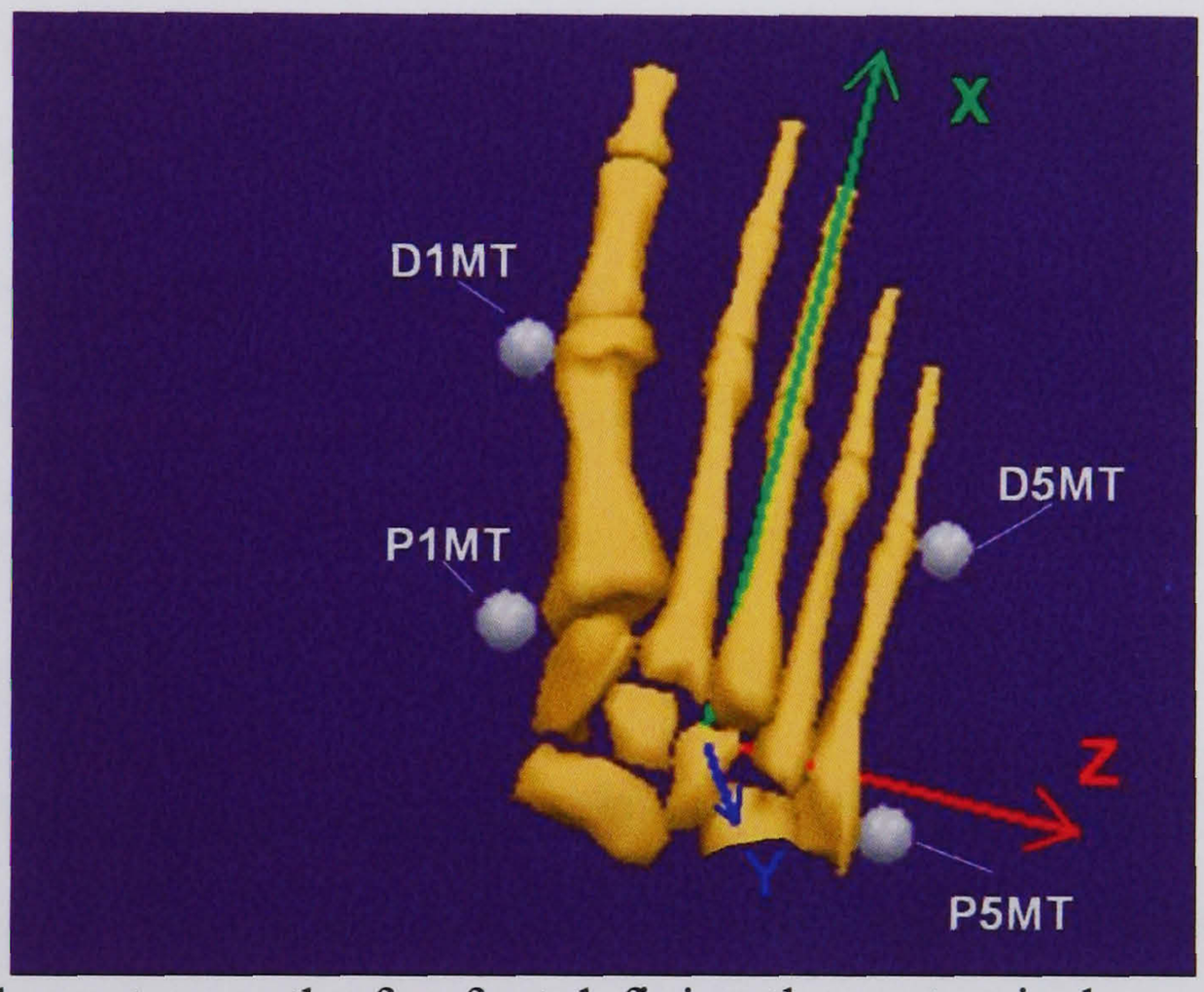

Figure 4.6. Marker setup on the forefoot defining the anatomical co-ordinate system.

4.3.7 Reconstructing Anatomical Landmarks in the Technical Co-ordinate System

By performing an anatomical landmark calibration procedure (Cappozzo et al., 1995) during the static trial it was possible to determine the position of segmental anatomical landmarks within the local technical co-ordinate system. By using equation 4.2 (section 4.1.1) it was then possible to reconstruct the position of the

anatomical landmarks using the position and orientation of the technical co-ordinate system during the subsequent running trials. This calibration procedure was carried out with the aid of Visual3D software (C-motion, USA). Due to the deformable nature of the technical co-ordinate system, a least squares algorithm was applied to reduce errors caused by the non-rigid behaviour of the marker cluster (Spoor and Veldpaus, 1980). This function was performed with the aid of Visual3D software (C-motion, USA).

4.3.8 Calculation of Three-Dimensional Joint Angles

Three-dimensional rotations between the segments were determined using the relative orientation of the distal segment relative to the proximal segment (using Visual3D software, C-motion, USA). Cardan angles were used to rotate the distal segment with respect to the proximal segment (equation 4.7; section 4.1.4) with the order of rotations being sagittal, frontal and then transverse plane of motion (*zxy*). This cardan sequence was selected to be equivalent to the joint co-ordinate system (Cole et al., 1993) recommended by the International Society of Biomechanics (Wu and Cavanagh, 1995). This enabled the interpretation of rearfoot motion in clinical terms of dorsiflexion-plantarflexion, inversion-eversion and shank external-internal rotation (equivalent to rearfoot adduction-abduction). Forefoot motion was interpreted in a similar manner using dorsiflexion-plantarflexion, inversion-eversion and adduction-adduction. The directions of dorsiflexion, inversion and adduction (external rotation) were defined as positive. All joint angles during gait were referenced relative to the standardised standing posture (section 4.2.3).

4.4 Determining the Cut-off Frequency of the Butterworth Filter

4.4.1 Introduction

Raw marker co-ordinate data was filtered using a fourth-order Butterworth filter with a cut-off frequency of 12Hz (section 4.1.2). The cut-off frequency is typically determined using residual analysis (Winter, 2005). Therefore, pilot testing was conducted to determine the optimum cut-off frequency for filtering the marker co-ordinate data collected within the context of this thesis.

4.4.2 Methods

Two subjects performed one running trial at a self selected jogging speed. Markers were attached (section 4.3.1) and co-ordinate data was captured using seven ProReflex cameras (section 4.2). The raw data of a period from 20 frames prior to touchtown until 20 frames after toe-off was exported for residual analysis on the x, y and z co-ordinates of markers D1MT, SCAL and SHN1 (2 subjects x 2 trials x 3 markers x 3 co-ordinate directions = total of 36 analyses). These markers were selected so that a single marker from each segment (forefoot, rearfoot and shank) was represented. The residual was calculated for each cut-off frequency (up to 30Hz) for a signal of N sample points in time as follows (Winter, 2005):

$$R(f_c) = \sqrt{\frac{1}{N}\sum_{i=1}^{N}\left(X_i - \hat{X}_i\right)^2} \qquad \text{Equation 4.8}$$

where X_i is the raw data at *i*th sample and $\hat{X}_i$ is the filtered data at the *i*th sample. For each analysis the residual was plotted against frequency (Figure 4.7).

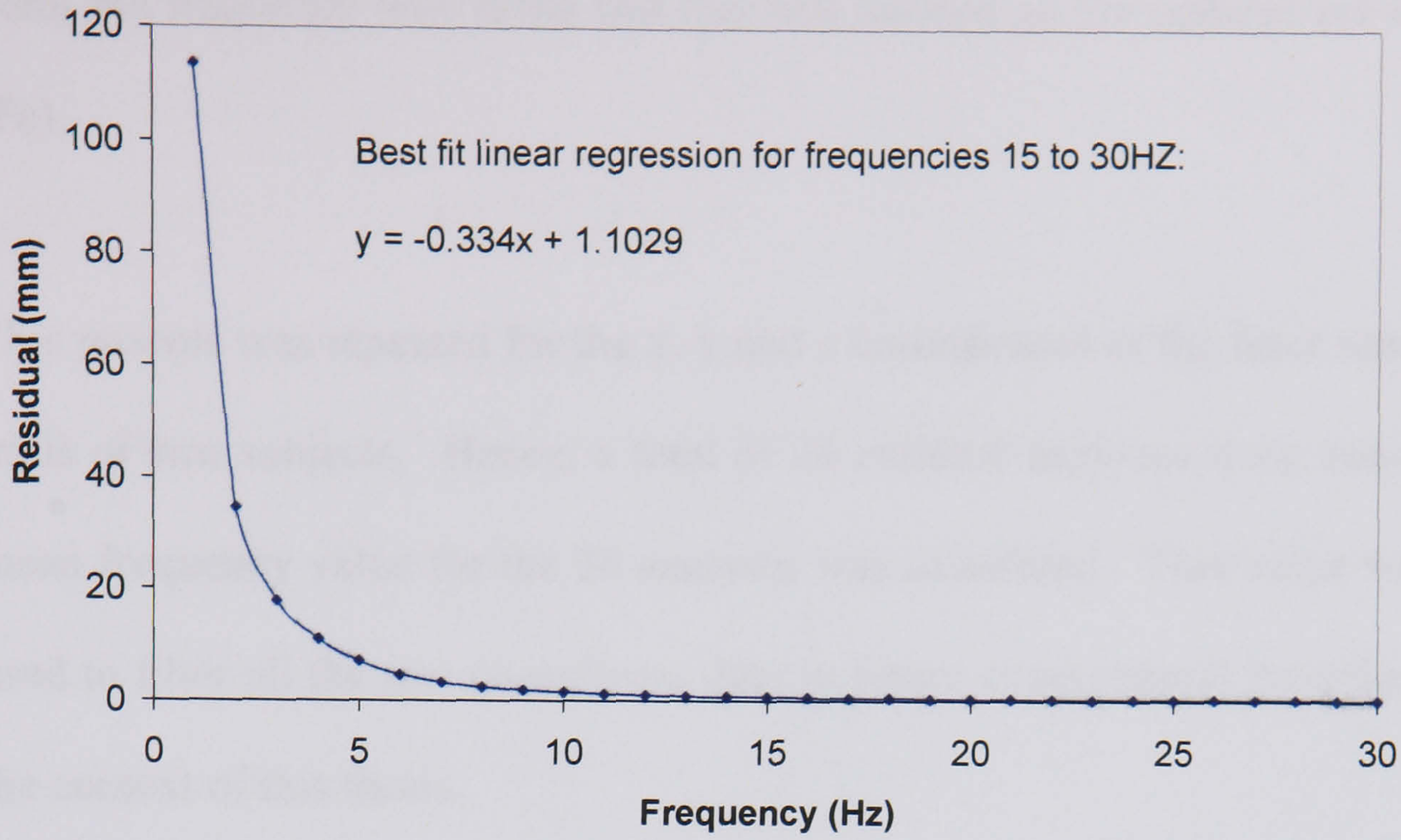

Figure 4.7. Sample plot of the residual versus frequency. The example shown is for the *y* direction displacement data of D1MT in one trial of one subject.

If the data contained only random noise then the residual plot would be a straight line. It can be seen that at the higher frequencies which are associated with noise, the line is indeed approximately linear in nature (Figure 4.7). However, since the data contained both true signal and noise, the residual increased exponentially at lower frequencies due to the increased signal distortion taking place as the cut-off frequency was reduced. Choosing where the cut-off frequency will fall is always a compromise between signal distortion (lower frequencies) and noise (higher frequencies). In this case it was decided that the cut-off frequency would be selected so that signal distortion and noise were equal. Therefore, a best fit linear regression for frequencies between 15 and 30Hz was calculated for the residual-frequency plot since it was deemed that the line was approximately linear at this point, thus contained only noise. Therefore, the intercept of this linear regression represented the noise content of the signal. Then a line was projected horizontally from the intercept point on the vertical axis to intersect with the residual-frequency plot (Figure 4.8). At the intersection

point the frequency was noted and this was defined as the optimal cut-off frequency (Fc).

This process was repeated for the x, y and z co-ordinates of the three markers for two trials of two subjects. Hence, a total of 36 residual analyses were undertaken. The mean frequency value for the 36 analyses was calculated. This value was to be later used to filter all the raw co-ordinate data in future experimental investigations within the context of this thesis.

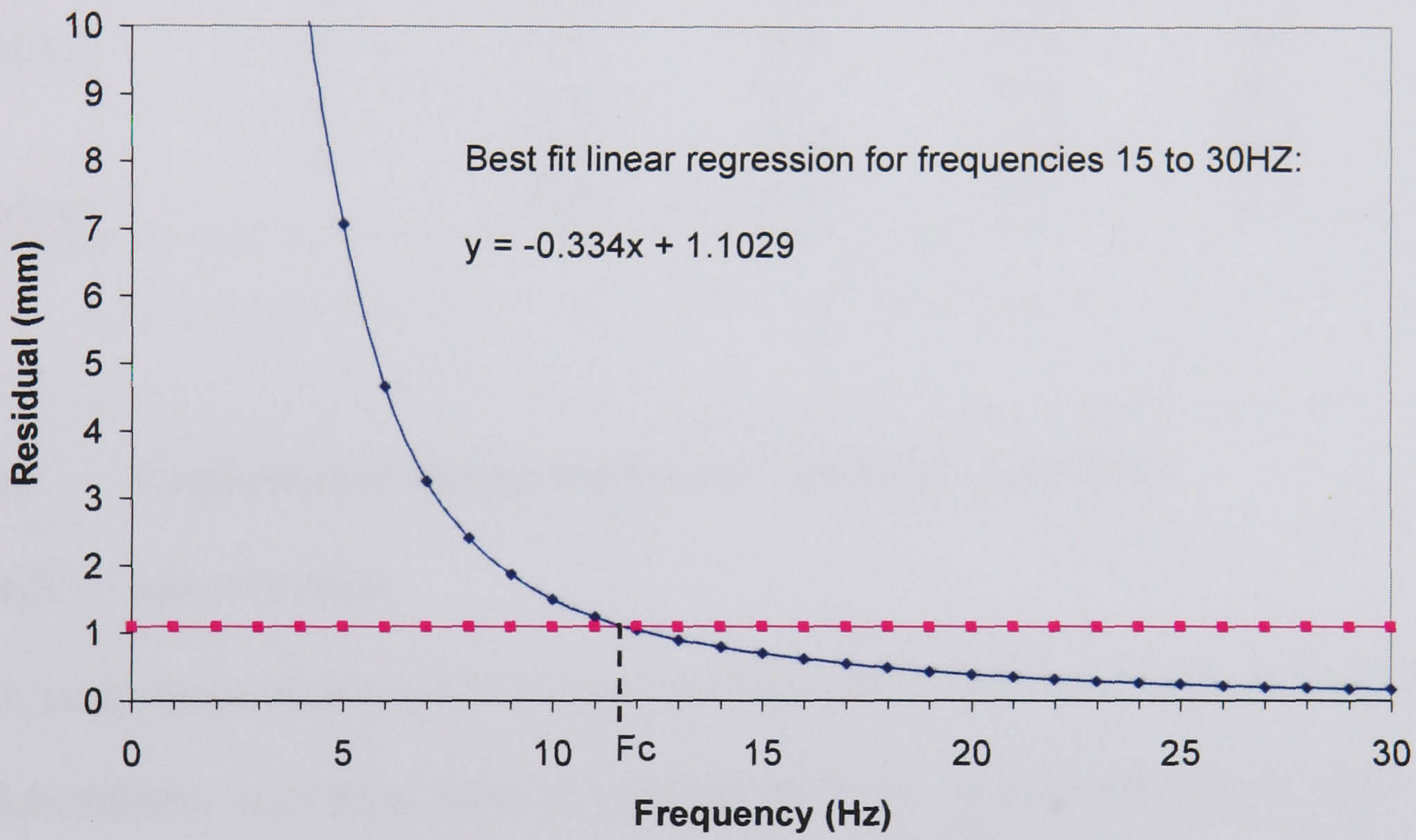

Figure 4.8. Residual plot indicating the chosen cut-off frequency. The cut-off frequency (Fc) was defined as the frequency where the horizontal projection intersected the residual-frequency plot.

4.4.3 Results and Discussion: Residual Analysis

The results of the residual analysis are presented in Table 4.2. The mean value for all the cut-off frequency was 12.1Hz. The values of the cut-off frequencies ranged from 10.6 to 13.5Hz. It was also noted that the three markers, each representing a different segment had similar cut-offs as determined by the residual analysis. Thus it was

concluded that a Butterworth fourth-order low-pass filter with a cut-off frequency of 12Hz would be suitable to smooth the marker raw co-ordinate data in the experimental studies within this thesis.

Table 4.2. Cut-off frequencies determined from residual analysis.

Marker		Subject A		Subject B		Mean
		Trial 1	Trial 2	Trial 1	Trial 2	
D1MT	x	12.4	12.3	11.4	11.3	11.9
	y	13.0	13.0	11.7	12.4	12.5
	z	11.4	11.9	11.1	10.6	11.3
SCAL	x	12.3	12.4	12.3	11.9	12.2
	y	13.2	13.0	12.3	12.5	12.8
	z	12.5	11.4	11.9	11.6	11.9
SHN1	x	11.6	11.4	11.2	11.7	11.5
	y	13.5	13.1	11.9	12.3	12.7
	z	12.2	12.6	11.7	12.7	12.3
Mean		12.5	12.3	11.7	11.9	**12.1**

4.5 Validation of Measurement and Analysis Equipment

4.5.1 Introduction

A large range of automatic tracking systems and analysis software are available to gait laboratories and these may be configured in an infinite manner of ways. For this reason, it is essential that the accuracy of each particular measurement/ analysis system is assessed with the setup identical to that used to capture data during gait (Myers et al., 2004). Both Hunt et al. (2001) and Liu et al. (1997) included a test for static accuracy but did not test for accuracy during dynamic movements when attempting to validate their measurement systems used for gait analyses. Since gait is a dynamic activity it would be advantageous to calculate the system accuracy during some form of dynamic test. Thus the aim of this investigation was to quantify the accuracy of the camera system and analysis software when used to determine both static and dynamic segmental kinematics.

4.5.2 Methods

The seven ProReflex cameras (Qualisys, Sweden) were arranged around the force plate (Kistler, Switzerland) in manner identical to the setup used for future gait analysis experiments. A calibration was performed prior to data capture using an L frame and wand kit (see section 4.2.2). Reconstruction residuals were reported to be less than 0.7mm. The accuracy of the angles obtained by the ProReflex/ Visual3D analysis system were assessed by comparing them with known angles determined using a potractor. This investigation was conducted in two parts: (a) static angular measures and (b) dynamic measures.

a) Static Angular Testing: A custom built device was used to assess the accuracy of the tracking system (Figure 4.9). The device consisted of a proximal and distal segment modelled to simulate the human shank and rearfoot. The distal segment remained stationary in the laboratory whilst the proximal segment could be rotated relative to the distal segment and the magnitudes of these rotations was measured using protractors mounted on the device. In the sagittal plane, a static reference trial was taken with the segments aligned with one another (Figure 4.9a). The proximal segment was then rotated 30° in each direction of the sagittal plane to simulate dorsiflexion and plantarflexion (Figures 4.9b and 4.9c). The same protocol was then applied to angular rotations in the frontal and transverse planes with all angles being referenced relative to a reference static trial with the segments aligned. Marker clusters placed on the segments were used to determine the angle between segments using the camera/ processing system. By rotating the proximal segment a known amount using the potractors, it was possible to determine the accuracy of the tracking

system / analysis software used to calculate the joint angles by comparing the calculated values with the actual values. The absolute error was presented as the difference between the angle measured by the protractor (actual) and the angle calculated using the cameras/ software (computed).

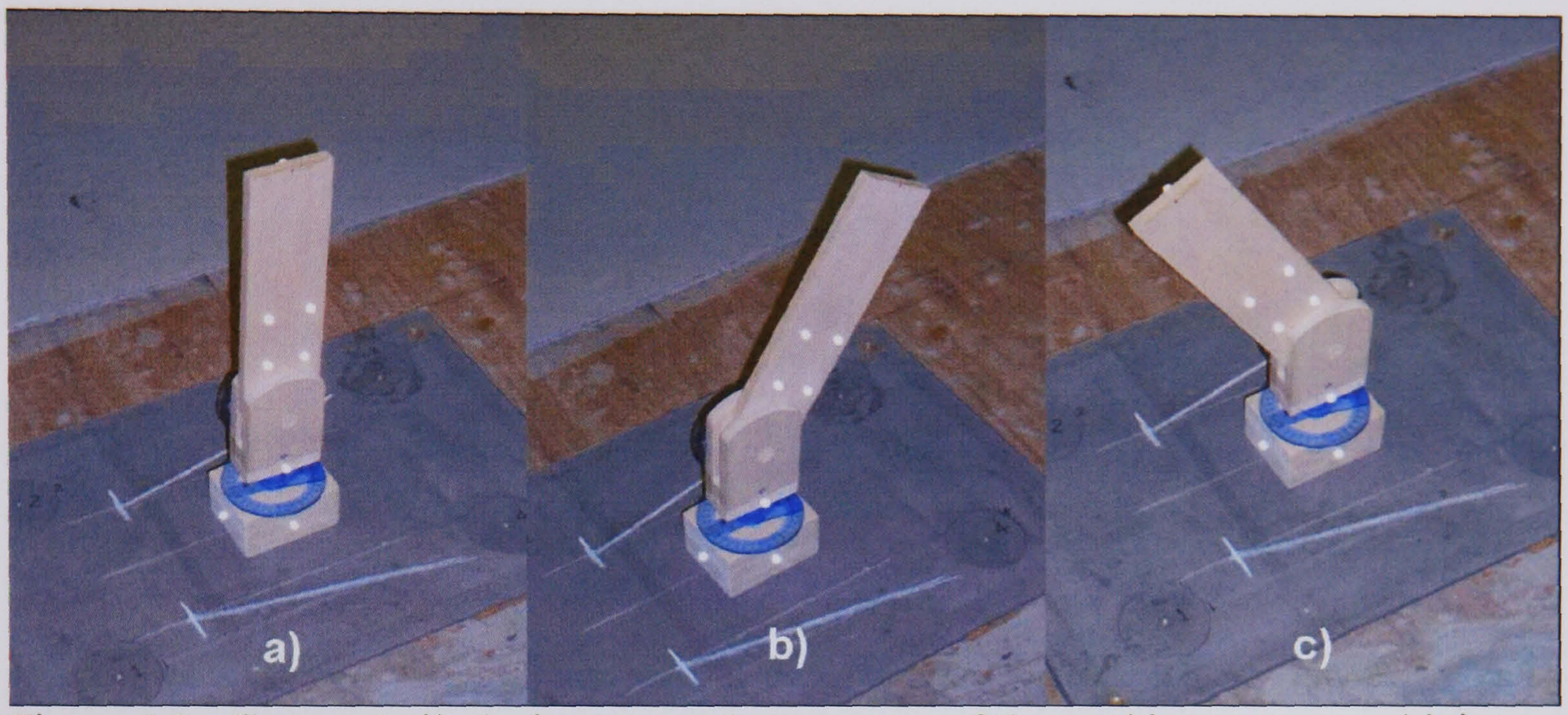

Figure 4.9. Custom built device to test the accuracy of the tracking system and joint angle calculations. Markers placed on the proximal segment represent the shank markers SHN1, SHN2, SHN3 and SHN4. Markers on the distal segment represent the rearfoot markers LCAL, SCAL and MCAL2. (a) Reference trial with segments aligned (0°). (b) Simulated 30° dorsiflexion. (c) Simulated 30° plantarflexion.

b) Dynamic Testing: A validation experiment was also conducted to assess the ability of the cameras/ software to measure an angle during dynamic movements through the data capture volume. The protocol used a goniometer with a proximal and distal arm on which marker clusters were placed. The marker clusters were designed so the marker separations were of a magnitude similar to those found on the rearfoot and shank. The proximal and distal arms were set at a fixed pre-determined angle with respect to one another and the goniometer was then moved through the capture volume in a random manner for five seconds whilst marker co-ordinate data was captured. This procedure was performed with angles of 0°, 30° and -30° set between the proximal and distal arms (these conditions are referred to as Gon0°,

Gon30° and Gon-30° respectively). Any deviations in the calculated angle from the actual angle would be due to the tracking/processing errors since the angle was fixed. The variation of the calculated angle during the captured trial was assessed using the 95% confidence interval (standard deviation multiplied by 1.96).

4.5.3 Results: Accuracy of Static and Dynamic Testing

The results for the static accuracy of the ProReflex tracking device are shown in Table 4.3. The greatest error was found during eversion with a difference of 1.4° found between the computed and the actual angle. The smallest errors were demonstrated in the transverse plane with values of 0.1° and 0.2° in tibial external and internal rotation respectively.

Table 4.3. Static angular validation testing results comparing the computed joint angles (kinematic) with the actual angles as measured using potractors.

Actual Joint Angle (using potractors)	Computed Angle (°)	Difference between actual and computed angle (°)
30° Dorsiflexion	31.1	+1.1
30° Plantarflexion	31.2	+1.2
30° Inversion	31.1	+1.1
30° Eversion	31.4	+1.4
30° Tib. Ext. Rotation	29.9	-0.1
30° Tib. Int. Rotation	29.8	-0.2

The results for the dynamic accuracy of the ProReflex tracking device are illustrated in Table 4.4. This table shows the ability of the ProReflex to measure a fixed angle of a goniometer moved through the capture volume over five seconds. The confidence interval highlights the variation in the computation of the angle over time. The maximum variation was found in the Gon30° condition where a confidence interval of 1.4° was found. This meant that the fixed angle on the goniometer was computed

accurately to within 1.4° with 95% confidence. The Gon0° condition yielded a confidence interval of only 0.7° indicating better accuracy.

Table 4.4. Dynamic validation testing results. The variation of the computed angle over five seconds is give by the confidence interval for three different fixed angles.

Condition	Angle of Goniometer (°)	Mean Angle Computed (°)	95%Confidence Interval (°)
Gon-30°	-30	-30.9	± 1.2
Gon 0°	0	-0.5	± 0.7
Gon30°	30	29.7	± 1.4

4.5.4 Discussion: Accuracy of Static and Dynamic Testing

The main findings of the validation testing was that static angles can be computed to within 1.4° of the actual angle and that during dynamic motion a fixed angle was found to vary by ± 1.4° due to errors in the tracking system. The errors in the calculation of static angles between segments are comparable to those found by Hunt et al. (2001), where the largest error found was 1.2° during the inversion condition. Hunt et al. (2001) simulated dorsiflexion/ plantarflexion and inversion/ eversion angles (actual) between two segments using accurately machined wedges to then compare with angles computed using the tracking system. A similar validation protocol using micrometers to rotate two segments known angles relative to each other found errors in the tracking system to be less than 1.0° (Liu et al., 1997). In the present investigation, however, the actual angle between segments was set using protractors and it was estimated that these actual angles could only be measured to within ± 1.0° using the protractors. This suggests that the computed static angle may actually be more accurate than it would first appear, since part of the error may have been attributed to inaccurate simulation of the actual angle to which it was compared.

Hunt et al. (2001) only used static angular measures to assess the validity of the tracking system and made no attempt to investigate errors associated during dynamic activity. Since gait is a dynamic activity it is desirable to investigate the ability of the tracking/ analysis system to determine angular measurements during dynamic motion. Myers et al. (2004) assessed dynamic linear accuracy by calculating the separation of markers placed on a dummy segment moved through the capture volume. They found that the marker separations determined by the tracking system contained errors of ± 0.53mm. Unfortunately, the effect of these tracking errors was not assessed for the angle between two adjacent segments, thus gives no indication of the accuracy of calculated joint angles during gait. In the present study, an estimate of the error found in the angle between segments was determined. It was estimated that the angle between the rearfoot and shank during gait can be calculated within 1.4° of the true value with 95% confidence.

4.5.5 Conclusion

The validation protocol determined the tracking system to be accurate to within ± 1.4°. Since the method of using protractors to measure the actual angle was also subject to measurement errors the accuracy of the tracking/processing system is likely to be even better than the results suggest. If a more accurate measurement method had been used to compare the computed angle with, such as micrometers or machined wedges, it is likely that even better accuracy would have been found for the tracking/ analysis system. The findings indicate that the measurement/analysis system had an acceptable level of accuracy to determine foot and lower limb segmental kinematics.

Chapter 5 - Subtalar and Tibiocalcaneal Joint Kinematics *In-Vitro*

5.1 Introduction

In vivo studies investigating subtalar joint function typically use external skin markers placed on the tibia and the calcaneus. There are two significant assumptions associated with this method. The first is that the markers placed on the skin are representative of the motion of the underlying bones. Reinschmidt et al. (1997a; 1997b) attempted to quantify the differences in the measurement of tibiocalcaneal rotations when using markers attached rigidly to the bones as opposed to external markers mounted on the shoe. They found that tibiocalcaneal rotations were generally well reflected with external markers in terms of curve pattern, but typically exceeded the true bone motions. Using skin mounted markers instead of external shoe markers would have been a more realistic comparison to make since the calcaneus may move within the shoe (Stacoff et al., 1992).

The second major assumption is that tibiocalcaneal joint rotations are representative of subtalar joint motion but this assumption may be flawed because angular rotations at the tibiocalcaneal joint consist of motion at two different joints (Scott and Winter, 1991); the talocrural joint and the subtalar joint. Furthermore, the range of motion of the tibiocalcaneal joint in any direction (sagittal/ frontal/ transverse plane) has been found to be larger than that of either the talocrural joint or the subtalar joint *in-vitro* (Siegler et al., 1988). However, Siegler and colleagues only investigated the tibiocalcaneal/ talocrural/ subtalar joint angles with the foot held in static positions so nothing is know about about the inter-relationship of the joints during dynamic

movements. Thus, an *in-vitro* investigation of the joints making up the ankle-joint-complex during dynamic movements was warranted.

In general, the aim of the present study was to investigate the coupling mechanisms between the rearfoot and lower leg *in-vitro*. The forefoot was excluded from this study because this segment consists of multiple bones, thus making a comparison between skin and bone marker based kinematics impossible. The investigation had two specific aims which were:

(a) To compare tibiocalcaneal joint rotations based on both skin and bone marker measurements during dynamic motion (*skin vs bone marker* study). It was hypothesised that there would be no difference between the two methods;

(b) To determine the similarity between tibiocalcaneal joint rotations and subtalar joint rotations during dynamic motion (*tibiocalcaneal vs subtalar joint* study). It was hypothesized that there would be no difference between the two methods;

The first aim (a) would address the issue concerning the validity of the measurements taken using external skin markers in the experimental gait studies within this thesis. This would confirm whether the results found in the gait studies were representative of the underlying bones. The second aim (b) would determine whether the biomechanical model of using the tibia and calcaneus to represent subtalar joint kinematics was valid. Hence it would be possible to know if the measurements conducted within the experimental gait studies of this thesis reflected subtalar joint motion.

5.2 Methods

Anatomical Specimens

Three fresh-frozen unembalmed human lower leg and foot specimens were used in this study. These specimens were chosen because they had no significant rear- and/or mid-foot deformity, joint stiffness, ankylosis or surface evidence of invasive surgery. The soft tissue of each anatomical specimen was removed from the proximal end of the tibia and fibula to expose the peroneus longus (PL), peroneus brevis (PB), tibialis posterior (TP) and triceps surae (TS) tendons to approximately 100mm proximal of the malleoli (Figure 5.1). To allow the specimen to be loaded vertically without slippage approximately 70mm of exposed proximal tibia and fibula were embedded in polymethylmethacrylate encased within an aluminium vessel. Intracortical bone pins were inserted into the medial border of the tibia, neck of the talus, and lateral surface of the calcaneus.

Protocol

Each specimen was mounted (Figure 5.1) in a Model 8500 servo-hydraulic materials testing unit (Instron Corporation, Canton, USA). A custom built bearing allowed the specimen to rotate freely in the transverse plane. The specimen rested on a Plexiglas plate fixed to the actuator arm of the test machine with the lower leg visually aligned to vertical and with the foot perpendicular in both the transverse and frontal planes.

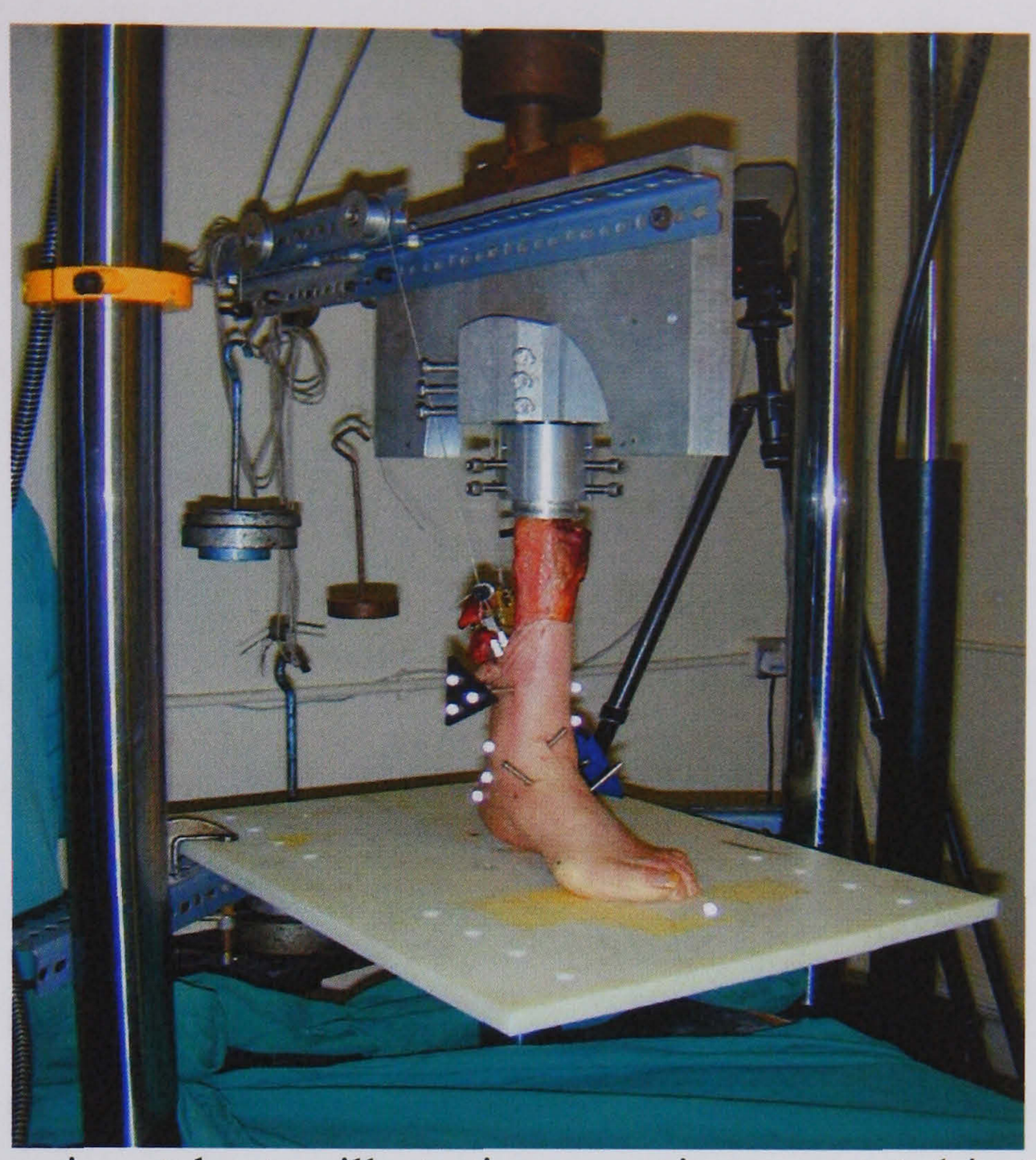

Figure 5.1. Experimental setup illustrating a specimen mounted in the Instron with loads attached to the tendons.

In an attempt to simulate muscle forces, a series of weights, wire cables, pulleys and clamps were used to secure and load the PL, PB, TP and TS tendons (Stahelin et al., 1997). The forces used to load the tendons during testing were determined using relative muscle physiological cross-sectional areas (PCSA) and normalised EMG values (Kitaoka et al., 2002; McCormack et al., 1998; Niki et al., 2001; Reeck et al., 1998). First, the force produced by the TS during maximum voluntary contraction (MVC) was determined from the literature (Inman et al., 1981; Sharkey and Hamel, 1998). Then the force for a MVC of each muscle was estimated using its PCSA relative to the PCSA of the TS (Friederich and Brand, 1990; Wickiewicz et al., 1983). Next, the load applied to each muscle tendon was determined from its percentage activation during the early mid-stance phase (15% of the gait cycle) of walking based on EMG values (Perry, 1992) e.g. EMG activity of the TS at 15% of the gait cycle

was 80% of its MVC, thus the load applied to the TS was 80% of the force value determined from the MVC. All of the calculated tendon loads were scaled down to one-quarter to avoid slippage of the tendons from the clamps. PL and PB were clamped together and loaded with 4.2N, TP was loaded with 20N and TS was loaded with 150N.

The general test protocol for each specimen involved collecting kinematic data for both static (reference position) and cyclic motion trials. Static reference testing consisted of applying a vertical compressive load of 280N (50% of body weight) through the tibia. Body weight was assumed to be approximately 560N. To minimise the effect of creep, the static load was applied for 20 seconds prior to the recording of the kinematic orientations of the bones and skin markers. Cyclic compressive loading ranging from 0N to a maximum force of 560N (i.e. 100% of body weight) was applied sinusoidally at a frequency of 1 Hz. The frequency was chosen to represent a normal cadence during walking and the magnitude of the force was selected to approximate the loading conditions found during the early mid-stance phase (15% of the gait cycle) of walking (Winter, 1991). This phase of the gait cycle was selected as it best represented the orientation of the loaded specimen in the Instron, since the foot was flat on the plate with the lower limb oriented vertically.

The testing protocol was divided into two phases: (a) the *skin vs bone marker* study, and (b) the *tibiocalcaneal vs subtalar joint* study. Each experiment contained the following stages:

1) The 280N static load was applied to the foot (reference trial) and kinematic data collected for three seconds;

2) The specimen was subjected to cyclic axial compressions (range 0 to 560N) and five cycles were recorded for kinematic analysis;

3) Only the loading phase of the cycle was selected for analysis i.e. when the actuator was compressing the foot (0N to 560N). The loading phase was determined using the vertical trajectory of a single marker placed on the actuator plate. As the actuator compressed (loading phase) the specimen the vertical displacement of the marker increased and as the specimen was unloaded the vertical displacement decreased. The onset of the loading phase was defined using the minimum vertical displacement of the marker and the offset using the maximum vertical displacement.

Kinematic Analysis and Marker Setup

Marker co-ordinates were recorded using five ProReflex MCU240 cameras (Qualisys, Sweden) sampling at 60Hz. The cameras were placed in an umbrella formation around the specimen. Prior to any kinematic analysis the testing volume was calibrated using a custom frame and wand. Residuals reported during the calibration of the capture volume indicated that marker position was determined accurately to within 0.8mm. Rigid marker clusters consisting of three 7mm diameter retro-reflective hemispherical markers were clamped to the three intracortical bone pins to represent motion of the individual bones (Figure 5.2). Lightweight shields were placed behind each marker cluster to limit tracking problems due to markers merging in the camera field of view (Michelson et al., 2002). Markers were also placed directly on the skin of the specimens using double-sided adhesive tape.

Skin vs Bone Marker Study

In this study tibial and calcaneal motion was measured using both bone and skin markers (Figure 5.2). Anatomical co-ordinate systems were created for the tibia and the calcaneus by placing markers on bony anatomical landmarks (see below). The position of the technical markers on the tibia and calcaneus (both skin and bone markers) were defined in the anatomical co-ordinate systems of the tibia and calcaneus respectively during a static reference trial (see section 4.1.1: *Anatomical and Technical Co-ordinate Systems*).

The tibial anatomical co-ordinate system was created using skin markers placed on the medial (MMAL) and lateral malleoli (LMAL) and a virtual knee joint centre based on anthropometric measurements of the specimen. The origin was located at the midpoint of the malleoli. The frontal plane was defined as the plane containing the malleoli and the virtual knee joint centre. The longitudinal (y) axis runs along the line from the malleoli mid-point to the virtual knee joint centre. The antero-posterior axis (x) was perpendicular to the frontal plane and faced anteriorly. The medio-lateral axis (z) was the cross-product of the y and z axes. Four skin tracking markers were placed on the lateral distal aspect of the shank (SHN1-SHN4) to measure the movement of the segment during the dynamic loading trials. In addition, the marker triad attached to the bone pin embedded in the tibia was used to measure the movement of the bone during the loading trials.

The anatomical co-ordinate system for the calcaneus created in the manner described earlier using the markers SCAL, ICAL, MCAL and LCAL (see methods section 4.3.5). The skin markers SCAL, MCAL2 and LCAL were used for tracking during

the cyclic loading. The marker triad attached to the bone pin embedded in the calcaneus was used to measure the movement of the bone during the cyclic loading. Three-dimensional rotations between the segments were determined using the cardan angle convention described earlier (section 4.3.8) and all angles were referenced to the static trial.

Figure 5.2. Marker setup for the *skin vs bone markers* experiment. The markers on the triads were used to track the motion of the bones.

Tibiocalcaneal vs Subtalar Joint Study

Tibial, talar and calcaneal motion were measured using only bone markers. The anatomical co-ordinate systems for the tibia and calcaneus were created in an identical manner to the *skin vs bone marker* study. The talus anatomical co-ordinate system was assumed to be coincident with the tibia co-ordinate system in the static trial (Michelson et al., 2002). The tracking markers of each bone (triad attached to the bone pins) were located with respect to the anatomical co-ordinate systems during the static reference trial as described earlier. Joint angles were calculated using the same Cardan angle sequence of rotations as the '*skin vs bone markers*' study. Subtalar and

tibiocalcaneal motion were expressed as rotation of the calcaneus relative to the talus, and rotation of the calcaneus relative to the tibia, respectively.

Data Analysis

All joint angles and arch heights were expressed as the mean value of the five cycles captured. The differences between tibiocalcaneal joint angles (inversion/ eversion, tibial external/ internal rotation) derived from skin and bone markers (*skin vs bone marker* study) were expressed in terms of the average root mean square (RMS) difference (Reinschmidt et al., 1997b). The RMS values were expressed in absolute terms (°), and as a percentage of the range of motion (%) of the rotation angles measured using the bone markers. For each specimen, the cross-correlation (Li and Caldwell, 1999) coefficient between the tibiocalcaneal angles (inversion/ eversion, tibial external/ internal rotation) determined using the skin markers and those using bone markers were also calculated to check for shape agreement. The RMS values and correlations were also used to compare the differences between rotations (inversion/ eversion, tibial external/ internal rotation) derived using the tibiocalcaneal joint and the subtalar joint (*tibiocalcaneal vs subtalar joint* study).

5.3 Results

Skin vs Bone Marker Study

There was a poor relationship between tibiocalcaneal inversion/ eversion determined using skin mounted and bone mounted markers, with the average RMS difference being 1.4°, which equated to 80.0% of the total range of motion (Table 5.1). Specimen 1 demonstrated the best agreement between skin and bone marker based

inversion/eversion values with an average RMS difference of 29.3% of the range of motion, and the curve correlation value of 0.92 indicated similar temporal characteristics. Specimens 2 and 3 both demonstrated opposing tibiocalcaneal joint rotations (negative cross-correlations) for the skin and bone marker based measurements (Figure 5.1), i.e. the bone markers illustrated an eversion pattern but the skin markers indicated inversion was occurring.

The agreement between skin and bone marker based tibiocalcaneal rotations was marginally better for transverse plane rotations with an average RMS difference of 0.5° or 67.5% of the total range of motion of this rotation (Table 5.1). Specimens 2 and 3 showed similar movement patterns for skin and bone based angular rotations (positive correlations) with both demonstrating predominant internal tibial rotation (Figure 5.4). The skin markers showed that a slight tibial external rotation preceded internal rotation in specimen 1, which was not evident in the rotations based on bone markers. This resulted in a poor and negative cross-correlation for this specimen (Table 5.1). The largest average RMS difference was also found in specimen 1 with an absolute value of 0.6° which corresponded to 100.7% of the range of motion.

Table 5.1. Agreement between skin and bone marker determined tibiocalcaneal rotations expressed in absolute (°) and relative (%) terms. Cross-correlations between skin and bone determined tibiocalcaneal rotations are also shown.

Rotation	Variable	Spec. 1	Spec. 2	Spec. 3	Mean
Calcaneal Inversion/Eversion	RMS Diff. (°)	0.9	1.2	2.0	1.4
	RMS Diff. (%)	29.3	115.7	94.9	80.0
	Cross-correlation	0.92	-0.94	-0.98	
Tibial External/ Internal Rotation	RMS Diff. (°)	0.6	0.5	0.4	0.5
	RMS Diff. (%)	100.7	28.8	73.0	67.5
	Cross-correlation	-0.15	0.96	0.70	

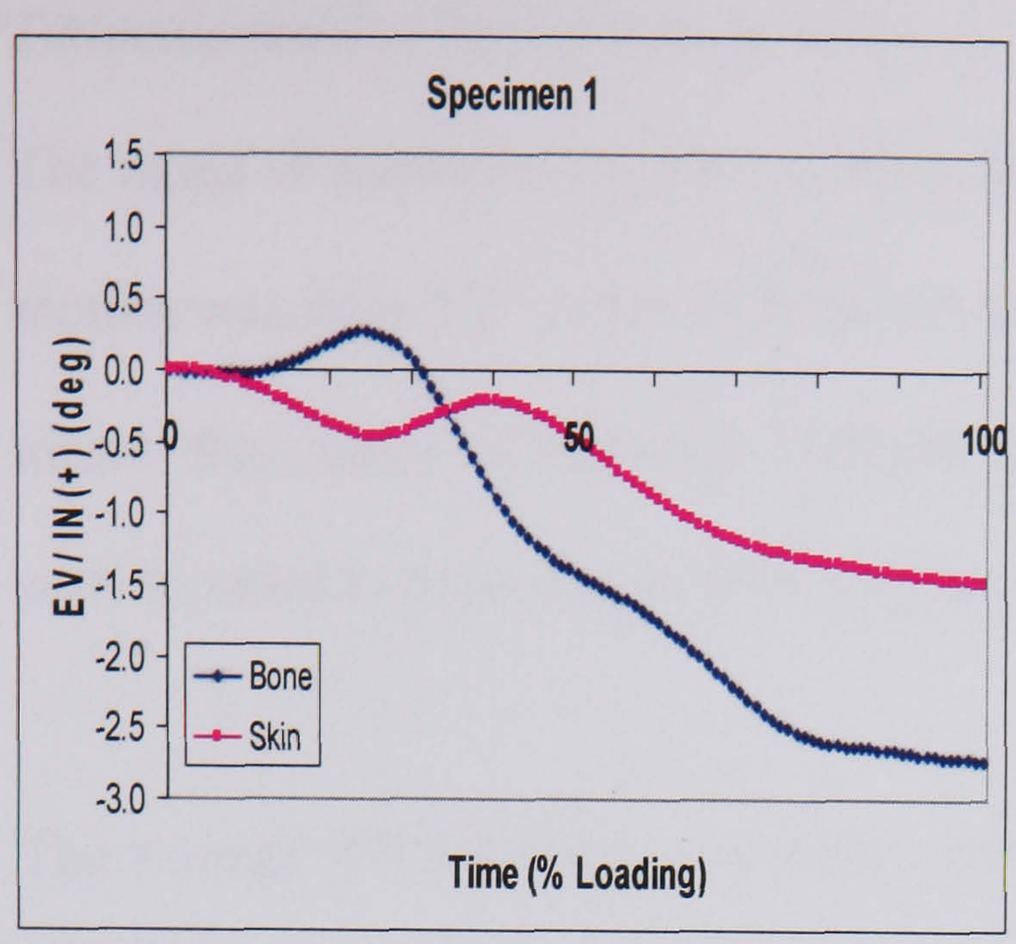

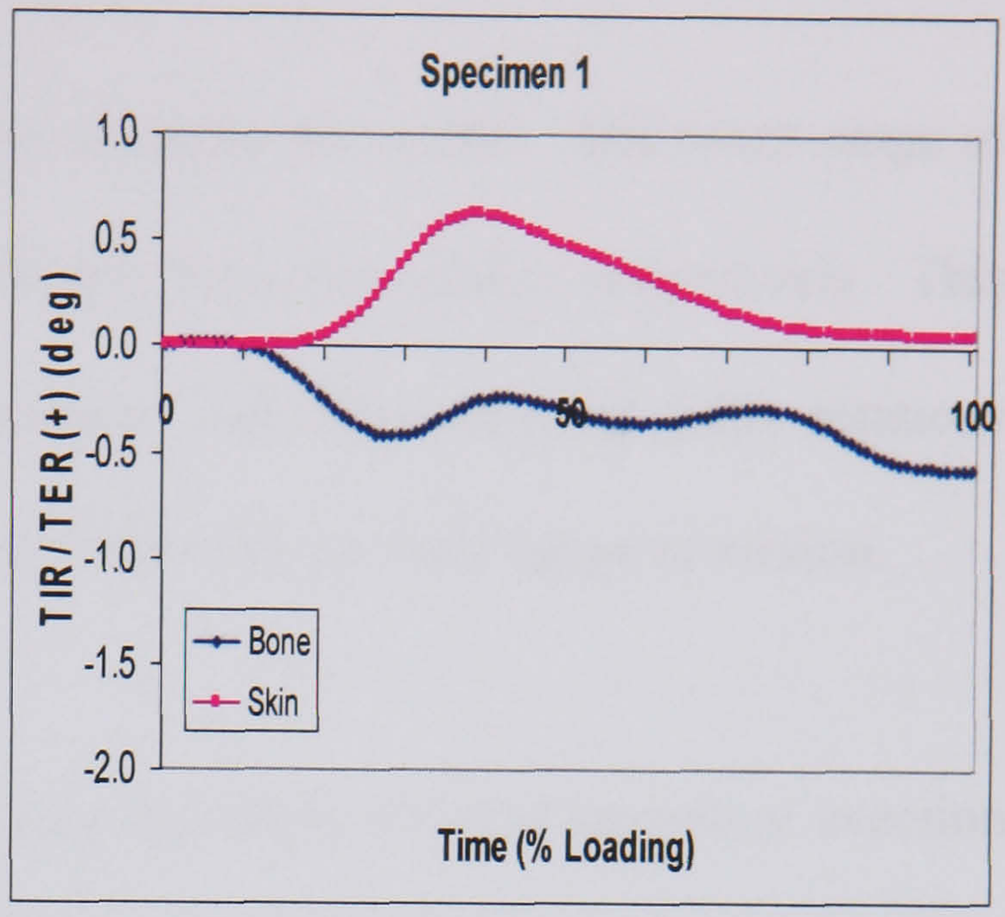

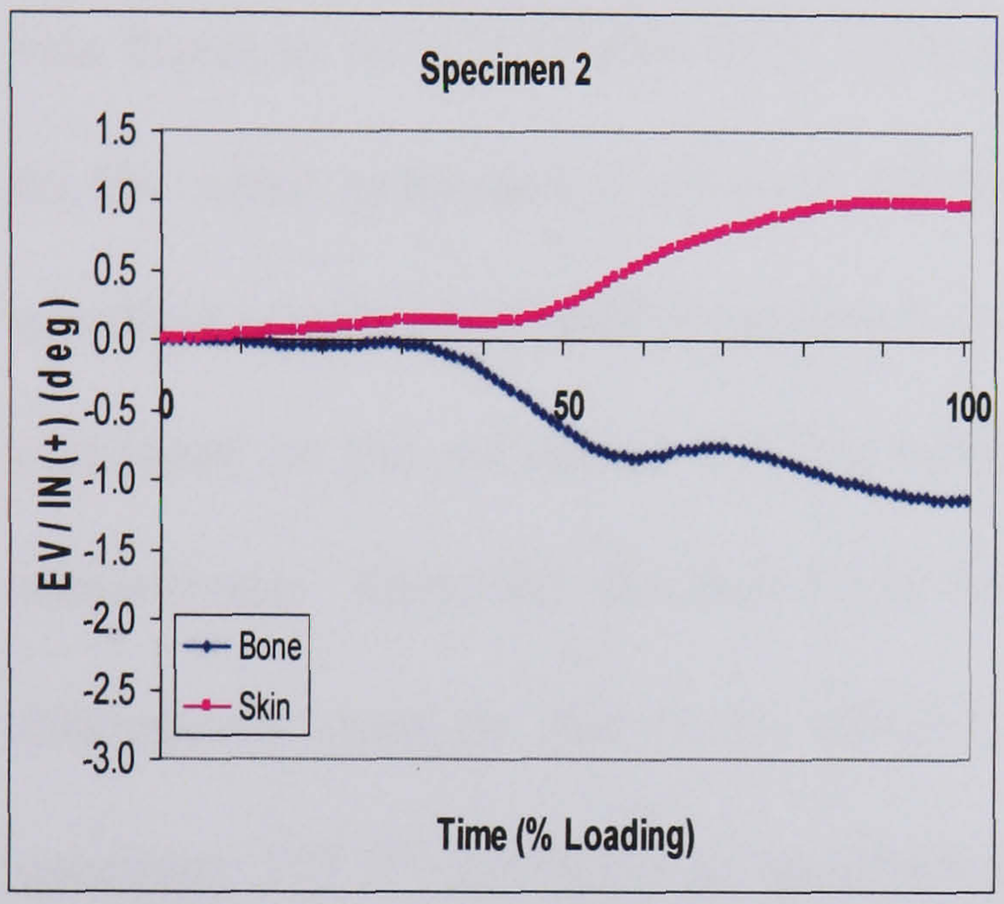

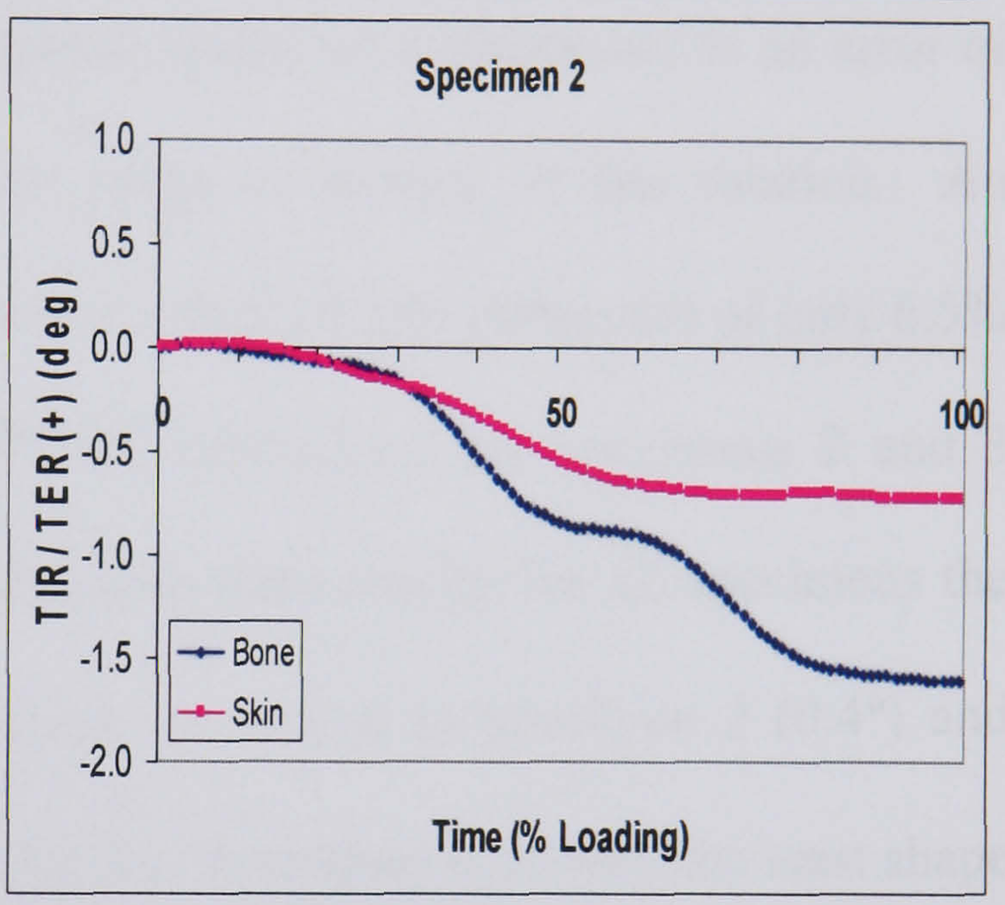

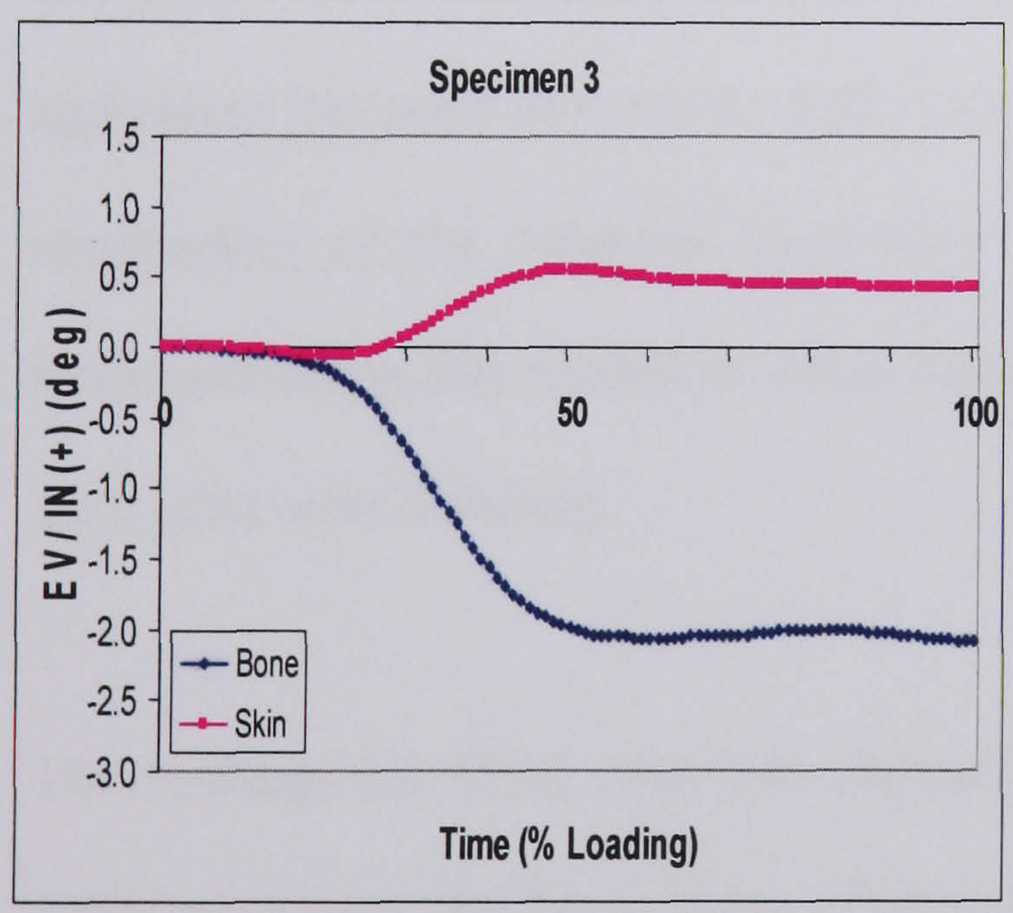

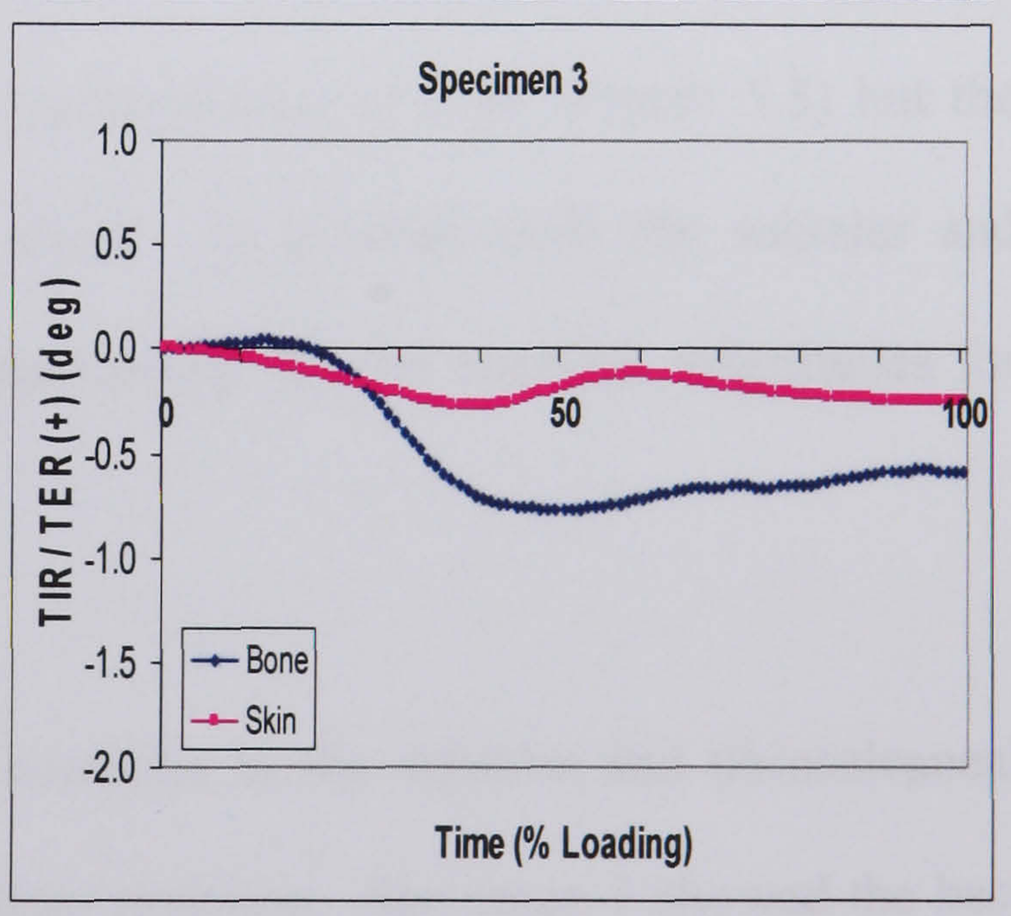

Figure 5.4. Tibiocalcaneal rotations based on bone and skin markers. Eversion (EV)/ inversion (IN) and tibial external (TER)/ internal rotation (TIR) are presented for each specimen.

Tibiocalcaneal vs Subtalar Joint Study

The range of motion found for subtalar joint rotations was small. The mean range of motion was only 2.2° and 1.6° in the frontal and transverse planes respectively. This meant that small differences between subtalar and tibiocalcaneal joint rotations corresponded to large errors when expressed relative to the total range of motion.

The average RMS difference between subtalar and tibiocalcaneal inversion/ eversion was found to be 0.5° (Table 5.2). This appears small but corresponds to an error of 63.1% when presented relative to the total range of motion of this rotation. An excellent match was found in specimen 1 with a relative RMS difference of only 6.5% compared to the values of 125.7% and 57.2% determined for specimens 2 and 3 respectively. Since the absolute RMS differences were similar for all specimens the discrepancy must be due to the smaller range of motion in specimen 2 (0.4°) and specimen 3 (1.2°) compared to specimen 1 (5.0°). Specimen 2 showed the least shape agreement between the curves with a cross-correlation of 0.48 (Figure 5.5) but the magnitudes of the rotations were very small. In general, both the subtalar and tibiocalcaneal joints tended to evert during loading but the eversion magnitudes for each joint were different.

The findings for tibial external/ internal rotations in the subtalar and tibiocalcaneal joints were very similar to those of inversion/ eversion. Specimen 1 showed the best match between subtalar and tibiocalcaneal external/ internal rotation with the lowest relative RMS difference of 4.2% (Table 5.2). Specimens 2 and 3 showed less agreement with relative RMS differences of 19.3% and 29.2% respectively. All specimens demonstrated a trend of tibial internal rotation during loading (Figure 5.5).

The similarity in temporal characteristics and curve shape was highlighted by the high curve correlation values (>0.91). The range of motion for this rotation was small in all specimens (i.e. less than 1.8°).

Table 5.2. Agreement between subtalar and tibiocalcaneal joint rotations expressed in absolute (°) and relative terms. Cross-correlations between the subtalar and tibiocalcaneal joint rotations are also shown.

Rotation	Variable	Spec. 1	Spec. 2	Spec. 3	Mean
Calcaneal Inversion/Eversion	RMS Diff. (°)	0.3	0.5	0.7	0.5
	RMS Diff. (%)	6.5	125.7	57.2	63.1
	Cross Correlation	0.99	0.48	0.95	
Tibial External/	RMS Diff. (°)	0.1	0.3	0.4	0.3
Internal Rotation	RMS Diff. (%)	4.2	19.3	29.2	17.6
	Cross-correlation	0.99	0.91	0.96	

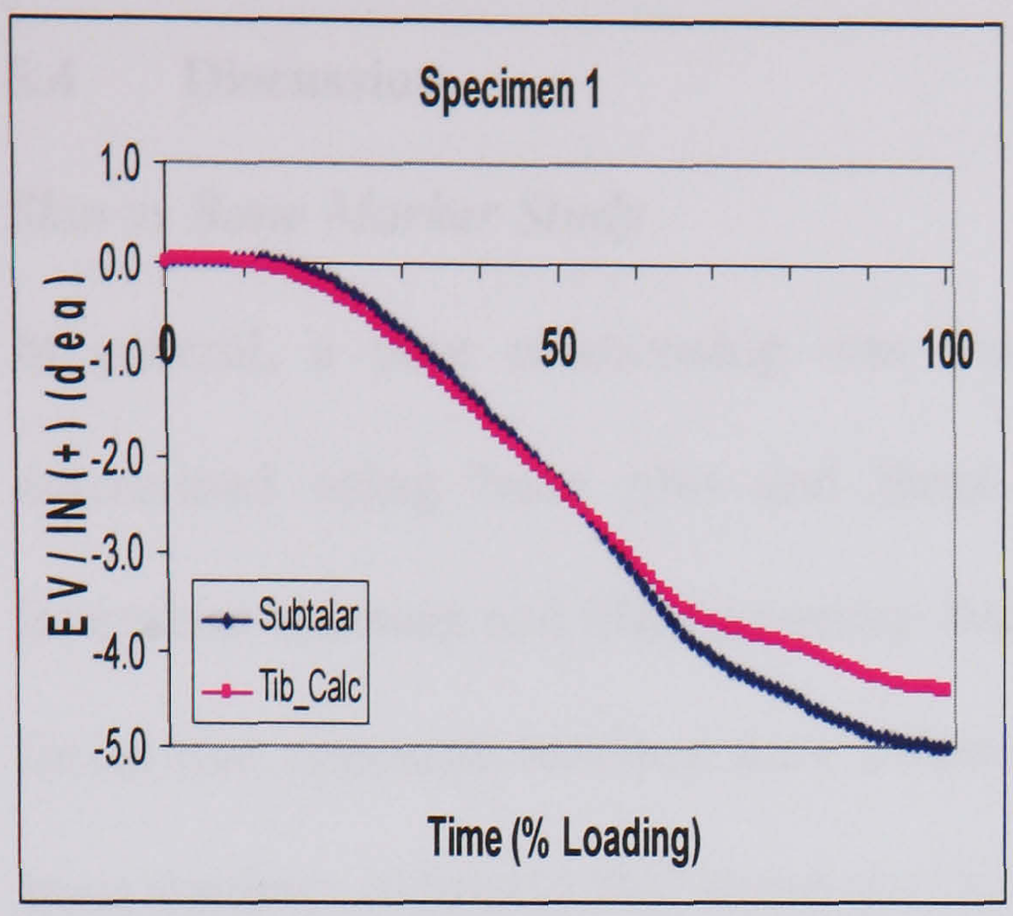

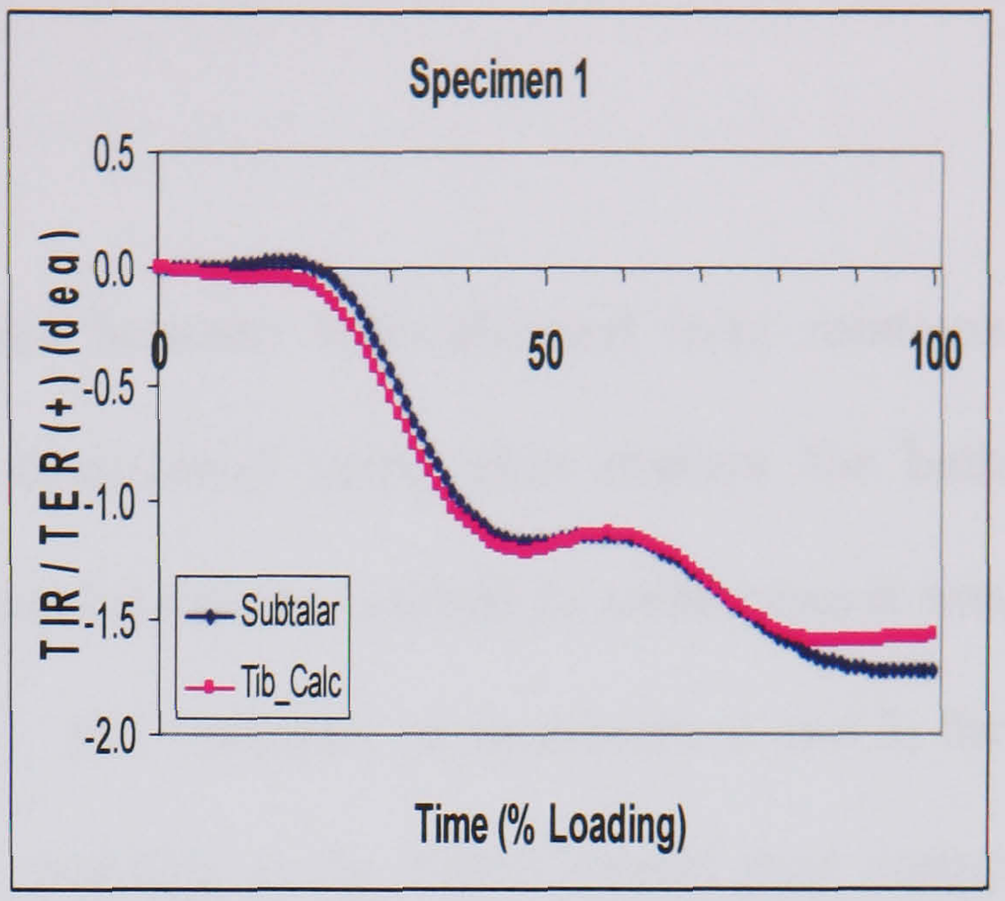

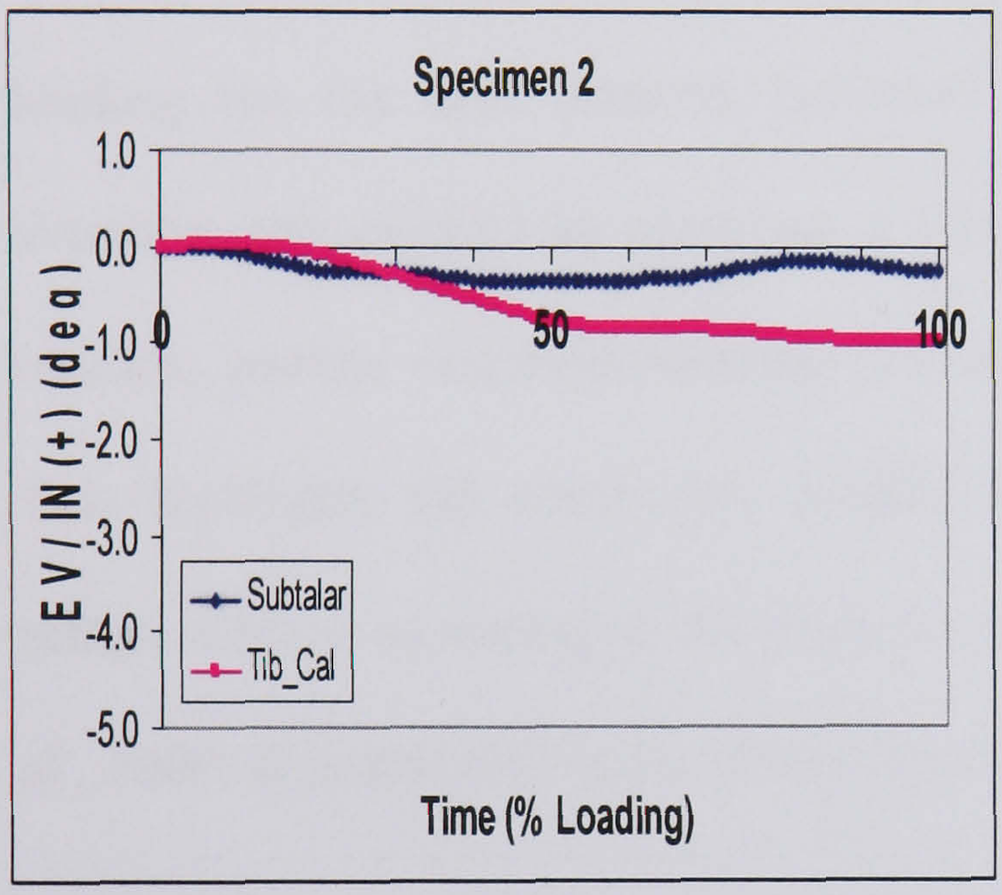

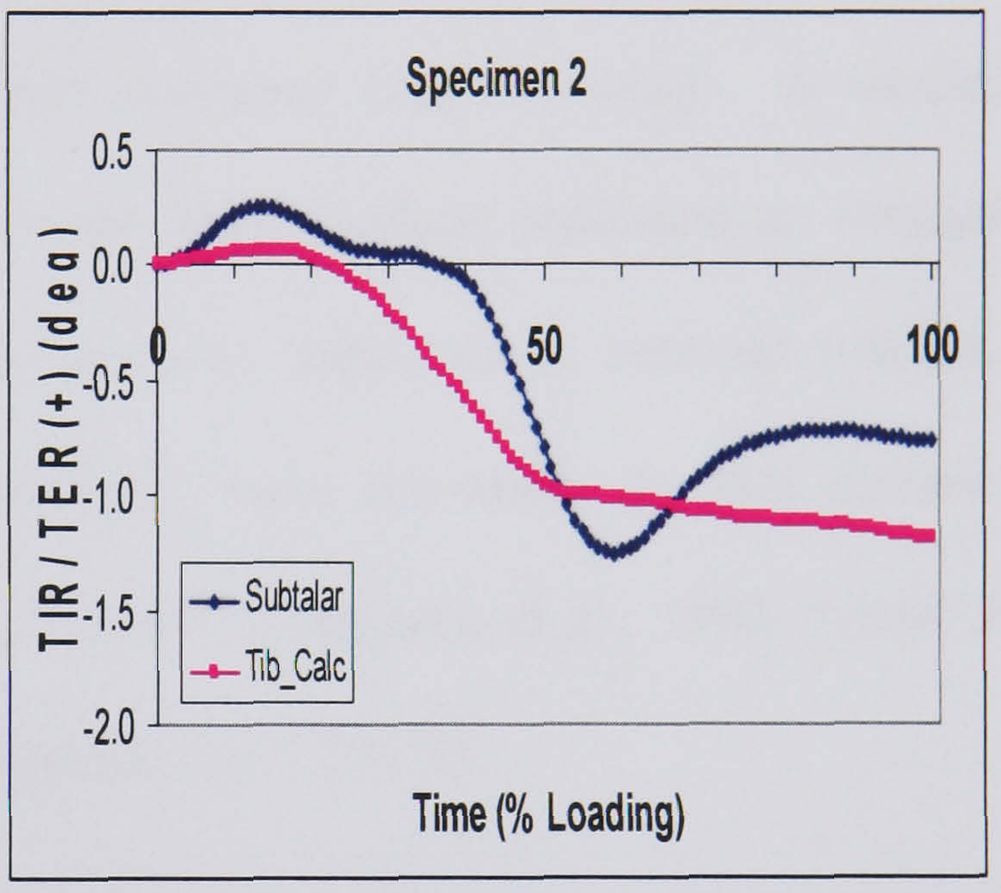

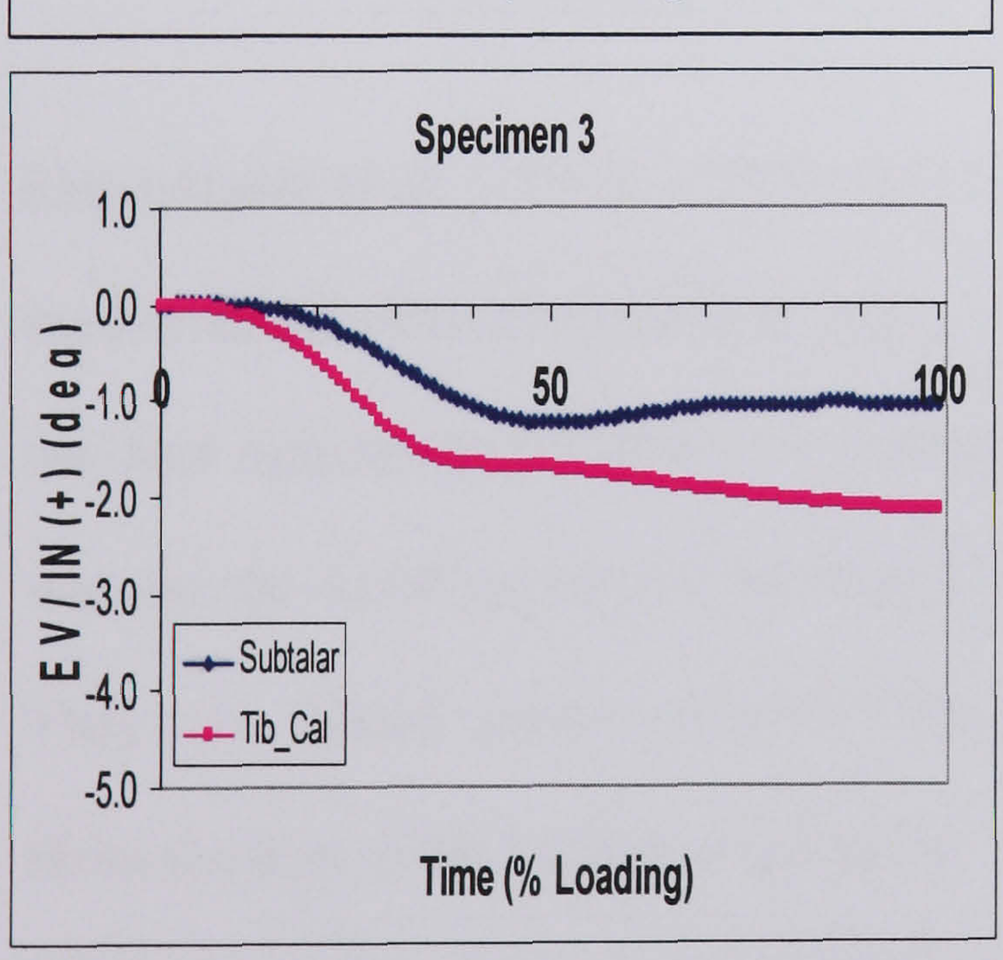

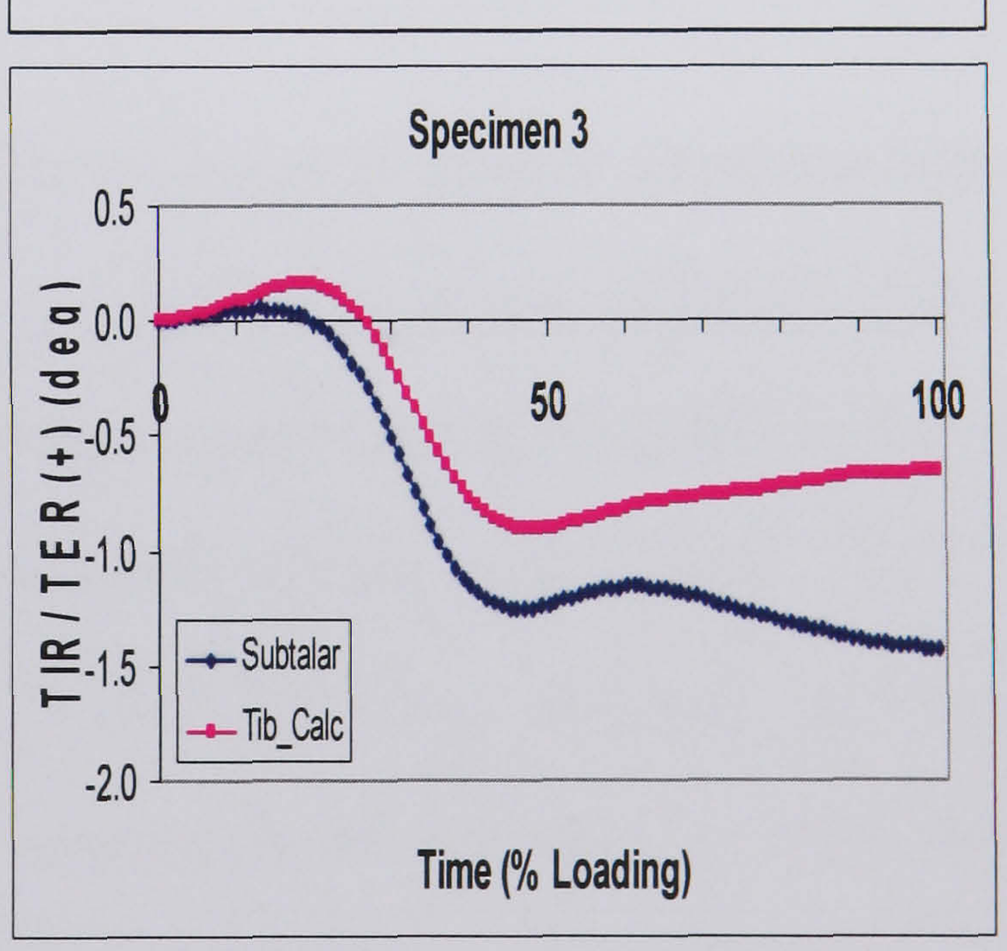

Figure 5.5. Subtalar and tibiocalcaneal joint rotations during cyclic loading. Eversion (EV)/ Inversion (IN) and tibial external (TER)/ internal (TIR) rotation are presented for each specimen.

5.4 Discussion

Skin vs Bone Marker Study

In general, a poor relationship was found between tibiocalcaneal joint rotations determined using bone pins and those determined using skin makers for both inversion/ eversion and tibial external/ internal rotations. Indeed in some cases it was found that opposing motions were evident. For example, in specimens 2 and 3, the bone markers indicated that eversion was occurring at the tibiocalcaneal joint during loading but the skin markers indicated that inversion was occurring. A similar situation was evident in specimen 1 where the bone markers indicated an internal rotation pattern occurred whereas the skin markers indicated an external rotation. This highlights the commonly debated question "how accurately do skin markers reflect motion occurring at the underlying bones?" (Cappozzo et al., 1996; Manal et al., 2000; Reinschmidt et al., 1997a; Reinschmidt et al., 1997b).

Reinschmidt et al. (1997a; 1997b) compared the shapes of external (shoe) and bone-marker-based tibiocalcaneal joint angle curves during running and walking and found the best agreement occurred for plantarflexion/dorsiflexion (RMS Diff. = 14.1%), whereas the worst agreement occurred for abduction/ adduction (RMS Diff. = 51.2%). They also found similar curve patterns in the frontal and transverse planes for tibiocalcaneal joint rotations determined using either external based or bone based markers. Joint rotations determined using external markers, however, were of a greater magnitude than those determined using bone markers. The present investigation found the worst agreement between the tibiocalcaneal inversion/ eversion determined using skin and bone markers (RMS Diff = 80.0%). Furthermore, little agreement was found between the joint rotation curve shapes. However, because

in the studies by Reinschmidt et al. (1997a; 1997b) the external markers were placed on the shoe rather than the skin, it is difficult to directly compare the results with the findings of the present study. Indeed, calcaneal slippage has been shown to occur in the shoe, especially when there is excess space between the heel and the shoe (Stacoff et al., 1992; van Gheluwe et al., 1999).

Tranberg and Karlson (1998) used roentgen photogrammetry to establish that skin markers placed on the medial calcaneus could move up to 2.6mm in relation to the underlying bone during dorsiflexion/ plantarflexion. It is plausible that skin markers on the lateral and posterior aspects of the calcaneus exhibit similar behaviour, thus creating errors in the calculation of the tibiocalcaneal joint angle. Since the joint angles found in the present study were relatively small (<2.7° for eversion excursion and <1.6° for tibial internal rotation), any errors of this magnitude due to skin markers would have a marked effect on the final joint angles calculated.

Tibiocalcaneal vs Subtalar Joint Study

During the normal loading condition subtalar and tibiocalcaneal joint rotation curves showed similar kinematic patterns. High cross-correlations (> 0.90) between subtalar and tibiocalcaneal joint rotations were found for all rotations with the exception of inversion/ eversion in specimen 2. However, the eversion excursion for this specimen was less than 1° and it seems unlikely that such small rotations can be measured accurately with such a degree of confidence. The average relative RMS difference of 63.1% for inversion/ eversion indicates that there were substantial differences between subtalar and tibicalcaneal joint motion. The nature of the difference did not appear to be systematic since subtalar eversion excursions were smaller than

tibiocalcaneal eversion excursions in specimens 2 and 3 but larger in specimen 1. Better agreement was found during tibial internal/external rotation with an average RMS difference of 17.6%.

The average absolute RMS differences between subtalar and tibiocalcaneal rotations were only 0.5° for inversion/ eversion and 0.3° for tibial internal/ external rotation. Due to the small range of motion measured during loading, these small angular differences translated into high percentage errors when expressed relative to the range of motion of the rotation. During walking, tibiocalcaneal joint rotations are typically much higher than the values obtained in the present study, with eversion and tibial internal rotation excursions found in the region of 6.9° and 4.3° respectively (Woodburn et al., 2002). The absolute RMS differences in the present study would equate to smaller errors if they were expressed relative to the joint ranges of motion found during walking. It could be, therefore, that tibiocalcaneal and subtalar joint motions are more closely matched during rotations with a larger range of motion. However, it is also possible that a larger range of motion of joint rotation may result in larger absolute RMS differences between subtalar and tibiocalcaneal joint rotations.

Limitations

There are a number of issues regarding the testing protocol which may explain the marked difference between the tibiocalcaneal joint angles calculated using skin and bone markers. Firstly, the specimens had resulted from amputations performed midway up the shank, and the soft tissue was then removed to approximately 100mm proximal of the malleoli. It is likely that this changed the tensile properties of the skin since it had no proximal attachment. This would have had a greater effect on the

shank markers which were closest to the dissected area. It is also suggested that steel pins which penetrate the skin disturb the 'natural' skin movement (Tranberg and Karlsson, 1998). During specimen preparation it was indeed, observed that the skin movement actually caused the pins to move. It was decided, therefore to make small incisions in the skin around the pin insertion area to prevent the skin from moving the pin. This could also have had an effect on skin marker displacement and may have been of even more importance to the markers on the calcaneus, which were situated close to the bone pin insertion.

In the present study the loading of certain tendons of the foot specimens during the cyclic compressions were undertaken to make the test more realistic to gait. Recent research has attempted to recreate loading conditions similar to phases during gait but due to slippage of the tendon clamps, the loads applied were scaled down to a quarter/ third of the physiological load, including the axial compressive loads applied to the specimens (Chu et al., 2001; Kitaoka et al., 2002; McCormack et al., 1998; Niki et al., 2001; Reeck et al., 1998; Stahelin et al., 1997). This problem was also encountered in the present study and similar scaling down was undertaken. In the present study it was found however, that by scaling down the axial load, the specimen did not visibly pronate during dynamic compressive loading. This is in agreement with Hintermann et al. (1994) who found that the transfer coefficient of tibiocalcaneal eversion to tibial internal rotation was decreased at lower axial loads. This implies the findings from studies which have used scaled down loading (axial and tendon) must be treated with caution. The axial load in the present study was not scaled down but this intervention evidently still did not enable enough joint angular rotation to occur as the angular displacements measured were of a small magnitude. It is plausible that the tendon

loads used in the present study were too low with respect to the high axial loads present during the cycling. This would result in a simulation that does not mimic in-vivo conditions and thus the joint properties may have behaved differently.

A recent development when applying load to tendons has been the use of freeze clamping (Sharkey et al., 1995). This method has demonstrated the tendon forces needed are much larger than those estimated using physiological cross-sectional areas and EMG data (Hansen et al., 2001; Sharkey and Hamel, 1998). Studies that lack physiological muscle forces may alter the kinematic properties of the foot. For instance, a good correlation has been reported between plantar aponeurosis tension and Achilles tendon force (Erdemir et al., 2004). Since the plantar aponeurosis is responsible for transmitting forces between the rearfoot and forefoot, any deficit in Achilles tendon force would consequently alter the rearfoot-forefoot relationship.

The present study simulated the early mid-stance (15% gait cycle) and the segment orientation and muscle forces applied were based on this phase of gait. Indeed, the way the leg could be orientated, the direction that axial load could be applied and the magnitude of the tendon forces that could be feasibly applied only allowed this phase of gait to be simulated. However, the coupling mechanism between the foot and leg may in fact alter throughout the stance phase. Attempts have been made to simulate different phases of the gait cycle such as heel-strike, mid-stance and toe-off (McCormack et al., 1998; Niki et al., 2001; Reeck et al., 1998) but these studies have all still relied on measurements using a static foot position. Sharkey and Hamel (1998) developed a dynamic gait simulator which mimics normal kinetics, kinematics and muscle forces of the tibia, foot and ankle during the stance phase from heel-strike

to toe-off. Initial findings using this equipment have revealed that the calcaneus rotated relative to the talus until 25% of stance, after which they moved together as one body for the remainder of the stance phase (Hamel et al., 2004). This demonstrates the coupling between the calcaneus and the talus will alter at different times of the stance phase, and thus studies which only simulate a single time point of the stance phase provide limited insight.

5.5 Conclusion

The "*skin vs bone marker*" study revealed poor agreement between tibiocalcaneal joint rotations determined using bone pins and those determined skin markers. This suggests that joint measurements using skin markers do not represent the true rotations of the underlying bones. The "*tibiocalcaneal vs subtalar joint*" study showed good agreement between subtalar and tibiocalcaneal joint rotations in the transverse plane but not in the frontal plane. Differences between subtalar and tibiocalcaneal joint rotations were highly variable between specimens. Therefore, it cannot be assumed that rotations measured at the tibiocalcaneal joint represent the rotations occurring at the subtalar joint.

A wide range of experimental issues made it very difficult to draw any conclusions based on this work. The altered mechanical properties of the skin and the mounting of the bone pins may have resulted in substantial errors in the "*skin vs bone marker*" study. The small joint angle displacement magnitudes in all studies ("*skin vs bone*" and "*tibiocalcaneal vs subtalar joint*") made comparisons across conditions difficult since the differences between them were of such a small magnitude. The use of a

single time instant in the stance phase and the scaled down tendon loads were seen as the main causes of the low angular displacements.

It was concluded that due to the methodological issues within this *in-vitro* study, the implications of the findings were of limited use to the *in-vivo* investigations conducted later within this thesis. There is a need for future *in-vitro* studies to incorporate physiological muscle forces and simulate multiple phases of the gait cycle to validate the common measurement practices used to determine subtalar joint kinematics.

Chapter 6 - Repeatability of Kinematic Measurements during Gait

6.1 Introduction

When attempting to quantify angular rotations at the subtalar and midtarsal joints it is desirable to assess the within- and between-day repeatability. The within-day repeatability gives an indication of how much the calculated angle can vary on a trial-to-trial basis, simply due to a person's natural variation during gait. The between-day repeatability demonstrates the magnitude that the measured joint angle can vary on a day-to-day basis where the experimental setup may have altered slightly (i.e. marker placement, camera position, calibration). It is important to assess the repeatability of a joint angle when this measure is being used to compare subgroups of people and formulate conclusions. For example, if the repeatability of a joint angle is equal to or greater than the difference in joint angle found between the subgroups, then it is difficult to draw any conclusions since any differences between subgroups could be masked by the variability in measuring the angle in each subject. Previous research has attempted to quantify the reliability of between-day joint angles by analysing the repeatability of the waveform of the joint angle curves (Growney et al., 1997; Hunt et al., 2001; Kadaba et al., 1989; Leardini et al., 1999; Liu et al., 1997; Moseley et al., 1996). This measure indicates the temporal similarity of the kinematic patterns but does not reflect absolute differences in the magnitudes of the angles. It would also be useful to quantify this error size of the measurement.

The objective of this study was to assess the repeatability of determining kinematic measurements at the ankle-joint-complex (subtalar and ankle joints) and midtarsal

joint during the stance phase of walking. This was conducted in terms of both similarity of the waveform pattern and the absolute magnitude of the error.

6.2 Methods

Experimental Protocol and Equipment

One female subject was used for this study. Inclusion criteria was that the subjects was currently participating for at least two hours per week in exercise involving running, had been free from injury of the lower extremity in the last six months, had no obvious malalignment and did not wear foot orthotics. The study was approved by the institutional ethics committee, and written informed consent was obtained from all subjects (see Appendices A and B). The marker and camera configurations were setup according to the description in the general methods chapter (see methods sections 4.2 and 4.3). After the skin markers were carefully applied to the right limb of the subject they assumed a standing standardised posture from which a reference trial was recorded (methods section 4.2.3). The subject then practiced walking along the runway until they could land the whole of their right foot repeatedly on the force plate. They were instructed to walk at a normal self-selected pace and to focus their vision on the wall ahead to prevent them 'spotting' the force plate. A single foot fall of the right foot was then captured for ten successful trials. A successful trial was defined as one where the subject's right foot landed fully on the force plate without under- or over-striding and running speed. This testing protocol was performed on the same subject on two separate occasions three days apart.

Data Reduction

Five trials from each day were randomly selected for analysis. Raw co-ordinate data of the markers was filtered using a fourth order low-pass Butterworth filter with a cutoff frequency of 12Hz (see methods section 4.4). The shank, rearfoot and forefoot were modelled as rigid segments (see methods section 4.3) adapted from those described by Carson et al. (2001). Calculation of three-dimensional joint rotations (see methods section 4.3.8) enabled interpretation of motion of the distal relative to the proximal segment in clinical terms of dorsiflexion/plantarflexion, inversion/eversion and adduction/abduction (or shank external/internal rotation). All angles were referenced to a standardised standing reference trial (see methods section 4.2.3). Ground reaction forces (GRF) were used to determine touchdown and toe-off for the stance phase. All kinematic parameter files were normalised to 100 data points from touch-down to toe-off using a cubic spline interpolation.

Data Analysis

The levels of within- and between-day repeatability of shank, rearfoot and forefoot angular displacements were evaluated using two methods. The adjusted coefficient of multiple correlation (CMC) was used to assess the temporal similarities (Kadaba et al., 1989) and the 95% limits of agreement (LOA) were calculated to assess the magnitude of the errors (Bland and Altman, 1986). The within-session (day) CMC for each planar motion was calculated using the five trials from the first day. The between-day CMC was calculated for each planar motion using the ten trials from both days. The 95% LOA were also computed in each planar motion to provide both within- and between-day measures.

6.3 Results

Rearfoot

The highest CMC values were found for frontal plane motion as indicated by within- and between-day values of 0.980 and 0.972 respectively (Table 6.1). This indicated that this planar motion was the most repeatable from a temporal perspective. Sagittal plane motion had an identical within-day CMC to the frontal plane but was slightly less repeatable between-day as indicated by the lower CMC of 0.964. Transverse plane motion demonstrated the least similar waveform agreement between trials both within- and between-day. In general, within-day CMCs were higher than between-day values indicating that the temporal characteristics were more reproducible within a day then across days.

The LOA showed that like the CMCs, within-day repeatability was much better than between-day in all four variables (Table 6.2). In fact, the within-day LOA values were approximately half of the between-day values. The best reproducibility was found for the transverse plane motion with values of ± 1.4° and ± 2.5° for within- and between-day. The weakest agreement was found between-days in the frontal plane where inversion/ eversion values had a between-day value of ± 3.4°. Observation of the joint angle curves for all three planes revealed a static offset in the inter-segment angles between-days (Figure 6.3). The inter-segment angles for the second day typically displayed a shift towards dorsiflexion, inversion and tibial external rotation rotated compared to the first day.

Table 6.1. Coefficient of multiple correlation (CMC) values for the walking trials of a single subject.

	Within-day CMC	Between-day CMC
Rearfoot Plantarflexion/ Dorsiflexion	0.980	0.964
Rearfoot Eversion/ Inversion	0.980	0.972
Shank Internal/ External Rotation	0.963	0.962
Forefoot Plantarflexion/ Dorsiflexion	0.980	0.881
Forefoot Eversion/ Inversion	0.862	0.847
Forefoot Abduction/ Adduction	0.992	0.989

Table 6.2. Limits of agreement (LOA) for the walking trials of a single subject.

	Within-day LOA	Between-day LOA
Rearfoot Plantarflexion /Dorsiflexion (°)	± 1.5	± 2.8
Rearfoot Eversion/ Inversion (°)	± 1.6	± 3.4
Shank Internal/ External Rotation (°)	± 1.4	± 2.5
Forefoot Plantarflexion /Dorsiflexion (°)	± 1.3	± 3.1
Forefoot Eversion/ Inversion (°)	± 1.9	± 2.6
Forefoot Abduction/ Adduction (°)	± 0.6	± 1.5

Forefoot

The transverse plane was the most repeatable motion of the forefoot for within- and between-day, yielding CMC values of 0.992 and 0.989 respectively (Table 6.1). Forefoot sagittal plane motion was slightly less reliable especially between-days with a CMC value of 0.881. The lowest CMC value for any kinematic curve was found to be between-day forefoot frontal plane motion but this was still in excess of 0.847.

As was the case with the rearfoot, all the within-day LOA values were less than between-day values in all forefoot planar motions (Table 6.2). The best reproducibility was found for transverse plane motion with values of ± 0.6° and ± 1.5° for within- and between-day. The lowest within-day LOA in the forefoot was observed in the frontal plane (± 1.9) with the worst between-day value being evident in the sagittal plane (± 3.1).

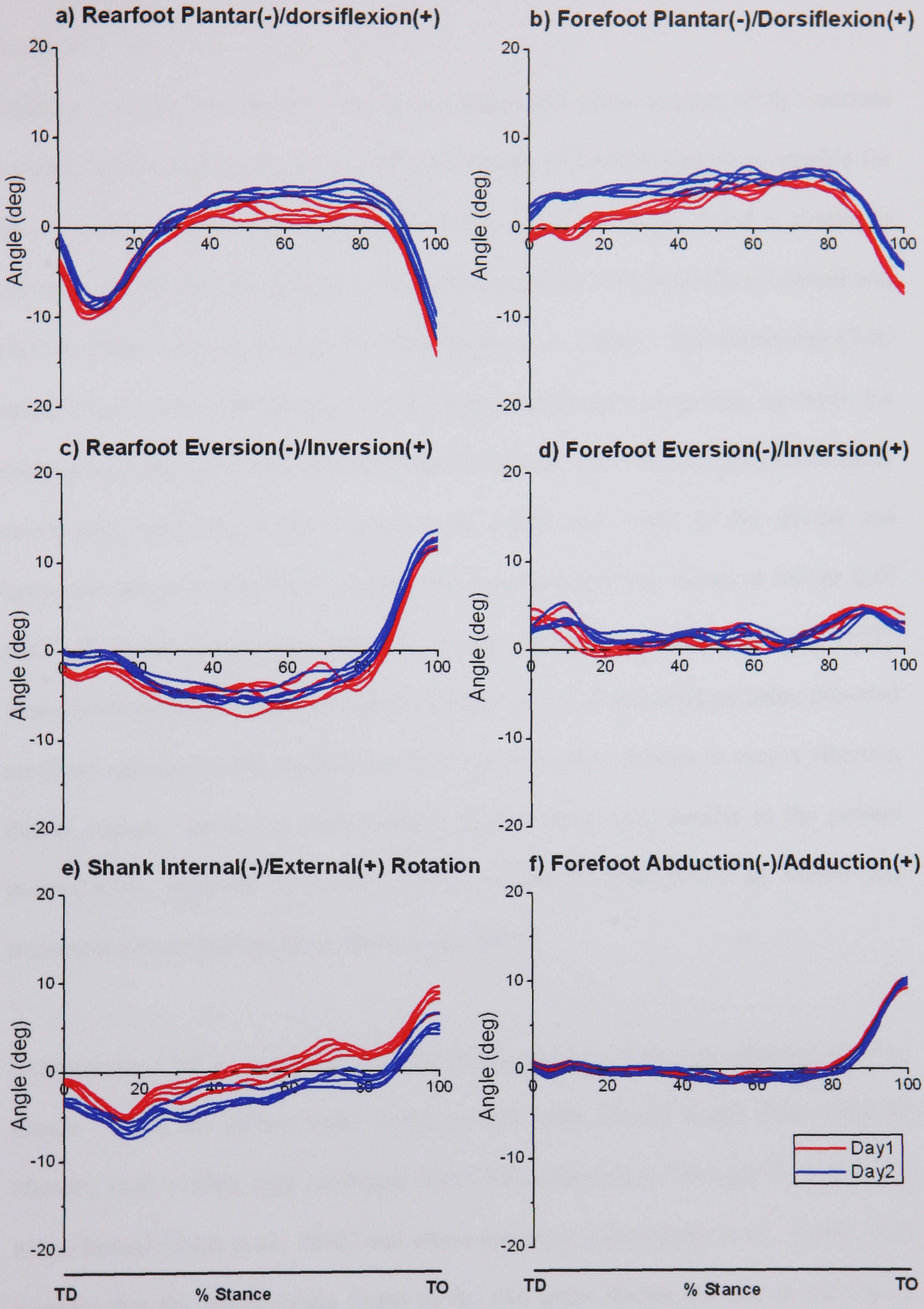

Figure 6.3. Angular displacement curves for the forefoot, rearfoot and shank. All ten trials are shown from touchdown (TD) to toe-off (TO).

6.4 Discussion

Rearfoot

Findings indicate that sagittal, frontal and transverse plane motion of the rearfoot during barefoot walking could be obtained reliably at a level deemed acceptable for future studies. In the sagittal plane the within-day CMC value found is similar to previous studies that have reported values ranging from 0.91 to 0.976 (Cornwall and McPoil, 2002; Leardini et al., 1999; Woodburn et al., 2004). The within-day CMC values found in the present study for the frontal and transverse planes, however, are much greater than those reported by the same authors. For instance, the present study determined within-day CMC values to be 0.980 and 0.963 in the frontal and transverse planes respectively, whereas the literature reported values as low as 0.85 and 0.76 in the frontal and transverse planes respectively (Leardini et al., 1999). These lower values may have been attributable to the all the markers being mounted on plates clamped to the segments, which may have been subject to excess vibration during impact. In fact, a study using a marker setup very similar to the present investigation, reported within-day CMCs of greater than 0.912 in frontal and transverse plane rotations (Woodburn et al., 2004).

Between-day CMCs were lower than the corresponding within-day values in all three planes. While the values found in the present study closely match those cited by Moseley et al. (1996), they are higher than CMCs reported in other papers, especially in the frontal (Hunt et al., 2001) and transverse plane (Woodburn et al., 2004). It is possible that the lower values found in the two latter studies are due to the use of multiple subjects during reliability testing, since the present study along with Moseley et al. (1996) used single subject designs. Indeed, it has been shown that the frontal

and transverse planes display a high degree of inter-subject variability (Leardini et al., 1999; Liu et al., 1997) and it is plausible that some subjects display more within-day variability than others, thus affecting a CMC value that has been calculated as a mean across a range of subjects.

The greater reproducibility of within-day measures in the present study was also evident in the LOA, with between-day values approximately twice the magnitude of the corresponding within-day values. The within-day LOA indicates that on a trial-to-trial basis the joint angle at any time can be calculated to ± 1.6° with 95% confidence. As the system accuracy was determined to be within 1.4° (see methods section 4.5), then it is plausible that tracking errors contribute to the majority of the variability found within-session. However, between-day LOA values were as a high as ± 3.4° in the frontal plane and are too high to be explained by the tracking accuracy. Carson et al. (2001) found between-day variability of a similar magnitude using confidence intervals. A possible cause of the elevated errors between-days is the re-application of the skin markers. Even though easily palpable landmarks were chosen as the sites for markers, it was still difficult to place the markers on exactly the same location on each landmark. An attempt was made to reduce the variability by referencing joint angles relative to a standardised static standing trial but a shift in the absolute value of the inter-segment angles was still present.

Forefoot

The high CMC values reported for forefoot motion ($r \geq 0.847$) indicated that this measure could also be obtained reliably at a level deemed acceptable for future studies. As with rearfoot motion, within-day CMCs were slightly higher than the

respective between-day values in each cardinal plane. The within-day values were of a similar magnitude to those found by Woodburn et al. (2004). The between-day values of this latter study were well matched with those of the present investigation, but a substantially lower CMC has been reported in the frontal (Hunt et al., 2001). This may have been due to large inter-subject variability in the angular displacement.

Within-day LOA indicate that on a trial-to-trial basis the forefoot angle at any time can be calculated to ± 1.9° with 95% confidence. However, between-day LOA values were as a high as ± 3.1° in the sagittal plane which is in agreement with Carson et al. (2001) who found between-day variability to be as high as ± 4.3° (transverse plane) using confidence intervals. The elevated errors found between-days are influenced by the same experimental factors as the rearfoot (i.e. marker re-application). However, observation of the kinematic curves (Figure 6.4b) reveals that the offset was much larger during early stance compared to the rest of stance, so the higher LOAs may have also been influenced by an alteration in the subject's gait at touchdown on the second day.

6.5 Conclusion

With LOA of ± 3.4° in rearfoot frontal plane motion, findings indicate that when comparing experimental conditions, the differences between conditions should be of a magnitude greater than ± 3.4° to be considered meaningful. Any conclusions based on differences of less than this must be interpreted with the understanding that the differences may in fact be attributable to experimental errors. Similar considerations must be taken into account for all other segmental rotations. Hence, any differences

found between conditions which are of a magnitude smaller than the respective LOAs, must also be treated with caution. High CMC values for all measures reflect the excellent repeatability of the kinematic patterns for the shank, rearfoot and forefoot.

Chapter 7 - Forefoot, Rearfoot and Shank Coupling: Effect of Variations in Step Width

7.1 Introduction

The coupling between movements of the foot and tibia during running has been suggested to be a possible mechanism of overuse injuries (Duffey et al., 2000; James and Jones, 1990; Kibler et al., 1991; Orchard et al., 1996; Powers et al., 2002; Sutlive et al., 2004; van Mechelen, 1992; Wen et al., 1997; Williams et al., 2001b). This coupling mechanism is a result of the function of the subtalar joint, which is suggested to act like a mitered hinge, whereby pronation and supination of the foot is transferred respectively into internal and external rotation of the shank (Inman et al., 1981). It has been suggested that excessive or prolonged pronation may cause excessive or prolonged internal rotation of the shank (Tiberio, 1987). As a consequence, this could alter the normal kinematics and kinetics of the lower limb and result in an increased risk of injury to bone and/or soft tissue structures.

Studies investigating foot function during gait have typically approximated foot pronation and supination using calcaneal eversion and inversion, as this component is the simplest to measure (Edington et al., 1990). However, Lundberg et al. (1989) and Nester et al. (2002) showed that significant amounts of rotation occur at the midfoot joints, and there is growing evidence that motion at the midfoot contributes significantly to overall foot motion during walking and running (Carson et al., 2001; Hunt et al., 2001; Leardini et al., 1999; Myers et al., 2004; Rattanaprasert et al., 1999; Woodburn et al., 2004). Despite this, little is known about how the midfoot joints influence the subtalar coupling mechanism during gait. In the present study, we

therefore investigated the association between midfoot joint motion (rotation of forefoot relative to the rearfoot) and the kinematic coupling at the subtalar joint (rotation of the rearfoot relative to the shank) during running. More specifically, we determine whether forefoot motion is coupled to rearfoot motion and thus has an effect on shank rotation.

Studies investigating the biomechanical coupling between the foot and shank have traditionally examined this relationship using kinematic data determined at discrete points in the stance phase, e.g. maximum rearfoot eversion (Liu et al., 1997; Moseley et al., 1996; Nawoczenski et al., 1998; Nigg et al., 1998; Reinschmidt et al., 1997; Stacoff et al., 2000; Williams et al., 2001a). However, this approach may not reveal the complete relationship between the segments since it does not measure the continuous coupling throughout the entire stance phase (DeLeo et al., 2004; Hamill et al., 1999). It is important to include measures of continuous coupling, as it has been suggested that asynchronous motion (poor coupling) between rearfoot eversion/inversion and knee flexion/extension may also contribute to overuse injuries at the knee (Hamill et al., 1992; Stergiou et al., 1999; Stergiou and Bates, 1997). It has been postulated that, during the initial phase of stance, both knee flexion and rearfoot eversion act to induce shank internal rotation and, during the latter phase of support knee extension and rearfoot inversion, induce shank external rotation (Hamill et al., 1992). This implies that if rearfoot inversion occurred at a different time than the onset of knee extension, then an antagonistic relationship would be present and thus the risk of injury would increase. This injury mechanism, however, is based on the assumption that rearfoot eversion and inversion, respectively, are strongly mechanically coupled with shank internal and external rotation; however, there has

been little research to determine if this relationship is continuous throughout the stance phase. In the present study, we therefore used continuous measures to quantify joint coupling.

Variations in step width occur frequently during running and have been shown to significantly affect the maximum rearfoot eversion (Williams and Ziff, 1991). Such changes in rearfoot eversion would presumably also alter tibial and forefoot kinematics since they are connected to the rearfoot via the subtalar and midfoot joints, respectively. Therefore, investigating if subtalar and midfoot joint coupling alters when the kinematics of rearfoot is manipulated should determine how rigidly shank, rearfoot and forefoot motions are linked during gait. Thus the purpose of the present study was to determine if the coupling relationship between the shank, rearfoot and forefoot changed when step width was manipulated during running.

7.2 Methods

Subject Population

Twelve subjects (six males, six female; mean age (SD), 29.9 (4.9) years; body mass, 61.2 (15.1) kg; and height, 171.2 (9.5) cm) volunteered to participate. Inclusion criteria were that subjects were currently participating for at least two hours per week in exercise involving running, had been free from injury of the lower extremity in the last six months, had no obvious malalignment and did not wear foot orthotics. The study was approved by the institutional ethics committee, and written informed consent was obtained from all subjects.

Experimental Protocol and Equipment

The marker and camera configurations were setup according to the description in the general methods chapter (see methods sections 4.2 and 4.3.1). In this study an additional marker was also placed on the left foot in the same location as D3MT. Before starting the dynamic trials, a calibration trial was recorded. All subjects assumed a standardised standing posture with the heel centres 0.18m apart and the long axes of the feet (heel to second metatarsal head) at an angle of 11.6° to each another (McIlroy and Maki, 1997). Kinematic data were collected at 240 Hz and ground reaction force (not presented here) at 960 Hz.

Participants then practised barefoot running along the runway at a self-selected jogging speed which was recorded using timing gates and then later used as the baseline self-selected speed for all subsequent trials. Subjects were asked to perform ten running trials at three different step widths, and were given time to practise running at each required step width. Step width was defined as the perpendicular distance from the line of progression to each D3MT marker, with a negative value indicating that the feet had crossed this line medially. A line along the centre of the runway (line of progression) was used by the experimenter to provide feedback to the subject (Williams and Ziff, 1991). The three step widths were determined by instructing the participants to run in the following manner: a crossover condition, where the lateral borders of both feet landed just inside the line (Xover); a wide condition, where the right and left feet stayed to the right and left of the line respectively (Wide); and a normal condition, where the subjects ran along the line (Norm). Using timing gates to monitor speed along with verbal feedback, subjects practiced until they acquired the target (baseline) speed within approximately ± 5%

(Hunt et al., 2001), after which the experimenter adjusted the start of their run-up so that the subject's right foot landed fully on the force plate. Following a short rest subjects then completed, in block random order, 10 trials using each step width pattern. A successful trial was defined as one where the subject's right foot landed fully on the force plate using the desired step width pattern (later confirmed by looking at the D3MT marker co-ordinate data) without under or over striding and running speed was within 5% of the target speed.

Data Reduction

Five trials for each foot strike condition were randomly selected for analysis. Raw co-ordinate data were filtered using a fourth order low-pass Butterworth filter with a cut-off frequency of 12Hz (see methods section 4.4).

The shank, rearfoot and forefoot were modelled as rigid segments (see methods section 4.3) adapted from those described by Carson et al. (2001). Three-dimensional joint rotations were calculated using cardan angles with the distal segment rotated with respect to the adjacent proximal segment (see methods section 4.3.8). This enabled interpretation of motion in clinical terms of dorsiflexion/plantarflexion (sagittal plane), inversion/eversion (frontal plane) and abduction/adduction (transverse plane). Rearfoot abduction/adduction was expressed as shank internal/external rotation throughout to be more in fitting with the literature. All angles were referenced to the standing position determined from the calibration trial. Ground reaction forces (GRF) were used to determine the onset (touch-down) and offset (toe-off) of the stance phase, and using cubic spline interpolation methods all kinematic parameter files were normalised to 100 data points from touch-down to toe-off. The

kinematic curves from the five trails of each condition (width) were averaged for each subject. This was done by calculating the mean angle at each of the 100 time points to create a new ensemble average curve. The average curves of all subjects were then processed in a similar manner to create a mean ensemble average curve for each step width condition (N =12).

Data Analysis

The following discrete variables were identified for each trial and subject: peak rearfoot eversion, rearfoot eversion excursion, time to maximum rearfoot eversion, peak shank internal rotation, shank internal rotation excursion, time to maximum shank internal rotation, forefoot dorsiflexion excursion, time to maximum forefoot dorsiflexion, forefoot abduction excursion and time to maximum forefoot abduction. Excursions were defined as the difference between the maximum value and the value at foot strike, and event timings were determined as a percentage of stance time. Data from all five trials for each subject were analysed using one-way repeated measures analysis of variance (ANOVA) with both repetition and step width as repeated measures. Post-hoc analysis was performed using Tukey's multiple comparison tests. Significance was set at an alpha level of $p<0.05$ and all statistical analysis was undertaken using Statistica 4.0 (SuperStat, USA).

To examine the continuous coupling between adjacent segments, kinematic data for one segment was compared to kinematic data for the adjacent segment by using cross-correlation technique (Derrick et al., 1994; Li and Caldwell, 1999). This involved calculating the cross-correlation coefficient between the angular displacement curves of adjacent segments across the stance phase. The cross-correlation was performed on

every trial (3 conditions x 5 trials = 15 trials) for each subject. The mean value for each step width condition was then calculated using the five cross-correlations obtained for each subject (N = 12). The following formula was used to calculate the cross correlation between the angular displacement curves:

$$r_{xy}(k) = \frac{\sum_{i=0}^{N-1}(x_i - \bar{x})(y_{i-k} - \bar{y})}{\sqrt{\sum_{i=0}^{N-1}(x_i - \bar{x})^2}\sqrt{\sum_{i=0}^{N-1}(y_{i-k} - \bar{y})^2}}$$

where k is a number indicating the time shift (number of time intervals) of one signal with respect to the other; thus $k = 0$ when the time series data for each segment are synchronised in time. Two correlation values were determined: one when there was zero phase shift ($k = 0$); and one where k was systematically altered until the maximum correlation coefficient (positive or negative) value was achieved. The number of phase shifts was limited to 15 in order to This approach was used to determine the coupling between the following segmental rotations: rearfoot eversion/inversion (EVE/INV) and shank internal/external (IR/ER) rotation, rearfoot EVE/INV and forefoot plantarflexion/dorsiflexion (PF/DF), rearfoot EVE/INV and forefoot EVE/INV, rearfoot EVE/INV and forefoot abduction/adduction (ABD/ADD). The correlation value with zero phase shift was considered to be of primary importance in this investigation since this measured the curve congruity of the segmental rotations occurring about a common joint as they occurred in real time. This was based on the premise that with good mechanical coupling there should be no evidence of a phase shift between the kinematics of adjacent segments. Correlation coefficients greater than 0.7 or (less than -0.7) indicated a strong coupling between the two segmental rotations. Coefficients of between 0.3 to 0.69 and -0.3 to -0.69

represented a moderate coupling, and coefficients of between -0.3 and 0.3 suggested zero or weak coupling.

7.3 Results

Step width was significantly different ($P < 0.001$) between all three running conditions (Table 7.1). The small step width standard deviations (<0.03m) indicate that all subjects were able to run at the required step width. Additionally, intra-subject variability (± SD) across the 5 trials for each step width condition was less than 0.02m in all subjects. This provides evidence that all subjects were able to run consistently at each given step width.

Repetition had no effect on any of the kinematic variables analysed ($P > 0.10$). This indicated that there was no learning effect between trials. It also indicates that the differences found between step width conditions were reliable. Ensemble group average angular displacement curves for the forefoot, rearfoot and shank are shown in Figure 7.1. In general, rearfoot dorsiflexion and eversion, forefoot dorsiflexion and abduction, and shank internal rotation occurred during the first half of stance, whereas rearfoot inversion and plantarflexion, forefoot plantarflexion and adduction, and external shank rotation occurred during the second. Step width did not appear to induce large alterations in curve shape in any of the angular displacements analysed, with the exception of forefoot eversion/inversion which showed a different kinematic pattern during the cross-over condition (Figure 7.1d).

Segmental kinematics

Group mean kinematic variables for the forefoot, rearfoot and shank are presented in Table 7.1. Peak rearfoot EVE (P = 0.046) and EVE excursion (P= 0.026) were significantly greater in the cross-over compared to normal condition, whereas the values for the wide condition were similar to those for normal running (P > 0.05). The time of peak EVE occurred approximately 6-7% earlier in stance compared to both the normal and wide conditions (P < 0.001). Differences between step width conditions for any of the shank rotation variables were not significant (P > 0.10). Forefoot DF excursion was significantly greater during cross-over running compared to the normal condition (P = 0.031) and the instance of peak forefoot DF occurred later in stance compared to normal and wide running (P < 0.001). Forefoot ABD excursion was reduced (P = 0.038) and peak forefoot ABD occurred earlier in stance during cross-over, compared to wide running (P = 0.029).

Table 7.1. Group mean (SD) foot and shank kinematic variables for the normal, wide and cross-over step width conditions. Significant differences between conditions ($P < 0.05$) are shown by superscript.

Variables	**Normal**	**Wide**	**Xover**
Step Width (m)	0.05 (0.02)	0.11^{norm} (0.01)	-0.07$^{norm, wide}$ (0.03)
Rearfoot peak EVE (°)	-11.1 (3.2)	-9.9 (3.3)	-12.5$^{norm, wide}$ (3.2)
Shank peak IR (°)	-9.1 (2.3)	8.7 (2.6)	-9.0 (2.4)
Rearfoot EVE excursion (°)	-13.3 (4.9)	-13.7 (5.0)	-16.1^{norm} (5.5)
Shank IR excursion (°)	-6.5 (3.2)	-7.0 (3.1)	-8.0 (2.8)
Forefoot DF excursion (°)	10.2 (3.3)	10.5 (3.4)	12.5^{norm} (5.9)
Forefoot ABD excursion (°)	-6.1 (2.5)	-6.6 (2.2)	-5.5^{wide} (2.3)
Time to peak rearfoot EVE (%stance)	46.3 (6.7)	47.7 (5.3)	40.4$^{norm, wide}$ (5.6)
Time to peak shank IR (%stance)	40.6 (11.2)	41.2 (11.2)	38.6 (6.6)
Time to peak forefoot DF (%stance)	54.2 (5.7)	52.4 ^{norm} (4.6)	59.3$^{norm, wide}$ (5.3)
Time to peak forefoot ABD (%stance)	49.7 (8.7)	50.5 (9.0)	46.0^{wide} (12.9)

Cross Correlation

Table 7.2 represents group mean cross-correlation values for the various segmental rotations at zero phase shift, and Table 7.3 shows the optimum cross correlation

coefficients together with the phase shifts undertaken to achieve these optimum correlations.

With zero phase shift, coupling between rearfoot EVE/INV and shank IR/ER was consistently high across all three step width conditions ($r \geq 0.92$). Similarly, coupling between rearfoot EVE/INV and forefoot PF/DF was high ($r \leq -0.85$), although the cross-over condition exhibited slightly lower values than the normal and wide conditions. Rearfoot EVE/INV and forefoot ABD/ADD was also highly coupled at all step widths ($r \geq 0.95$). Coupling for rearfoot EVE/INV and forefoot EVE/INV was poor ($-0.02 \leq r \leq 0.31$), with the correlation value for the cross-over condition the only one to suggest a weak relationship ($r = 0.31$).

Table 7.2. Mean (SD) cross-correlation values (zero phase shift) between rearfoot eversion/inversion and shank internal/external rotation and forefoot motion in each plane.

Variables	**Normal**	**Wide**	**Xover**
Rearfoot EVE/INV _ Shank IR/ER	0.93 (0.07)	0.92 (0.08)	0.96 (0.03)
Rearfoot EVE/INV _ Forefoot PF/DF	-0.93 (0.07)	-0.94 (0.04)	-0.85 (0.11)
Rearfoot EVE/INV _ Forefoot EVE/INV	-0.02 (0.52)	-0.21 (0.45)	0.31 (0.40)
Rearfoot EVE/INV _ Forefoot ABD/ADD	0.95 (0.04)	0.95 (0.04)	0.95 (0.05)

Even after determining the optimum correlation, by incorporating a phase shift of up to 7 time intervals, correlation values for rearfoot EVE/INV and forefoot EVE/INV (r

≤ 0.59) were still much weaker than the other three joint angle pairs, which also marginally improved after incorporating a small (< 3 time intervals) phase shift (Table 7.3).

Table 7.3. Mean (SD) optimum cross-correlation values along with the mean (SD) phase shift required to achieve the optimum correlation.

Variables		**Norm**	**Wide**	**Xover**
Rearfoot EVE/INV _ Shank IR/ER	Correlation	0.97 (0.02)	0.97 (0.04)	0.98 (0.02)
	Phase shift	3 (5)	3 (5)	0 (3)
Rearfoot EVE/INV _ Forefoot PF/DF	Correlation	-0.97 (0.03)	-0.97 (0.02)	-0.94 (0.04)
	Phase shift	2 (5)	0 (4)	7 (6)
Rearfoot EVE/INV _ Forefoot EVE/INV	Correlation	-0.32 (0.76)	-0.01 (0.82)	0.59 (0.63)
	Phase shift	-2 (14)	-7 (14)	4 (17)
Rearfoot EVE/INV _ Forefoot ABD/ADD	Correlation	0.98 (0.01)	0.98 (0.01)	0.98 (0.02)
	Phase shift	1 (4)	0 (4)	2 (4)

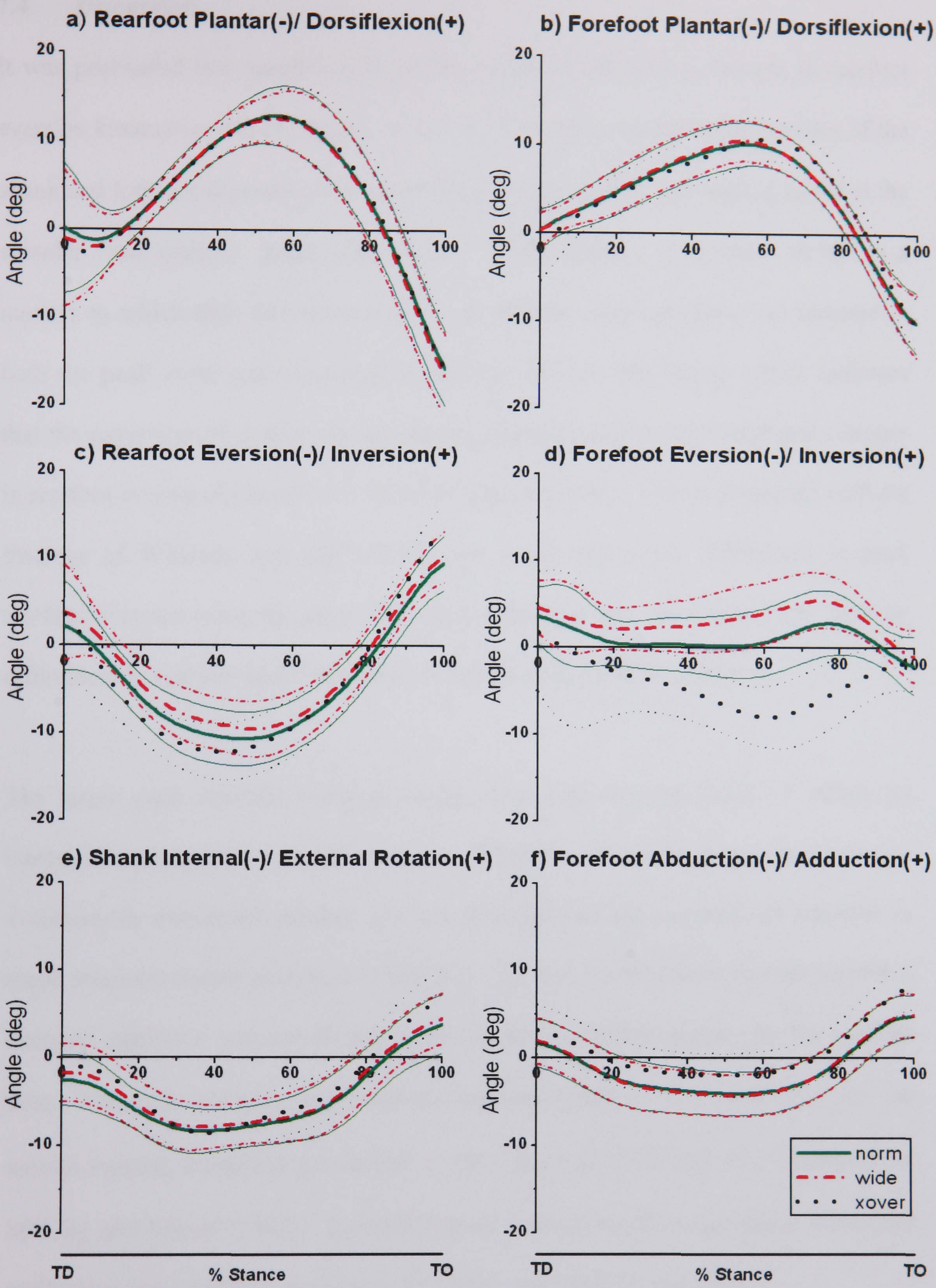

Figure 7.1. Angular displacement curves for the forefoot, rearfoot and shank for each step width condition. The ensemble mean and standard deviation for all subjects are shown from touch-down (TD) to toe-off (TO).

7.4 Discussion

It was postulated that manipulation of step width would induce changes in rearfoot eversion kinematics and depending on how such changes altered the kinematics of the shank and forefoot segments, this would highlight the rigidity of coupling found at the subtalar and midfoot joints respectively. When subjects were asked to run in a manner in which their feet crossed over 'the midline of progression,' an increase in both the peak value and excursion of rearfoot eversion was found, which indicates that the experimental design was indeed successful in facilitating significant changes in rearfoot eversion kinematics in the cross-over condition. This is consistent with the findings of Williams and Ziff (1991) who found significant differences in peak rearfoot eversion using the same step width manipulations. However, there were no differences in rearfoot kinematics induced by the wide running condition.

The larger peak rearfoot eversion during cross-over running failed to induce an increase in peak shank internal rotation. Similarly, the increased rearfoot eversion excursion in cross-over running was not accompanied by a significant increase in shank internal rotation excursion (Table 7.1). Thus, it would appear that the increased eversion excursion was not all transferred to shank internal rotation by the subtalar joint. The peak eversion and eversion excursion values of 11.1° and 13.3° for the normal running condition are similar to the values of 11.2° and 12.7° reported by McClay and Manal (1997). Similarly, shank internal rotation excursion values fall within the range reported by Nigg et al. (1998) and Stacoff et al. (2000).

Perhaps the most important finding of the study was the apparent lack of coupling between rearfoot EVE/INV and forefoot EVE/INV. This was despite there being a

strong coupling relationship between rearfoot EVE/INV and both forefoot PF/DF ($P \leq$ -0.85) and forefoot ABD/ADD ($P \geq 0.95$). This finding suggests that frontal plane motion of the forefoot has limited effect on frontal plane rearfoot motion, and *vice versa*. Even when one of the curves was phase shifted with respect to the other, the correlation coefficients indicated little more than moderate coupling (Table 7.3). The slightly better coupling value between rearfoot EVE/INV and forefoot EVE/INV found in the cross-over condition (0.31), compared to the normal (-0.02) and wide (-0.21) step width conditions, may be reflective of a change in foot-strike pattern in the cross-over condition. It was observed during data collection that some subjects tended to land more on their forefoot in the cross-over condition. In addition, compared to the other planar movements at the shank, rearfoot and forefoot, the movement of the forefoot in the frontal plane was highly variable between subjects, consistent with an earlier study (Carson et al., 2001; Hunt et al., 2001). This is emphasised by standard deviation values in excess of 0.51, compared to values for the other planar movements of less than 0.11 (Table 7.2).

The relationship between forefoot frontal plane and rearfoot frontal plane movement in the present study is in contrast to segmental motion patterns found by Cornwall and McPoil (2002) for walking. They highlighted that forefoot motion about a longitudinal axis can occur in the opposite direction to rearfoot frontal plane motion. More specifically, during initial loading they showed that the navicular was inverting relative to the rearfoot while the rearfoot was everting. In contrast, in the present study the forefoot was found to evert during initial loading (Figure 7.1d). A possible reason for these seemingly contradictory findings may be the methods used to model the midfoot. Cornwall and McPoil (2002) measured the motion of the navicular

relative to the calcaneus, whereas the present study measured motion of the entire forefoot segment relative to the rearfoot. It is also likely that midfoot behaviour is very different between walking and running due to both the period of 'double support' in walking and the potentially different loading patterns between the two modes of gait.

Rearfoot EVE/INV and shank IR/ER rotation coupling was high (>0.92) for all three step width conditions. This is comparable with the observations of Moseley et al. (1996) who found a mean correlation of 0.95 throughout the stance phase between rearfoot frontal plane and shank transverse plane motion during walking. Interestingly, we found the best coupling to occur in the cross-over condition (r = 0.96). This higher value may have been due to the peak rearfoot eversion and peak shank internal rotation occurring closer together in the stance phase in the cross-over, compared to both wide and normal conditions (Table 7.1). This is supported by the finding that optimum correlation between the joint rotations in the cross-over condition occurred at zero phase shift, whereas in both the wide and normal conditions optimum correlation occurred at a phase shift of 3 time intervals. This suggests that the changes in rearfoot frontal plane kinematics induced by the cross-over running served to enhance the coupling between the rearfoot and shank. The fact that changing step width slightly altered subtalar joint coupling suggests that coupling is not related to anatomy solely, but may also be influenced by the geometry of the external loads applied.

Correlation values between rearfoot frontal plane and forefoot sagittal plane motion were in excess of -0.93 in both normal and wide conditions. A good, but slightly

lower, correlation value of -0.85 was found in the cross-over condition. During cross-over running, the angular displacement curve was shifted so that the forefoot was in a more adducted position throughout the entire stance phase (Figure 7.1d), which may explain why segmental kinematics were significantly different for this condition (Table 7.1). However, coupling between rearfoot frontal plane motion and forefoot transverse plane was similar between the three step widths (>0.95). The coupling relationships between the rearfoot and forefoot (discussed above) indicate that rearfoot eversion was accompanied by forefoot dorsiflexion and abduction, and during rearfoot inversion the forefoot plantarflexed and adducted (Figure 7.1). Since rearfoot eversion occurred in conjunction with shank internal rotation, our results indicate that transverse/sagittal forefoot motion is coupled with transverse plane shank motion. This is in agreement with the findings of Nester et al. (2002), although in their study internal/external rotations of the shank were induced whilst subjects were in a stationary standing position. However, the same authors also reported that forefoot inversion and eversion accompanied forefoot dorsiflexion/abduction and forefoot plantarflexion/adduction respectively. This synchronised motion of forefoot frontal plane motion with the other forefoot planar movements was not found in the present study, but this may be due to the different experimental protocols and midfoot joint models utilised.

The findings of the present study indicate that forefoot motion was 'out of phase' in relationship to the rearfoot. Table 7.1 illustrates how peak rearfoot EVE (40.4-47.7%) occurred prior to both peak forefoot ABD (46-50.5%) and peak forefoot DF (52.4-59.3%). This is also highlighted by the finding that the phase shifts to achieve optimum correlation between rearfoot EVE/INV and forefoot DF/PF were higher (up

to 7 time intervals) than that required to achieve optimum coupling between other joint pairings. This 'out of phase motion' indicated that as the rearfoot began to invert, the forefoot continued to abduct and dorsiflex. Hunt et al (2001) showed that forefoot sagittal plane motion pattern was linked to the collapsing of the medial longitudinal arch. Therefore, the results of the present study suggest that when the rearfoot began to supinate, the medial longitudinal arch was still collapsing. This out-of-phase motion was more pronounced in the cross-over condition, where peak rearfoot EVE occurred 19% earlier than peak forefoot DF. These findings are in contrast to the previous concept that rearfoot eversion is reflective of whole foot pronation.

There are two important limitations/assumptions which should be taken into account when interpreting the results of this study. Firstly, the movement of the forefoot relative to the rearfoot was used to represent midtarsal joint rotation. However, it has been shown that the first metatarsal may move relative to the navicular (Cornwall and McPoil, 2002) and therefore, the measurements cannot be construed to strictly represent that of the midtarsal joint. Secondly, to enable tracking of markers on the forefoot, subjects performed the running trials barefoot. Although calcaneal and tibial movement patterns have been shown to not differ substantially between barefoot and shod running (Stacoff et al., 2000), it is likely that the midtarsal joint behaves differently between bare and shod-foot running due to rigidity of the shoe in the midfoot area. Although future research will need to continue improving multi-segment foot models, the results of this study provide a useful preliminary insight into how the forefoot, rearfoot and shank interact during running.

7.5 Conclusions

Rearfoot frontal plane motion was found to have strong continuous coupling with transverse shank rotation, forefoot sagittal plane motion and forefoot transverse plane motion regardless of alterations in step width. In contrast, coupling between rearfoot frontal plane motion and forefoot frontal plane motion was poor to non-existent. These findings suggest that forefoot motion has an important influence on subtalar joint kinematics.

Chapter 8 - Forefoot, Rearfoot and Shank Coupling: Effect of Variations in Speed and Mode of Gait

8.1 Introduction

The link between foot pronation and shank internal rotation has long been a focus of injury research due to the theory that the two segments are mechanically coupled as a consequence of anatomy at the ankle-joint-complex (Hicks, 1953). It has been suggested that rearfoot frontal plane motion (eversion/inversion) is transferred into transverse tibial rotation (internal/external) via the subtalar joint, which is believed to function as a mitered hinge (Inman et al., 1981). Consequently, abnormal foot movements can alter normal kinematics and kinetics of the lower limb, resulting in increased risk of injury to bone and/or soft tissue structures (James and Jones, 1990; Tiberio, 1987).

Although extensive research into the mechanical coupling between the foot and shank exists, it remains unclear whether the relationship is stable across different speeds and modes of gait. For example, inconsistencies appear between walking and running in terms of kinematic coupling at the subtalar joint. During running, research has shown the general pattern of motion as being rearfoot eversion accompanied by shank internal rotation during the first half of stance, with these motions reversed during the latter half of stance (McClay and Manal, 1998; Nigg et al., 1993). However, evidence indicating a similar kinematic coupling relationship during walking is less compelling. While studies generally agree that the shank internally rotates until approximately 14-21% of stance and then externally rotates (Hunt et al., 2001; Leardini et al., 1999), there is no clear consensus regarding rearfoot frontal plane motion. For instance,

some studies found that the rearfoot everts until 25-35% of stance before it inverts (Hunt et al., 2001; Liu et al., 1997), while others suggest the rearfoot continues to evert until after 50% of stance (Cornwall and McPoil, 2002; Woodburn et al., 2002). The latter studies suggest that kinematic coupling is different during walking and running but a study confirming this has yet to be conducted.

It has been shown that changes in running speed can alter the timing between rearfoot frontal plane and knee sagittal plane motion (Hamill et al., 1992; Stergiou et al., 1999). During running it has been postulated that both rearfoot eversion and knee flexion induce shank internal rotation, whereas rearfoot inversion and knee extension induce shank external rotation (Tiberio, 1987). Therefore, any disruption in the co-ordination of rearfoot eversion/inversion and knee flexion/extension would result in opposing torques at the proximal and distal ends of the tibia, thus increasing stresses placed on the joints (Hamill et al., 1992; Stergiou et al., 1999). However, no study has yet investigated whether the kinematic coupling between the rearfoot eversion/inversion and shank internal/external rotation changes with running speed.

The recent use of multi-segment foot models has provided a deeper insight into the kinematic relationship between the foot and lower limb (Carson et al., 2001). Such research has provided evidence that the midfoot joints contribute more to overall foot motion than was previously believed. As the talus, which transfers motion of the calcaneus to the tibia, also shares an articulation with the navicular (talonavicular joint), motion of the rearfoot must have some affect on motion of the midfoot and visa versa. It is therefore pertinent to include an analysis of the midfoot joints when examining the coupling mechanisms between the foot and shank. In the present study

we use such an approach to determine whether the kinematic coupling between the forefoot, rearfoot and shank differed between walking and running, and/or across running speeds.

8.2 Methods

Subjects

Sixteen subjects (eight males, eight females; mean (SD) age, 22.8 (4.1) years; body mass, 62.2 (11.3) kg; and height, 171.8 (8.2) cm) volunteered to participate. Inclusion criteria were that subjects were currently engaging in at least two hours per week of exercise involving running, had been free from injury of the lower extremity in the last six months, had no obvious anatomical malalignment and did not wear foot orthotics. The study was approved by the institutional ethics committee, and written informed consent was obtained from all subjects.

Experimental protocol and Equipment

The marker and camera configurations were setup according to the description in the general methods chapter (see methods sections 4.2 and 4.3.1). Prior to commencement of the dynamic trials a calibration trial was recorded: subjects assumed a standardised standing position with the heel centres 0.18m apart and the feet angled 12° to each other (McIlroy and Maki, 1997).

Four different speeds were compared during this study. These speeds were determined by asking subjects to walk barefoot on a treadmill (Quinton Fitness Equipment, USA) while the speed was gradually increased by the experimenter.

Subjects were instructed to maintain a walking gait until they could no longer refrain from running, at which point the treadmill speed was recorded as maximum walking speed (W_{max}). Four experimental speeds were then computed: a walking condition (Walk) at 50% of W_{max}; and three running speeds conducted at W_{max} (Slow), 120% of W_{max} (Medium) and 140% of W_{max} (Fast). This protocol enabled the experimental speeds for each subject to be standardised relative to their maximum walking speed.

Subjects then practised over-ground barefoot walking/running at each of the four pre-determined speeds. Using timing gates to monitor speed along with verbal feedback, subjects practiced until they acquired the target speed to within ± 5%, after which the experimenter adjusted the start of their run-up so the subject's right foot landed fully on the force plate without under- or over-striding. Following a short rest subjects completed, in block random order, 10 trials at each speed. Data collection was conducted using seven ProReflex cameras (Qualisys Medical AB, Sweden) arranged around a force plate (Kistler, Switzerland) positioned in the middle of the runway. Kinematic data were collected at 240Hz and ground reaction force (not presented here) at 960Hz.

Data Reduction

Five trials for each speed condition were randomly selected for analysis. Raw co-ordinate data were filtered using a fourth order low-pass Butterworth filter with a cut-off frequency of 12Hz. The cut-off frequency was determined by residual analysis of markers SHN1, SCAL, D1MT (methods section 4.4)

The shank, rearfoot and forefoot were modelled as rigid segments adapted from those described by Carson et al. (2001). Calculation of three-dimensional joint rotations (for details see methods section 4.3.8) enabled interpretation of motion in clinical terms of dorsiflexion/plantarflexion (sagittal plane), inversion/eversion (frontal plane) and abduction/adduction (transverse plane). Rearfoot abduction/adduction was expressed as shank internal/external rotation throughout to be more in fitting with the literature. All angles were referenced to the standing position determined from the calibration trial. Ground reaction forces (GRF) were used to determine the onset (touch-down) and offset (toe-off) of the stance phase. All kinematic parameter files were normalised to 100 data points from touch-down to toe-off using a cubic spline interpolation. The kinematic curves from the five trails of each condition (speed) were averaged for each subject. This was done by calculating the mean angle at each of the 100 time points to create a new ensemble average curve. The average curves of all subjects were then processed in a similar manner to create a mean ensemble average curve for each speed condition (N =16).

Data Analysis

The following discrete variables were identified for each trial and subject: peak rearfoot eversion, rearfoot eversion excursion, time to maximum rearfoot eversion, peak shank internal rotation, shank internal rotation excursion, time to maximum shank internal rotation, forefoot dorsiflexion excursion, time to maximum forefoot dorsiflexion, forefoot abduction excursion and time to maximum forefoot abduction. Excursions were defined as the difference between the maximum value and the value at foot strike, and event timings were determined as a percentage of stance time. Data from all five trials for each subject were analysed using one-way repeated measures

analysis of variance (ANOVA) with both repetition and speed as repeated measures. Post-hoc analysis was performed using Tukey's multiple comparison tests. Significance was set at an alpha level of $P < 0.05$ and all statistical analysis was undertaken using Statistica 4.0 (SuperStat, USA).

To examine the continuous coupling between adjacent segments, kinematic data for one segment was compared to kinematic data for the adjacent segment. This involved calculating the cross-correlation coefficient between the angular displacement curves of adjacent segments across the stance phase (Li and Caldwell, 1999). This involved calculating the cross-correlation coefficient between the angular displacement curves of adjacent segments across the stance phase. The cross-correlation was performed on every trial (4 conditions x 5 trials = 20 trials) for each subject (see section 7.2 for calculation formula). The mean value for each speed condition was then calculated using the five cross-correlations obtained for each subject (N = 16). This approach was used to determine coupling between the following segmental rotations: rearfoot eversion/inversion (EVE/INV) and shank internal/external (IR/ER) rotation, rearfoot EVE/INV and forefoot plantarflexion/dorsiflexion (PF/DF), rearfoot EVE/INV and forefoot EVE/INV, rearfoot EVE/INV and forefoot abduction/adduction (ABD/ADD). Correlation coefficients greater than 0.7 (or less than -0.7) indicated a strong coupling between the two segmental rotations. Coefficients of between 0.3 to 0.69 and -0.3 to -0.69 represented a moderate coupling, and coefficients of between -0.3 and 0.3 suggested weak or no coupling. The correlation value with a zero phase shift was considered of primary importance in the investigation since this measured the curve congruity of the segmental rotations occurring about a common joint as they happened in real time. This was based on the premise that with good mechanical

coupling there should be no evidence of a phase shift between the kinematics of adjacent segments. For this reason an exact measure of phase relationships was not considered necessary.

To indicate whether adjacent segments had similar angular excursion magnitudes or whether one segment had a greater angular excursion than the adjacent segment, vector coding values were determined (Heiderscheit et al., 2002). First an angle-angle diagram for the two segments of interest was constructed, then the angle of the resultant trajectory between two successive data points was calculated (Ferber et al., 2005):

$$\phi_i = \text{abs}\left[\tan^{-1}\left(y_{i+1} - y_i / x_{i+1} - x_i\right)\right]$$

where y represented the distal segment, x the proximal segment and i = 1,2, and n. The vector coding was performed on every trial (4 conditions x 5 trials = 20 trials) for each subject. The mean value for each speed condition was then calculated using the five vector coding values obtained for each subject (N = 16). A coupling angle of 45° indicated that equal amounts of angular displacement occurred in the two segments. An angle greater than 45° indicated a greater movement of the distal segment relative to the proximal segment. In addition the vector coding curves (across stance) from the five trails of each condition (speed) were averaged for each subject. This was done by calculating the mean angle at each of the 100 time points to create a new ensemble average curve. The average curves of all subjects were then processed in a similar manner as highlighted above to create a mean ensemble vector coding curve for each speed condition (N =16).

8.3 Results

Group ensemble angular displacements of the shank, rearfoot and forefoot are shown in Figure 8.1 In general, there was no difference in the kinematic curve patterns between the three running speeds, but segmental kinematics for walking were different to those for running. Specific differences between walking and running and across the running speeds are described in the following sections.

Segmental Kinematics

Repetition had no effect on any of the kinematic variables analysed ($P > 0.10$) indicating there was no learning effect between trials. It also indicated that the differences found between speed conditions were reliable. Group mean kinematic variables for the forefoot, rearfoot and shank are presented in Table 8.1. The only variable which significantly changed between the three running speeds was that peak shank internal rotation occurred earlier in the stance phase in slow running compared to fast running ($P < 0.05$). There were, however, a number of notable differences between walking and running. Both peak rearfoot eversion ($P < 0.001$) and peak shank internal rotation ($P < 0.05$) were significantly lower in walking. Rearfoot eversion excursion during walking was reduced compared to running, as was both forefoot dorsiflexion and abduction excursion. Peak shank internal rotation was found to occur substantially earlier in walking but peak eversion occurred approximately 11% later ($P < 0.001$). Additionally, the time to peak forefoot abduction remained unchanged between conditions but peak forefoot dorsiflexion occurred later in stance during walking ($P < 0.001$). No significant differences were observed between conditions for shank internal rotation excursion.

Table 8.1. Group mean (SD) foot and shank kinematic variables for walking and slow, medium and fast running conditions. Significant differences between conditions ($P < 0.05$) are shown by superscript.

Variables	**Walk**	**Slow run**	**Medium run**	**Fast run**
Speed (ms^{-1})	1.2* (0.1)	2. 5* (0.3)	2.9* (0.3)	3.5* (0.4)
Rearfoot peak EVE (°)	-5.5* (2.5)	-10.4 (3.3)	-10.4 (3.4)	-10.6 (3.5)
Shank peak IR (°)	-6.5* (2.8)	-8.2 (2.8)	-8.2 (2.8)	-8.1 (3.1)
Rearfoot EVE excursion (°)	-7.3* (2.2)	-12.4 (3.3)	-12.7 (2.7)	-13.1 (2.7)
Shank IR excursion (°)	-5.5 (2.2)	-6.8 (3.1)	-6.8 (2.9)	-6.7 (2.7)
Forefoot DF excursion (°)	7.0* (1.6)	9.6 (3.4)	9.9 (3.1)	10.5 (3.1)
Forefoot ABD excursion (°)	-4.3* (1.4)	-6.0 (1.7)	-6.0 (1.7)	-6.2 (1.6)
Time to peak EVE (%stance)	54.7* (11.1)	44.0 (5.7)	44.6 (6.0)	44.5 (4.6)
Time to peak Shank IR (%stance)	17.0* (5.0)	36.5**fast (14.5)	38.9 (12.3)	42.7**slow (11.3)
Time to peak forefoot DF (%stance)	71.2* (8.2)	51.2 (5.6)	52.2 (5.3)	52.7 (4.8)
Time to peak forefoot ABD (%stance)	48.2 (19.6)	52.4 (6.3)	52.2 (9.2)	51.4 (8.6)

* Significantly different from all other speeds
** Significantly different from the speed condition shown by the superscript

Joint Coupling

Table 8.2 presents group mean cross-correlation values for the various segmental rotations. Once again, values were very similar between the three different running

conditions for all variables assessed, and there were some obvious differences between walking and running. During running, correlations between rearfoot EVE/INV and shank IR/ER were consistently high ($r \geq 0.95$) whereas a much lower value was observed during walking ($r = 0.49$). Slightly lower cross-correlation values were also observed for walking compared to running for the segmental coupling of rearfoot EVE/INV with both forefoot PF/DF (walking, $r = -0.80$; running, $r = -0.96$) and forefoot ABD/ADD (walking, $r = 0.91$; running, $r = 0.97$). The only segmental coupling where walking resulted in higher cross-correlations than running was between rearfoot EVE/INV and forefoot EVE/INV, which returned an r value of 0.41 compared to a maximum r value in running of 0.15 (Table 8.2).

Table 8.2. Mean (SD) cross-correlations between rearfoot eversion/inversion, and shank internal/external rotation and forefoot motion in each plane.

Variables	**Walk**	**Slow run**	**Medium run**	**Fast run**
Rearfoot EVE/INV _ Shank IR/ER	0.49 (0.22)	0.95 (0.04)	0.96 (0.03)	0.96 (0.03)
Rearfoot EVE/INV _ Forefoot PF/DF	-0.80 (0.19)	-0.97 (0.03)	-0.97 (0.03)	-0.96 (0.04)
Rearfoot EVE/INV _ Forefoot EVE/INV	0.41 (0.37)	0.08 (0.51)	0.13 (0.52)	0.15 (0.57)
Rearfoot EVE/INV _ Forefoot ABD/ADD	0.91 (0.05)	0.97 (0.02)	0.97 (0.02)	0.97 (0.02)

Mean (standard deviation) vector coding angles are presented in Table 8.3. Values of 56 to 58° between rearfoot EVE/INV and shank IR/ER during running suggest that rearfoot frontal plane excursions exceeded those of transverse shank rotation. There

was also greater rearfoot EVE/INV compared to forefoot ABD/ADD during running and walking indicated by values of 24 to 32°. Rearfoot EVE/INV and forefoot PF/DF were found to occur with similar excursion magnitudes as highlighted by coupling angles of 41 to 43°. Group ensemble vector coding plots over the entire stance phase are shown for the different modes of gait and running speed conditions in figure 8.2. The coupling angle curves (vector coding) when rearfoot EVE/INV was paired with shank IR/ER (Figure 8.2a) and all forefoot planar movements (Figures 8.2b-8.2d) were very similar between the three running speeds. Walking, however, induced a markedly different response to running in all four coupling angle curves.

Table 8.3. Mean (SD) vector coding angles (in degrees) between rearfoot eversion/inversion, and shank internal/external rotation and forefoot motion in each plane.

Variables	**Walk**	**Slow run**	**Medium run**	**Fast run**
Rearfoot EVE/INV _ Shank IR/ER	48.6 (5.6)	56.4 (5.0)	56.4 (5.6)	57.5 (5.4)
Rearfoot EVE/INV _ Forefoot PF/DF	40.9 (5.4)	42.2 (5.7)	41.9 (5.7)	42.0 (5.6)
Rearfoot EVE/INV _ Forefoot EVE/INV	40.3 (4.3)	26.9 (6.0)	26.7 (5.6)	25.2 (4.9)
Rearfoot EVE/INV _ Forefoot ABD/ADD	31.7 (5.3)	25.5 (3.3)	24.7 (3.0)	24.9 (3.7)

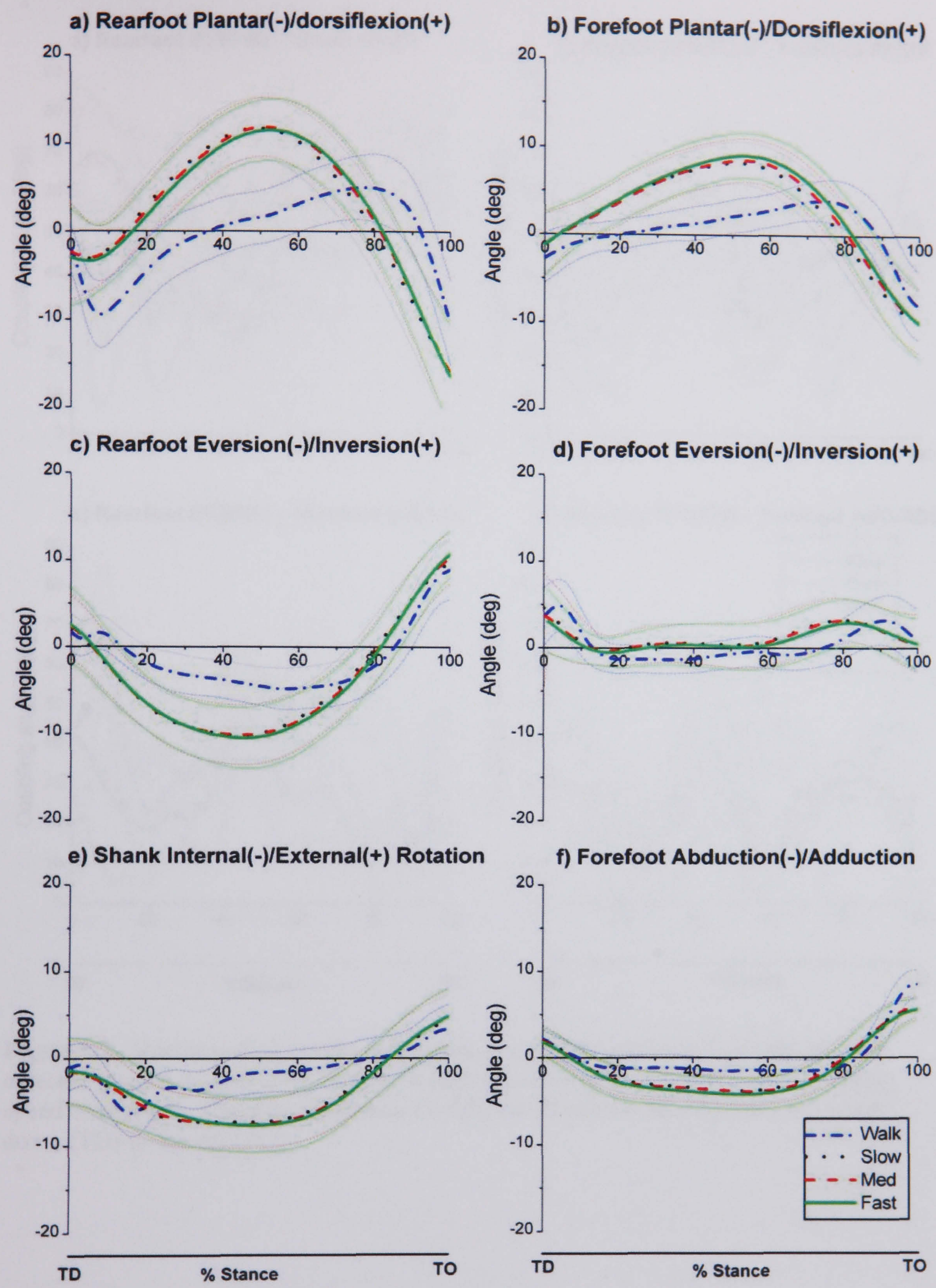

Figure 8.1. Angular displacement curves for the forefoot, rearfoot and shank for walking and slow, medium and fast running conditions. The ensemble mean (±SD) for all subjects are shown from touch-down (TD) to toe-off (TO).

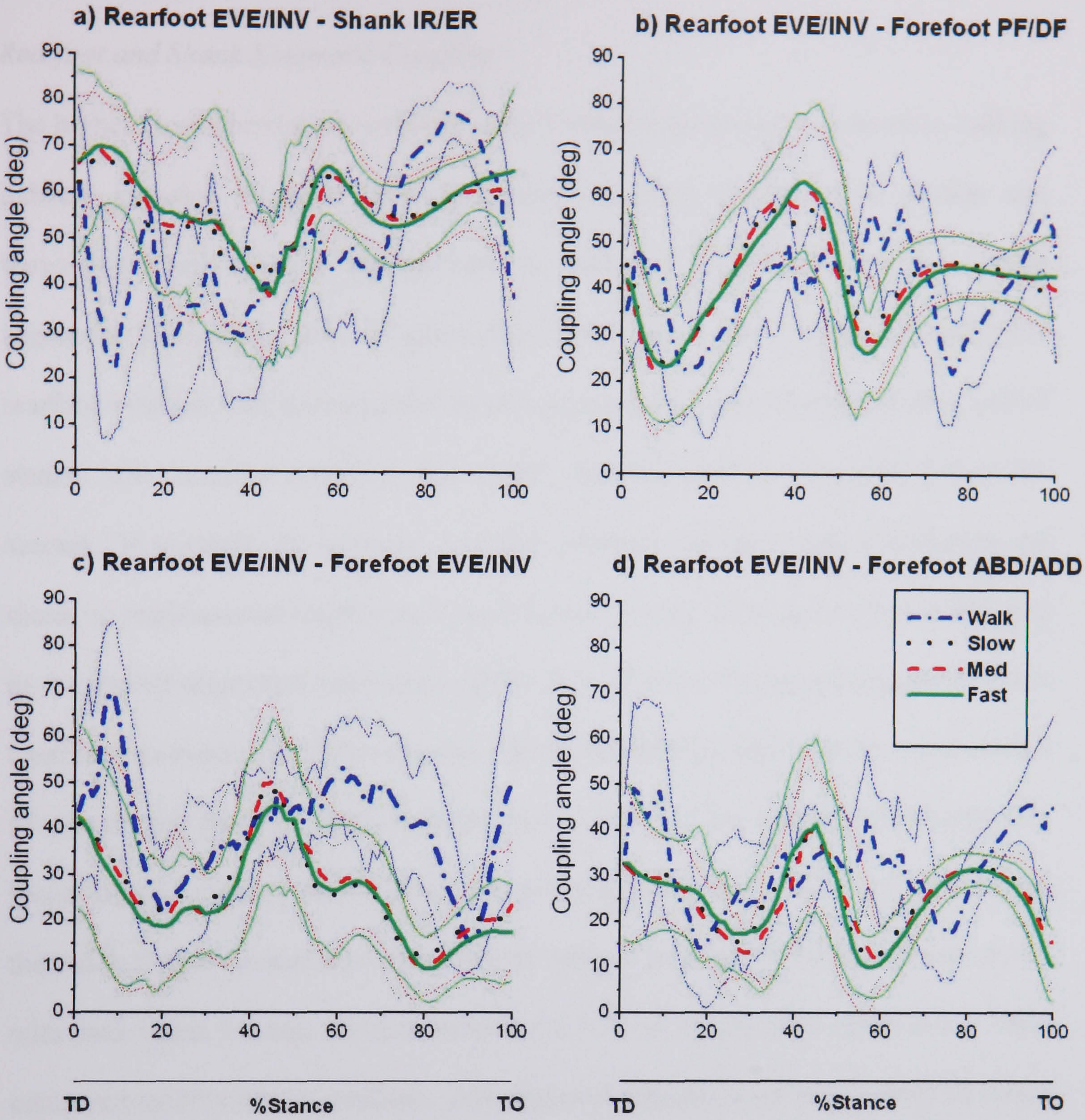

Figure 8.2. Vector coding curves of rearfoot eversion/inversion with shank internal/ external rotation and forefoot motion in each plane for walking and different running speed conditions. The ensemble mean (± SD) are shown for all subjects from touch-down (TD) to toe-off (TO).

8.4 Discussion

Rearfoot and Shank Kinematic Coupling

The higher cross-correlation coefficients for running (all speeds) compared to walking indicate superior temporal coupling between rearfoot frontal plane motion and transverse shank rotation during running, which is highlighted by the similar segmental kinematic curves (Figures 8.1c and 8.1e). These figures indicate that rearfoot eversion was accompanied by shank internal rotation during the first half of stance, with rearfoot inversion and shank external rotation occurring during the second. In contrast, the temporal coupling between rearfoot eversion/inversion and shank internal/external rotation was much weaker during walking, and this is reflected in the altered segmental kinematics (Table 8.1). Firstly, during walking the rearfoot continued to evert until 55% of stance which corresponds well with previous studies (Cornwall and McPoil, 2002; Moseley et al., 1996). This was approximately 10% longer into the stance phase compared with running. Secondly and more importantly, the shank began to externally rotate earlier when compared to running (Figure 8.1e), with peak shank internal rotation occurring at 17% of stance (Woodburn et al., 2002) compared to 37% during running. This demonstrates that for a large period of stance in walking, the shank was externally rotating even though the rearfoot continued to evert. This suggests there was not always temporal coupling between rearfoot frontal plane motion and transverse shank plane motion since, for a period of stance, the two segments underwent angular displacements in opposing directions. This finding has important implications for the theory that asynchronous timing between the knee and subtalar joint is a risk factor in chronic injuries of the lower extremity (Hamill et al., 1992) since it demonstrates that rearfoot eversion/inversion is not necessarily coupled

with shank internal/external rotation. Thus in walking the actions of the subtalar and knee joints cannot be assumed to be coupled via transverse rotation of the shank.

In contrast, during running good kinematic coupling in terms of curve congruity was found between rearfoot frontal and shank transverse plane motion, even though the magnitude of angular displacements that each segment underwent were different. Rearfoot eversion excursion values were greater than internal rotation excursions of the shank, a finding consistent with the literature (McClay and Manal, 1997; Nigg et al., 1998). This pattern of greater angular displacement of the rearfoot relative to the shank is reflected by the vector coding values which exceeded 45°. This implies that not all the frontal plane motion of the rearfoot was transferred to the shank, and instead some may have been absorbed by the talus, which supports previous findings indicating that the tibia and talus rotate relative to each other (Arndt et al., 2004). The vector coding plots (Figure 8.2a) also indicated that the coupling angle curves were of a very similar pattern across the stance phase for all three running conditions. This implies that the kinematic coupling between rearfoot frontal plane and shank transverse plane motion across the entire stance phase was not significantly affected by changes in running speed. Contrastingly, the coupling angle curve for walking was very different to those found during running indicating that weaker kinematic coupling was evident throughout the whole of stance. The largest discrepancies between walking and running curves, however, were found close to touch-down or toe-off as indicated by the largest differences in coupling angle (Figure 8.2a).

Peak shank internal rotation, which was achieved earlier during the fast condition relative to the slow condition, was the only discrete kinematic variable that changed

with running speed. This is in contrast to Andrew (1990), who found greater rearfoot eversion excursions occurred with increasing speed. This may be attributable to the range of running speeds utilised in the different studies; Andrew (1990) tested at speeds up to 6.0 ms^{-1} whereas the maximum speed in the present study was 3.5 ms^{-1}.

Forefoot and Rearfoot Kinematic Coupling

The temporal coupling of rearfoot frontal plane motion and forefoot sagittal plane motion was high during running and walking (Table 8.2) and vector coding values of 40-43° (Table 8.3) suggest that the magnitude of angular displacements of both segments were similar. In general, rearfoot eversion was accompanied by forefoot dorsiflexion during the first half of stance and forefoot plantarflexion occurred in conjunction with rearfoot inversion during the latter half of stance (Figures 8.1c, 8.1b). Although there is limited literature regarding forefoot kinematics during running, the walking curves show good pattern agreement with previous studies that have used a forefoot model (Carson et al., 2001; Hunt et al., 2001). A slightly lower cross-correlation was found during walking (-0.80) compared to running (-0.97), which may be a result of the prolonged period of forefoot dorsiflexion during walking (Figure 8.1b). During running, the forefoot began to plantarflex 8% later in stance than the beginning of rearfoot inversion, whereas during walking, this delay was extended to 17% of stance (Table 8.1). Sagittal plane forefoot motion has been shown to be synonymous with motion of the medial longitudinal arch of the foot (Hunt et al., 2001), a common measure of foot pronation/supination. Therefore, forefoot dorsiflexion could be implied to represent the collapse of the medial arch and thus foot pronation, and forefoot plantarflexion the rebound of the medial arch and foot supination. In the present study, the motion of the rearfoot during walking indicated

that the foot began to supinate after 55% of stance, whereas motion of the forefoot suggests that pronation was still occurring until 71% of stance. This implies that rearfoot eversion may not be reflective of whole foot pronation since the subtalar and midtarsal joints appear to be acting independently of one another.

Poor kinematic coupling was found between the motions of rearfoot eversion/inversion and forefoot eversion/inversion as indicated by low cross-correlation values (Table 8.2), which is in agreement with the previous study (chapter 7). Although a slightly better cross-correlation was evident during walking, the low values suggest that the angular displacements of these two segments in this plane are largely independent of one another. The kinematic pattern of forefoot eversion/inversion closely matched those previously published (Hunt et al., 2001; Woodburn et al., 2004). However, the high standard deviations for the cross-correlations indicated that coupling between rearfoot and forefoot frontal plane motion was subject dependent, thus the general trends should be interpreted with caution.

Coupling between rearfoot frontal and forefoot transverse plane motion was high during both running and walking (Table 8.2), even though forefoot transverse plane motion was minimal, especially during mid-stance (Figure 8.1d). Vector coding values of less than 32° reflect the reduced forefoot transverse motion compared to rearfoot frontal plane motion (Table 8.3). Closer inspection of the vector coding graphs reveals that the coupling angle was below 45° for most of the stance phase which means that forefoot transverse excursions were smaller then rearfoot excursions across the entirety of stance (Figure 8.2d). In general, the forefoot underwent

abduction during the first 20% of stance followed by a period of minimal motion during midstance, after which adduction occurred until toe-off. The kinematic patterns of forefoot transverse plane motion are in accord with those reported by Hunt et al. (2001).

There was no difference in the coupling relationship between the three running speeds when any of the forefoot planar motions were paired with rearfoot frontal plane motion. This implies that the different running speeds used within this study did not induce any alterations in midtarsal joint coupling.

Midfoot (midtarsal) Joint Function

The sagittal and transverse movements of the forefoot in the present study lend partial support to a theoretical model of midtarsal joint function (Elftman, 1960; Manter, 1941). In this model, two axes of motion are said to exist through the midtarsal joint. One of these axes is oblique, and movement about this consists of dorsiflexion in conjunction with abduction, or plantarflexion in conjunction with adduction. The findings in the present study indicate that during running dorsiflexion and abduction occurred during loading followed by plantarflexion and adduction during propulsion. Additionally, this forefoot motion occurred in conjunction with rearfoot eversion/inversion, suggesting a kinematic link between rearfoot frontal plane motion and motion about the midtarsal joint. However, since the forefoot continued to dorsiflex after the rearfoot had already begun to invert, the kinematic coupling between rearfoot frontal plane motion and midtarsal joint function may not be as interdependent on one another as has previously been believed (Donatelli, 1996).

The second axis in the proposed midtarsal joint model (Elftman, 1960; Manter, 1941) runs longitudinally through the foot. It is speculated that inversion and eversion are the primary rotations about this axis, with inversion occurring during the loading phase of walking and eversion occurring during midstance and propulsion (Cornwall and McPoil, 2002). In their study midtarsal joint motion was modelled as angular motion between the navicular and calcaneus, and they also reported rotation of the first metatarsal relative to the navicular (2002). Interestingly they found that rotations between the metatarsal and navicular in the frontal plane were essentially opposite in direction to the rotations occurring between the navicular and calcaneus. In the present study a very different kinematic pattern was evident (Figure 8.1d), which may have been partly due to how the midtarsal joint was modelled. The present study modelled the midtarsal joint based on angular displacement of the forefoot segment relative to the rearfoot. Consequently, it was difficult to differentiate movements that occurred proximal (midtarsal joints) or distal to the navicular (tarsometatarsal joints). Therefore, caution must be taken when applying the findings of the present study to represent the actual motion of the midtarsal joint. Further research aimed at developing more advanced multi-segment foot models may help to unlock the intricate mechanics of the foot in more detail.

8.5 Conclusion

Rearfoot frontal plane motion had strong temporal coupling with transverse shank rotation, forefoot sagittal plane motion and forefoot transverse plane motion regardless of running speed. Kinematic coupling of the rearfoot frontal plane with shank rotation and forefoot sagittal plane was lower in walking compared to running.

In both walking and running, there was little evidence of coupling between rearfoot frontal plane and forefoot frontal plane motion. These findings suggest that kinematic coupling between the forefoot, rearfoot and shank is much stronger during running relative to walking. In particular, the low coupling between rearfoot eversion/inversion and shank internal/external rotation implies that rearfoot frontal plane motion and knee sagittal plane motion are not necessarily linked via transverse shank rotation, which has been assumed in previous injury models.

Chapter 9 - Forefoot, Rearfoot and Shank Coupling: Effect of Variations in Foot Strike Pattern

9.1 Introduction

It has been previously shown that changes in step width can alter rearfoot kinematics (Williams and Ziff, 1991), and the earlier experimental chapter (chapter 7) was undertaken to determine if such changes would also effect the kinematic coupling between the foot and shank. Similarly, Stacoff et al. (1989) found that the position of the foot at touchdown could influence rearfoot motion during early stance. They reported that when using a forefoot touchdown during running, rearfoot eversion excursion was lower in comparison to when a rearfoot touchdown was used. Thus it was postulated in the present study that any changes in rearfoot motion would in turn alter shank and forefoot kinematics if they were kinematically coupled with the rearfoot via the subtalar and midtarsal joints respectively.

Stacoff et al. (1989) also observed that forefoot frontal plane kinematics were affected by the foot strike pattern used. It was found that an increased amount of forefoot eversion was evident during heel strike running compared to forefoot strike running. This was confirmed in a later study, which demonstrated that forefoot kinematics in forefoot strike running was influenced by whether subjects touched the ground with their heel or not (Stacoff et al., 1991). In the previous experimental chapter, foot-strike pattern was not controlled for and this may explain the large between-subject variation present in the kinematic curves. This begs the question whether the variation observed was due to different subjects adopting different foot strike patterns. Thus the purpose of the present study was to determine if the kinematic coupling

between the forefoot, rearfoot and shank differed due to the type of foot strike pattern used.

9.2 Methods

Subject Population

Twelve subjects (six males, six females; mean (SD) age, 21.3 (1.9) years; body mass, 67.5 (13.1) kg; and height, 1.74 (0.09) m) volunteered to participate. Inclusion criteria were that subjects were currently engaging in at least two hours per week of exercise involving running, had been free from injury of the lower extremity in the last six months, had no obvious anatomical malalignment and did not wear foot orthotics. The study was approved by the institutional ethics committee, and written informed consent was obtained from all subjects.

Experimental Protocol

Participants practised barefoot running along the runway at a self-selected jogging speed which was recorded using timing gates and then later used as the baseline self-selected speed for all subsequent trials. Subjects were then given time to practise barefoot running using three different foot strike patterns. These were: a heel strike condition (HFS) where the heel was first part of the foot to touchdown; a forefoot strike condition (FFS) where the forefoot was the first part of the foot to touchdown, with the heel subsequently making contact with the ground; and a toe running condition (TFS) where the forefoot was the first part of the foot to touchdown but the heel remained off the floor throughout the whole of stance. Using timing gates to monitor speed along with verbal feedback, subjects practiced until they acquired the

target (baseline) speed within approximately ± 5%, after which the experimenter adjusted the start of their run-up so that the subject's right foot landed fully on the force plate. Following a short rest subjects then completed, in block random order, 10 trials using each foot strike pattern. A successful trial was defined as one where the subject's right foot landed fully on the force plate using the desired foot strike pattern (later confirmed by looking at the marker trajectory paths in the QTM software) without under or over striding and running speed was within 5% of the target speed. All subjects were able to comfortably and successfully complete the testing session within a two hour period and no subjects took more than 60 trials to complete the entire data collection session.

Data Reduction

Five trials for each foot strike condition were randomly selected for analysis. Raw co-ordinate data were filtered using a fourth order low-pass Butterworth filter with a cut-off frequency of 12Hz (see methods section 4.4).

The marker and camera setups were identical to the previous experimental chapters (sections 4.2 and 4.3.1). The shank, rearfoot and forefoot were modelled as rigid segments (section 4.3) adapted from those described by Carson et al. (2001). Calculation of three-dimensional joint rotations (section 4.3.8) enabled interpretation of motion of the distal relative to the proximal segment in clinical terms of dorsiflexion/plantarflexion, inversion/eversion and adduction/abduction (or shank external/internal rotation). All angles were referenced to a standardised standing reference trial (see methods section 4.2.3). Ground reaction forces (GRF) were used to determine touchdown and toe-off for the stance phase. All kinematic parameter

files were normalised to 100 data points from touch-down to toe-off using a cubic spline interpolation. The kinematic curves from the five trails of each condition (foot strike) were averaged for each subject. This was done by calculating the mean angle at each of the 100 time points to create a new ensemble average curve. The average curves of all subjects were then processed in a similar manner to create a mean ensemble average curve for each foot strike condition (N =12).

Data Analysis

The following discrete variables were identified for each trial and subject: rearfoot eversion excursion, time to maximum rearfoot eversion, shank internal rotation excursion, time to maximum shank internal rotation, forefoot dorsiflexion excursion, time to maximum forefoot dorsiflexion, forefoot abduction excursion and time to maximum forefoot abduction. Data from all five trials for each subject were analysed using one-way repeated measures analysis of variance (ANOVA) with both repetition and speed as repeated measures. Post-hoc analysis was performed using Tukey's multiple comparison tests. Significance was set at an alpha level of $P < 0.05$ and all statistical analysis was undertaken using Statistica 4.0 (SuperStat, USA).

To examine the continuous coupling between adjacent segments, kinematic data for one segment was compared to kinematic data for the adjacent segment. This involved calculating the cross-correlation coefficient between the angular displacement curves of adjacent segments across the stance phase (Li and Caldwell, 1999). This involved calculating the cross-correlation coefficient between the angular displacement curves of adjacent segments across the stance phase. The cross-correlation was performed on every trial (3 conditions x 5 trials = 15 trials) for each subject (see section 7.2 for

calculation formula). The mean value for each foot strike condition was then calculated using the five cross-correlations obtained for each subject (N = 12). This approach was used to determine coupling between the following segmental rotations: rearfoot eversion/inversion (EVE/INV) and shank internal/external (IR/ER) rotation, rearfoot EVE/INV and forefoot plantarflexion/dorsiflexion (PF/DF), rearfoot EVE/INV and forefoot EVE/INV, rearfoot EVE/INV and forefoot abduction/adduction (ABD/ADD). Correlation coefficients greater than 0.7 (or less than -0.7) indicated a strong coupling between the two segmental rotations. Coefficients of between 0.3 to 0.69 and -0.3 to -0.69 represented a moderate coupling, and coefficients of between -0.3 and 0.3 suggested weak or no coupling. The correlation value with a zero phase shift was considered of primary importance in the investigation since this measured the curve congruity of the segmental rotations occurring about a common joint as they happened in real time. This was based on the premise that with good mechanical coupling there should be no evidence of a phase shift between the kinematics of adjacent segments. For this reason an exact measure of phase relationships was not considered necessary.

To indicate whether adjacent segments had similar angular excursion magnitudes or whether one segment had a greater angular excursion than the adjacent segment, vector coding values were determined (Heiderscheit et al., 2002). The vector coding was performed on every trial (3 conditions x 5 trials = 15 trials) for each subject (see section 8.2 for calculation formula). The mean value for each foot strike condition was then calculated using the five vector coding values obtained for each subject (N = 12). A coupling angle of 45° indicated that equal amounts of angular displacement occurred in the two segments. An angle greater than 45° indicated a greater

movement of the distal segment relative to the proximal segment. In addition the vector coding curves (across stance) from the five trails of each condition (foot-strike) were averaged for each subject. This was done by calculating the mean angle at each of the 100 time points to create a new ensemble average curve. The average curves of all subjects were then processed in a similar manner to create a mean ensemble vector coding curve for each speed condition (N =12).

9.3 Results

The mean (SD) running speed for all subjects of 3.5 (0.2) ms^{-1} indicated small between-subject variability. This speed was comparable to the running speeds used in the previous experimental studies (chapters 7 and 8). Repetition had no effect on any of the kinematic variables analysed ($P > 0.05$). This indicated there was no learning or fatigue effects between trials and thus that any differences between conditions were due to the manipulation of foot-strike pattern.

Segmental Kinematics

Mean ensemble angular displacements of the rearfoot relative to the shank and forefoot relative to the rearfoot are shown in Figure 9.1. These curves are the ensembled average for the group and as they have relatively small standard deviations the figure highlights the consistency across subjects. Group mean kinematic variables for the forefoot, rearfoot and shank are presented in Table 9.1. There were a number of differences between heel strike, forefoot strike and toe running. Excursion values for rearfoot EVE ($P < 0.001$), shank IR ($P < 0.01$), forefoot DF ($P < 0.001$) and forefoot ABD ($P < 0.001$) were all significantly lower during heel strike running.

Rearfoot peak EVE ($P < 0.001$) and shank peak IR ($P < 0.001$) were greater in heel strike running compared to both forefoot strike and toe running, and values for rearfoot peak EVE in toe running were lower than those found in the forefoot strike condition ($P < 0.001$). There was no difference between conditions in terms of time of peak rearfoot EVE ($P = 0.514$) or peak shank IR ($P = 0.138$) but both peak forefoot DF ($P < 0.01$) and peak forefoot ABD ($P < 0.01$) occurred significantly later in heel strike running.

Table 9.1. Group mean (SD) foot and shank kinematic variables for heel strike (HFS), forefoot strike (FFS) and toe (TFS) running conditions. Significant differences between conditions ($P < 0.05$) are shown by superscript.

Variables	**HFS**	**FFS**	**TFS**
Rearfoot peak EVE (°)	-11.1 (2.8)	-9.1$^{heel, toe}$ (3.0)	-6.2$^{heel, fore}$ (2.6)
Shank peak IR (°)	-8.4 (2.9)	-7.2^{toe} (3.2)	-5.0$^{heel, fore}$ (3.4)
Rearfoot EVE excursion (°)	-12.0 (2.7)	-17.9^{heel} (4.3)	-17.6^{heel} (3.2)
Shank IR excursion (°)	-5.8 (2.0)	-8.2^{heel} (2.6)	-7.4^{heel} (2.2)
Forefoot DF excursion (°)	7.3 (1.8)	13.0^{heel} (2.4)	13.9^{heel} (2.1)
Forefoot ABD excursion (°)	-3.7 (1.2)	-6.4^{heel} (1.7)	-6.5^{heel} (1.4)
Time to peak rearfoot EVE (%stance)	43.6 (4.8)	42.6 (5.5)	43.9 (5.4)
Time to peak Shank IR (%stance)	37.7 (10.9)	40.0 (8.3)	41.2 (8.9)
Time to peak forefoot DF (%stance)	58.2 (4.9)	53.9 (5.4)	52.1^{heel} (6.8)
Time to peak forefoot ABD (%stance)	53.8 (11.5)	51.4 (10.0)	45.9$^{heel, fore}$ (8.4)

Segmental Coupling

Table 9.2 reports group mean cross-correlation values (zero phase shift) for the various segmental rotations. Coupling between rearfoot EVE/INV and shank IR/ER was consistently high regardless of foot strike pattern ($r \geq 0.94$). Similarly, cross-correlations between rearfoot EVE/INV and forefoot PF/DF were high ($r \leq -0.86$), although the heel strike condition exhibited a slightly lower value than the forefoot

and toe running conditions (Table 9.2). Rearfoot EVE/INV and forefoot ABD/ADD was also highly coupled during all three foot strike running conditions ($r \geq 0.92$). Cross-correlations between rearfoot EVE/INV and forefoot EVE/INV were poor in all cases ($-0.20 \leq r \leq -0.06$) with the standard deviations exceeding 0.37.

Table 9.2. Mean (SD) cross-correlations of rearfoot eversion/inversion with shank internal/external rotation and forefoot motion in each plane for different foot strike running conditions.

Variables	**HFS**	**FFS**	**TFS**
Rearfoot EVE/INV _ Shank IR/ER	0.96 (0.03)	0.95 (0.03)	0.94 (0.05)
Rearfoot EVE/INV _ Forefoot PF/DF	-0.86 (0.10)	-0.92 (0.08)	-0.96 (0.04)
Rearfoot EVE/INV _ Forefoot EVE/INV	-0.06 (0.42)	-0.20 (0.41)	-0.19 (0.38)
Rearfoot EVE/INV _ Forefoot ABD/ADD	0.92 (0.04)	0.95 (0.02)	0.96 (0.02)

The means and standard deviations of the vector coding angles are presented in Table 9.3. In general the values were found to be similar between foot strike conditions for all segmental movement pairs. Values of 55 to 58° between rearfoot EVE/INV and shank IR/ER during running suggest that rearfoot frontal plane excursion exceeded the amount of transverse shank rotation. There was also greater rearfoot EVE/INV compared to both forefoot EVE/INV and forefoot ABD/ADD, which is indicated by vector coding values ranging from 24 to 29°. Rearfoot EVE/INV and forefoot PF/DF were found to occur with similar excursion magnitudes as highlighted by coupling

angles of 40 to 46°. The coupling angle curves (vector coding) when rearfoot EVE/INV was paired with shank IR/ER (Figure 9.2a) and all forefoot planar movements (Figures 9.2b-9.2d) were similar between forefoot strike and toe running. The coupling angle between rearfoot EVE/INV and shank IR/ER was lower for heel-strike running during initial stance (~15% stance) compared to the other two foot-strike conditions (Figure 9.2a). There was also a lower coupling angle between rearfoot EVE/INV and forefoot PF/DF for the same initial period during stance (Figure 9.2b).

Table 9.3. Mean (SD) vector coding of rearfoot eversion/inversion with shank internal/external rotation and forefoot motion in each plane for different foot strike running conditions.

Variables	**Heel**	**Fore**	**Toe**
Rearfoot EVE/INV _ Shank IR/ER	58.1 (3.9)	55.7 (3.8)	57.0 (3.8)
Rearfoot EVE/INV _ Forefoot PF/DF	39.9 (4.0)	44.8 (5.1)	45.5 (4.7)
Rearfoot EVE/INV _ Forefoot EVE/INV	28.4 (5.2)	27.4 (5.6)	28.1 (4.9)
Rearfoot EVE/INV _ Forefoot ABD/ADD	21.7 (4.01)	24.5 (4.7)	25.1 (4.4)

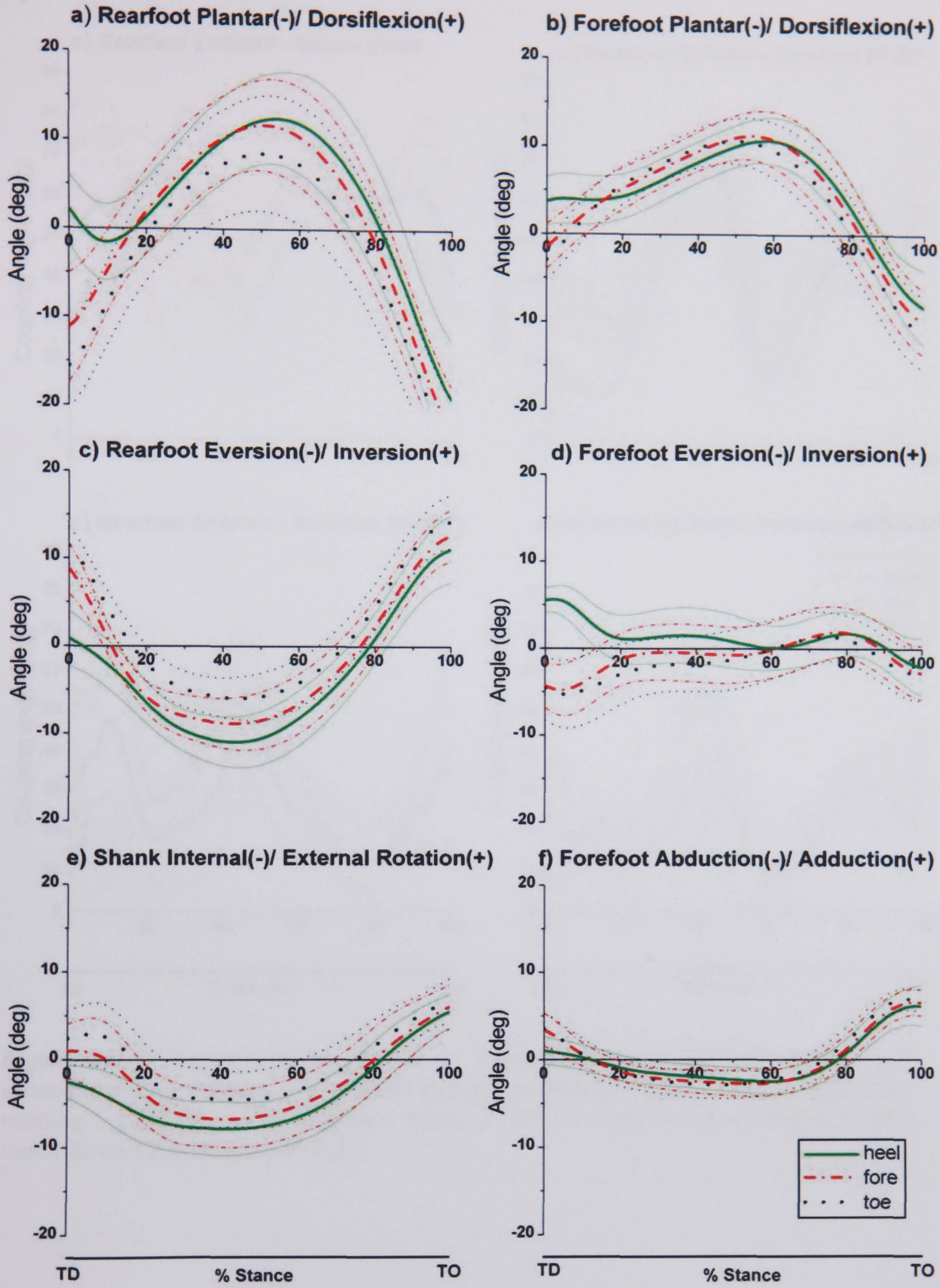

Figure 9.1. Angular displacement curves for the forefoot, rearfoot and shank for heel strike, forefoot strike and toe running conditions. The ensemble mean (±SD) for all subjects are shown from touch-down (TD) to toe-off (TO).

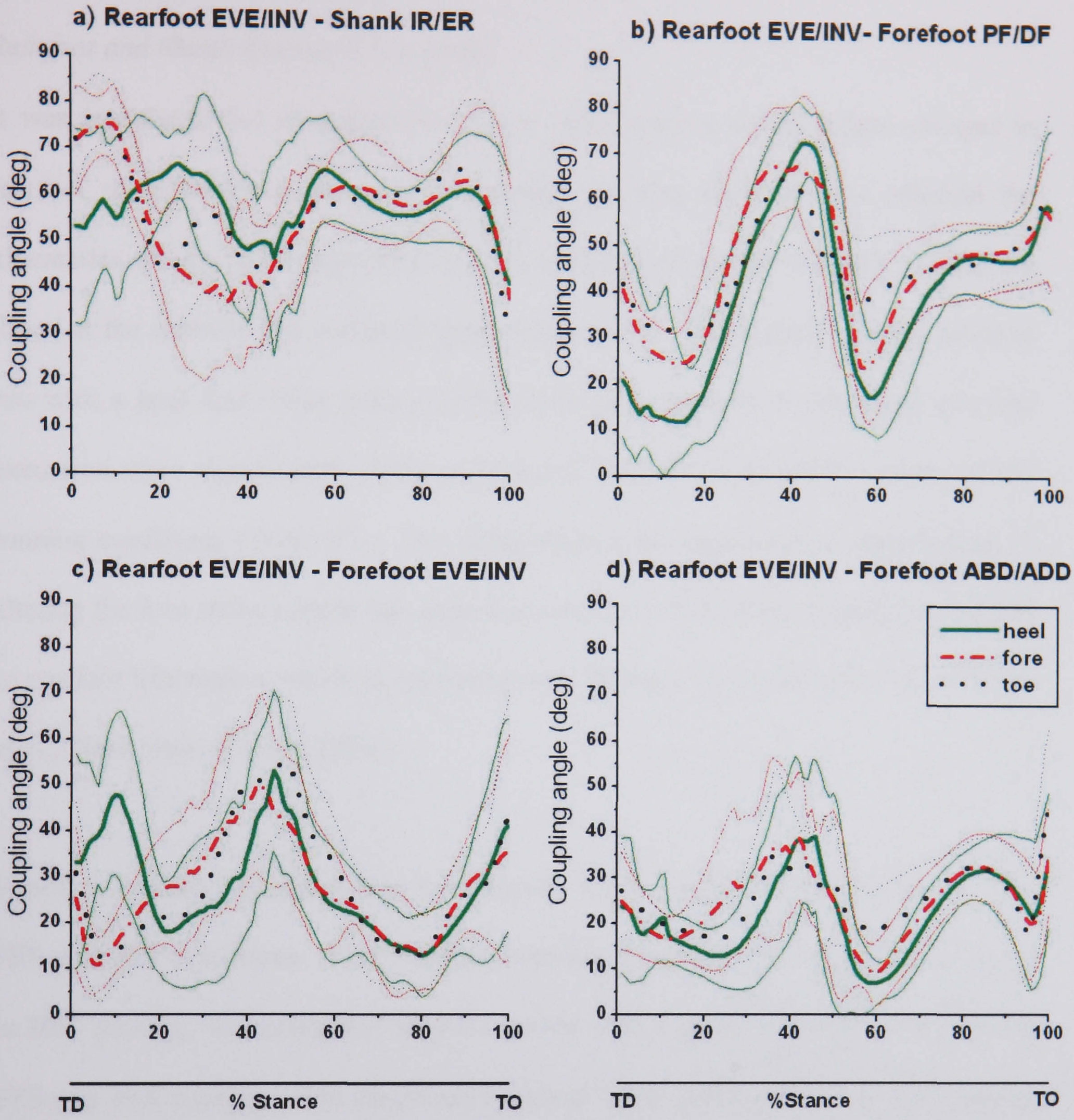

Figure 9.2. Vector coding curves of rearfoot eversion/inversion with shank internal/external rotation and forefoot motion in each plane for different foot-strike running conditions. The ensemble mean (± SD) are shown for all subjects from touch-down (TD) to toe-off (TO).

9.4 Discussion

Rearfoot and Shank Kinematic Coupling

It was postulated that manipulation of foot strike pattern would induce changes in rearfoot eversion kinematics, and depending on how such changes affected the kinematics of the shank and forefoot, this would highlight the rigidity of coupling found at the subtalar and midtarsal joints respectively. When subjects were asked to run with a heel foot strike pattern (HFS) both peak rearfoot eversion and eversion excursion were significantly different from the forefoot strike (FFS) and toe (TFS) running conditions (Table 9.1). This indicates that the experimental manipulation of altering the foot strike pattern was indeed successful in facilitating significant changes in rearfoot kinematics which is consistent with findings in the literature (Stackhouse et al., 2004; Stacoff et al., 1989).

Rearfoot eversion excursion was significantly lower in HFS in comparison to both FFS and TFS conditions. Peak rearfoot eversion, however, was significantly greater in HFS running, indicating that subjects landed with a more inverted rearfoot during FFS and TFS running. The excursion values of 12.0° (HFS) and 17.9° (FFS) in the present study correspond well with the magnitudes reported by Stackhouse et al. (2004) of 13.7° and 16.4° respectively. Similarly, peak eversion values of 11.1° (HFS) and 9.1° (FFS) in the present study closely match the values of 10.5° (HFS) and 8.8° (FFS) found by Stackhouse et al. (2004).

The lower rearfoot eversion excursion during HFS running was accompanied by a significant lower shank internal rotation excursion. The internal rotation excursion values of 5.8° (HFS) and 8.2° (FFS) are in good agreement with the excursion values

of 6.0° (HFS) and 7.5° (FFS) approximated from the kinematic curves presented by Stackhouse et al. (2004). The corresponding changes in eversion and internal rotation excursion suggest the two angular motions are coupled to some degree. Rearfoot frontal plane motion was not converted directly into transverse plane rotation of the shank, however, since the magnitude of the increase in rearfoot eversion excursion (from RFS to FFS or TFS) was larger than that of the subsequent change in shank internal rotation excursion. For example, during FFS running eversion excursion was 5.9° greater compared to HFS, whereas shank internal rotation excursion was only 2.4° greater. This dominance of rearfoot eversion/inversion over shank rotation motion is also supported by vector coding values in excess of 45° suggesting that greater excursions were occurring in the distal segment (Table 9.3). The vector coding graphs also provide evidence that the rearfoot was undergoing greater angular displacements than the shank across the whole stance phase, since the coupling angle rarely dropped below 45°.

The high cross-correlations evident between rearfoot frontal plane and shank transverse plane motion in all foot strike patterns ($r \geq 0.94$) provide evidence for strong temporal coupling between the two angular motions. The cross-correlation analysis together with the fact that the time to peak eversion and peak internal rotation are not altered between conditions indicates that foot strike pattern does not disrupt the temporal coupling between rearfoot frontal plane and shank transverse plane motion. However, closer inspection of the kinematic curves (Figure 9.1) revealed that HFS running displayed less eversion excursion during the first 15% of stance. Indeed an analysis of the vector coding curves reveals that the coupling angle was lower in HFS running during this part of stance (Figure 9.2a), which means that less rearfoot

eversion was transferred into shank internal rotation in the HFS condition compared to both FFS and TFS running. Interestingly, Hintermann et al. (1994) found that during *in vitro* loading of the foot, the transfer of calcaneal eversion into tibial rotation was reduced when the ankle-joint-complex was placed in a dorsiflexed position. Observation of the rearfoot sagittal plane kinematic curve in the present study (Figure 9.1a) highlights that the ankle-joint-complex was in a more dorsiflexed position during the initial period of stance in HFS running. Hintermann et al. (1994) postulated that the transfer mechanism can be altered by the ligaments around the joint being moved into a functionally inefficient position during dorsiflexion. It may also be possible that the talus' articulation with the tibia was altered by the dorsiflexed position of the talocrural joint, and this affected the transfer of motion from the calcaneus to the tibia via the talus.

Forefoot and Rearfoot Kinematic Coupling

In general good temporal coupling was found between forefoot sagittal plane and rearfoot frontal plane motion as indicated by the high cross-correlation values ($r \leq -0.86$). This is in agreement with the step width chapter which also found high coupling (between -0.85 and -0.94). Further support for kinematic coupling between forefoot sagittal plane and rearfoot frontal plane motion is evident in the fact that the lower rearfoot eversion excursion found during HFS running was also accompanied by a significantly lower forefoot dorsiflexion excursion (Table 9.1). A slightly lower cross-correlation, however, was found during HFS running and examination of the angular displacement curve (Figure 9.1b) reveals this may have been mainly due to a lack of forefoot dorsiflexion excursion occurring during the first 15% of stance. In addition, the lower vector coding value in HFS compared to the FFS and TFS

conditions implies less forefoot excursion occurred relative to rearfoot excursion (Table 9.2). Further analysis of the vector coding curves reveals that the lowered mean coupling angle found in HFS running was largely due to the difference during the initial 15% of stance (Figure 9.2b). These findings lend support to the theory that the forefoot and rearfoot are strongly coupled since alteration in the kinematics of the rearfoot induced changes in the forefoot. Since the two segments are linked via the action of the midtarsal joint, these findings suggest that the midtarsal joint has some influence on the transfer of movement between the rearfoot and shank.

Forefoot abduction and adduction also appeared to be strongly coupled with rearfoot eversion and inversion respectively. Good coupling throughout the entire stance phase was evident with cross-correlation values of 0.92 and above (Table 9.2). The vector coding values indicated that the rearfoot was undergoing greater excursion relative to the forefoot particularly so during the HFS condition (Table 9.3). Inspection of the kinematic curves (Figure 9.1f) suggests that this may be due to the forefoot undergoing slightly less abduction during early stance, a fact which is supported by the lower abduction excursion found in this condition (Table 9.1). This is a similar trend to that reported earlier in this study for the forefoot sagittal plane, which suggests that both the transverse and sagittal plane motions of the forefoot are coupled. This is in agreement with the theoretical model of the midtarsal joint (Elftman, 1960; Manter, 1941) where dorsiflexion occurs in conjunction with abduction, or plantarflexion in conjunction with adduction about the oblique axis. In addition as well as undergoing a lower amount of dorsiflexion and abduction excursion during early stance in HFS running, the forefoot was actually in a more dorsiflexed and abducted position at touchdown. The different forefoot position may

have altered the articulation between the navicular and talus at the midtarsal joint, which in turn may have influenced the manner in which the talus transferred motion from the calcaneus to the tibia.

Poor kinematic coupling was found between forefoot frontal plane and rearfoot transverse plane motion in the present study. This supports the findings of the previous chapters which found a lack of coupling between these two planar motions when step width and speed were altered during running. The standard deviations of the cross-correlations were as high as those reported in the previous experimental chapters (see chapters 7 and 8) investigating the effect of step width, speed and mode of gait. This suggests that the large between-subject variations reported in these previous experimental studies (and present study), were not a result of subjects adopting different foot strike patterns. However, during the first 15% of stance, there was a notable difference between the kinematic curves in the HFS condition compared to FFS and TFS running. At touchdown the forefoot was in an inverted position during HFS running and then underwent a period of eversion until approximately 20% stance. In contrast during both FFS and TFS running the forefoot was in a more everted position at touchdown, and then underwent a small period of eversion followed by inversion until 20% stance. These patterns are similar to those reported by Stacoff et al. (1989). This implies that midtarsal joint motion about a longitudinal axis (Elftman, 1960; Manter, 1941) may also have contributed to the altered transfer of rearfoot motion to the shank.

As has been mentioned in the previous experimental chapters, expressing forefoot motion relative the rearfoot does not differentiate between movements that may have

occurred at the midtarsal joint or at the more distal joints (i.e. tarsometatarsal joints). However, the present study still highlights that the distal joints of the foot can influence the kinematic coupling at the subtalar joint. Another limitation of the present study was that only acute changes in running mechanics were being examined. It has been shown that the kinematic and kinetic variables of habitual HFS runners who were trained to run with a FFS running pattern did not differ from those found in habitual FFS runners (Williams et al., 2000). Future research is thus needed to investigate if the kinematic coupling relationships between the shank, rearfoot and forefoot found in the present study are similar to those found between habitual FFS runners and habitual HFS runners.

9.5 Conclusion

Good kinematic coupling was found between rearfoot eversion/inversion and shank internal/external rotation regardless of foot strike pattern. Some subtle differences were noted in the amount of rearfoot eversion transferred into shank internal rotation in the first 10-15% of stance during HFS running. In addition, forefoot kinematics in all three planes were also slightly altered during HFS in the same initial period of stance. This implies that forefoot motion may have influenced the kinematic coupling at the subtalar joint via the action of the midtarsal joints articulation with the talus.

Chapter 10 – General Discussion

The aim of this thesis was to develop a more comprehensive understanding of kinematic coupling between the foot and lower limb. In addition, by developing a foot model that included both the rearfoot and forefoot it was possible to investigate the association between midtarsal joint motion (rotation of forefoot relative to the rearfoot) and the kinematic coupling at the subtalar joint (rotation of the rearfoot relative to the shank) during running. More specifically, to determine whether forefoot motion was coupled to rearfoot motion and thus could influence shank rotation. By conducting experimental gait manipulations that altered rearfoot motion and then observing the consequent effect on the adjacent segments of the shank and forefoot, it was possible to deduce how rigidly/robustly coupled the segments were at the subtalar and midtarsal joints respectively. As well as using traditional methods to quantify kinematic coupling between segments such as variables measured at discrete time points in the stance phase, a measure of continuous coupling throughout the entire stance phase was included to give a more complete picture of the relationship.

Prior to conducting the studies that determined the robustness of foot and leg coupling by manipulating certain gait parameters, an *in-vitro* investigation was carried out to assess the validity of using external skin mounted markers on the heel and shank to represent subtalar joint motion (chapter 5). It was found that there was a poor agreement between tibiocalcaneal joint kinematics determined from using skin or bone mounted markers. However, tibiocalcaneal joint kinematics (using bone pins) did provide a good reflection of subtalar joint kinematics. Unfortunately these findings had to be treated with caution since there were a number of significant

limitations in the methodology. This included the possible alteration of natural skin movement due to both the insertion of steel bone pins and removal of all soft tissue 100mm proximal of the malleoli. Other important limitations concerned the lack of realistic *in-vivo* physiological forces applied to the tendons and the ability to only simulate one instantaneous period of the stance phase (15% stance). These short-comings limited the external validity of the results and thus the conclusions drawn from this chapter were not used to adapt the methods applied in the experimental gait studies (chapters 6-9).

When attempting to assess the level of kinematic coupling between two adjacent segments it is essential to have reliable assessment methods. Chapter 6 thus determined the repeatability of determining shank, rearfoot and forefoot planar angles in terms of both the kinematic curve pattern (CMCs) and the absolute magnitudes of the angles obtained (LOAs) both within- and between-days. Excellent reliability was found in terms of the kinematic curve pattern over the stance phase (CMCs $\geq$ 0.847). This meant that any differences found in the gait manipulation studies (chapters 7-9) in terms of continuous coupling (cross-correlation) were due to the independent variable (i.e. experimental gait factors) and not the inability to reliably measure the coupling parameters. In addition, the reliability with which the magnitude of joint angles, peak or excursions, could be calculated was determined by calculating the LOAs. LOAs were found to be relatively low ($\leq 3.4°$) which meant that any changes in discrete angular variables greater than this could be attributed to the experimental gait manipulations.

The subsequent three chapters (chapters 7-9) investigated the rigidity/robustness of the kinematic coupling between the forefoot, rearfoot and shank by using a number of gait manipulations to induce alterations in rearfoot kinematics. The findings from these chapters (step width, chapter 7; speed/mode of gait, chapter 8; foot-strike pattern, chapter 9) highlight the kinematic coupling between the rearfoot and shank, the forefoot and rearfoot, and in a more general sense how motion of the foot is coupled to motion of the lower leg. Each of the aspects of coupling is discussed separately below.

10.1 Rearfoot and Shank Kinematic Coupling

In general, findings indicate that there is high/strong kinematic coupling between the rearfoot and shank during running but there is almost no coupling between the rearfoot and shank during walking. In running rearfoot eversion was accompanied by shank internal rotation during the first half of stance with rearfoot inversion and shank external rotation occurring in the second half. This relationship was present regardless of the experimental gait condition i.e. regardless of changes in running speed, step width or foot-strike pattern. There were, however, some confounding findings in the discrete variable measurements that suggest the kinematic coupling between the shank and rearfoot is not absolutely rigid. The findings from the three gait manipulation studies (running speed, step width and foot strike pattern) indicated that an increase in peak eversion or peak eversion excursion was related to an accompanying increase in the peak and range of shank internal rotation. However, the time at which peak rearfoot eversion and shank internal rotation occurred was not exactly synchronised, with peak shank internal rotation occurring earlier than peak

rearfoot eversion in all instances. In addition, when the time to peak excursion of one of the segments was altered by an experimental manipulation, the timing of the peak value of the adjacent segment was not always altered in a similar manner. This was observed when increasing running speed resulted in peak shank internal rotation occurring later in stance despite the time of peak rearfoot eversion remaining unchanged (chapter 8).

This highlights that even though robust coupling was found during running this relationship was not absolutely rigid due to slight timing discrepancies. The fact that the shank began to externally rotate before the rearfoot started to invert suggests that the motion of the lower leg was driving the motion of the foot. Since the shank and rearfoot are separated by the talus it may be that the delay was due to rotation occurring at the talocrural joint prior to the subtalar joint. Although the *in-vitro* investigation (chapter 5) attempted to address the question of how accurately tibiocalcaneal joint kinematics represent subtalar joint kinematics, the study was limited in terms of its applicability to in-vivo loading conditions during the entire stance phase of gait. It has been shown in the literature, however, that internal/external rotation may indeed occur at the talocrural joint (Arndt et al., 2004; Lundberg, 1989). To confirm whether this timing discrepancy between shank rotation and calcaneal eversion was indeed attributable to motion occurring at both the subtalar and talocrural joints, future investigations tracking markers placed directly on the bones during gait are required. Although studies involving bone mounted markers have recently been conducted (Arndt et al., 2004) the sample size has been limited due to the invasive procedures entailed. Future research using greater subject numbers would be necessary to present more universally applicable results.

The high degree of coupling between the shank and rearfoot in all running conditions confirms that altering the loading pattern of the subtalar joint does not significantly influence its kinematic behaviour. For instance, it is reasonable to expect that altering step width would influence the mediolateral GRFs and thus the inversion/eversion moments acting at the ankle-joint-complex. However, even though rearfoot eversion excursion and the eversion moment are increased in cross-over running (McClay and Cavanagh, 1994) the continuous kinematic coupling between the rearfoot and shank remained relatively unchanged. This highlights that during running, the subtalar joint was capable of maintaining its normal mechanical behaviour regardless of the changes to the loading pattern at the joint applied within this thesis. However, the information provided by the vector coding graphs in the foot-strike study revealed that cross-correlations or mean vector coding values averaged across stance may be slightly misleading in some cases (Chapter 9). No difference was reported between the three foot strike conditions in terms of cross correlation or mean vector coding values. Inspection of the vector coding graphs, however, showed that the coupling angle was altered during early stance in heel-strike running compared to both forefoot strike and toe running. This highlights the need for future research to incorporate an analysis of vector coding trends in specific regions of the stance phase.

The findings describing the kinematic coupling relationship between the shank and rearfoot during running have important implications for theoretical injury models proposed in the literature. It has been speculated that alterations in the timing between the motions of rearfoot eversion/inversion and knee flexion/extension may result in antagonistic torques being exerted at either end of the shank, thus placing

excessive stress on the joints (Hamill et al., 1992; Stergiou et al., 1999; Stergiou and Bates, 1997; Stergiou et al., 2003). This is based on the assumption that both rearfoot eversion and knee flexion act to internally rotate the shank whilst rearfoot inversion and knee flexion externally rotate the shank. The findings of this thesis suggest that although slight timing discrepancies between rearfoot eversion/inversion and shank internal/external rotation was present during running, in general rearfoot eversion/inversion and shank internal/external rotation coupling was strong. Thus, the asynchronous timing found between the rearfoot and knee in the literature may have been due to altered kinematics between the shank and knee, rather than between the rearfoot and shank. Future research should be conducted to ascertain how tightly rearfoot and shank motion is coupled with motion at the knee joint.

During walking there was little evidence of any coupling and for a substantial part of the stance phase, the shank was externally rotating while the rearfoot was still everting. Hence, this appears to challenge the theory that asynchronous timing between the shank and rearfoot is always problematic in terms of being an aetiological factor for injury. It could be that a lack of kinematic coupling at the subtalar joint is of less importance during walking compared to running. For instance, it may be that higher ground reaction forces during running induce a different kinematic behaviour in the subtalar joint. Indeed, Hintermann et al. (1994) found that the amount of movement transferred from the calcaneus to the tibia was highly dependant upon the downward vertical load applied to the tibia. In fact the vector coding graphs (Figure 8.2a) indicate that the transfer ratio of rearfoot eversion to shank internal rotation was highly variable during walking compared to running. The greater forces between the talus and calcaneus during running may mean that relative motion between the two

bones is strongly dependant upon the anatomy of the articulating facets, while lower joint forces present during walking might allow the subtalar joint to behave in a more flexible manner. It was speculated earlier in this discussion that the mechanical coupling between the rearfoot and shank appears to contain some elastic element since there is always a delay between the onset of shank external rotation and rearfoot inversion. This elastic element could be attributable to the muscles and ligaments across the ankle-joint-complex. Since more eversion and shank internal rotation occur in running compared to walking, it is likely that the ligaments are placed under greater tension due to greater range of motion at the subtalar joint. In addition, elevated muscular activity is required to stabilise the ankle-joint complex during the stance phase of running. It is possible that this increased muscle/ligament stiffness serves to decrease the elastic element at the subtalar joint. This would make coupling between the rearfoot and shank more dependant on bony anatomy and hence more rigid in nature. In walking, however, the lower GRFs means that decreased muscular activity would be required during stance. Also the lower range of motion at the subtalar joint would decrease the tensile strain on the proximate ligaments. The soft tissues would therefore be more compliant, thus allowing more flexibility at the subtalar joint.

During walking, the kinematic coupling relationship between the rearfoot and shank breaks down approximately 17% into the stance phase where the shank begins to externally rotate while the rearfoot is still everting. It is interesting to note that this coincides with the first modal peak of the vertical GRF which has been shown to occur at 19% stance (Chao et al., 1983). After this point in stance (19%), the vertical GRF decreases during walking, whereas at the equivalent period in running it

continues to rise. This meant that the discrepancy in GRF became even more apparent between walking and running, which also seemed to coincide with the period where the kinematic coupling between the rearfoot and shank was disrupted during walking. This provides further evidence to speculate that the disruption in subtalar joint coupling during walking may have been attributable to the different loading patterns between walking and running.

The fact that muscular stiffness may play a role in subtalar joint kinematics has broader implications when considering the effect that fatigue may have on the normal coupling relationship between the rearfoot and shank. Indeed, strengthening of the ankle dorsiflexors has been associated with reduction in rearfoot eversion excursion (Feltner et al., 1994). It may be that towards the end of an exhaustive run, the extrinsic muscles across the ankle-joint-complex become fatigued and thus the subtalar joint kinematics would be altered. Most comparative studies of injured and non-injured populations involve a kinematic analysis of running mechanics when both groups of subjects are rested. The nature of the testing protocol usually consists of subjects running for a short duration and is not sufficient to cause substantial fatigue in the extrinsic muscles. However, it is possible that subjects who have bony abnormalities of the foot (e.g. pes planus, calcaneal valgus) rely more on muscular function to maintain normal coupling at the subtalar joint. On the other hand, subjects with normal bone anatomy would rely less on muscular activity to maintain normal subtalar joint function. Thus a comparison of these subjects using running of short duration/intensity may not produce any notable differences in terms of subtalar joint coupling. However, following a prolonged run that served to fatigue the muscles around the ankle-joint complex, a significantly different coupling relationship might

be revealed between the two groups. Hence, future work should be conducted to determine whether subtalar and midtarsal joint coupling are similar between symptomatic and asymptomatic subjects following a prolonged run.

10.2 Forefoot and Rearfoot Kinematic Coupling

Similar to the asynchronous timing between peak rearfoot eversion and shank internal rotation, the results of all three gait manipulation studies showed that peak forefoot dorsiflexion and abduction did not coincide with peak rearfoot eversion. In general the rearfoot began to invert before the forefoot had stopped dorsiflexing and abducting. Forefoot sagittal plane motion has been linked to the collapse of the medial longitudinal arch (Hunt et al., 2001), a common measure of foot pronation. Therefore, the findings of this thesis suggest rearfoot eversion may not be reflective of whole foot pronation.

All three gait manipulation studies show that sagittal and transverse forefoot plane motions were both strongly coupled with rearfoot eversion/inversion during stance. The synchronous actions of forefoot dorsiflexion with abduction and then plantarflexion with adduction provides evidence for the existence of an oblique axis at the midtarsal joint as proposed by Manter (1941) and Elftman (1960). Since these forefoot motions also occurred in conjunction with rearfoot eversion/inversion, findings suggest the rearfoot and forefoot are kinematically coupled via the action of the midtarsal joint. However, there was no evidence that forefoot frontal plane motion was coupled with rearfoot frontal plane motion. Therefore, the results of the thesis do not support the existence of an additional longitudinal axis at the midtarsal joint about which inversion and eversion occurs (Elftman, 1960; Manter, 1941).

Chapter 9 provided a new insight into the interdependency of the midtarsal and subtalar joints by examining the effects of foot strike pattern. It was expected that the toe running condition would simulate a similar loading pattern to that found during the propulsion phase of stance i.e. the midtarsal joint was locked rigid to provide a rigid lever for push-off. Given that a rigid midfoot is associated with subtalar joint supination, it was speculated that the toe-running conditions would serve to limit the amount of rearfoot eversion excursion occurring compared to heel strike running. However, the findings indicated that toe running and forefoot-strike running produced significantly greater amounts of rearfoot eversion compared to heel-strike running. This was a surprising result as it implies that rearfoot motion and midtarsal joint flexibility are not as interdependent on one another as has been previously believed. This implies that there may be a substantial degree of elasticity in the coupling relationship between the midtarsal and subtalar joints.

The foot model utilised within the context of this thesis determined the relative motion between the forefoot and rearfoot to represent rotations occurring at the midtarsal joint. Such an approach does not distinguish between rotations occurring at the midtarsal joint and those at the joints distal to this (metatarsal joints). In addition, the forefoot was assumed to be a rigid segment even though the metatarsal are capable of moving relative to one another. Therefore, caution must be applied when using the results to generalise about motion occurring at the midtarsal joint. Future research should attempt to create multi-segment foot models that can distinguish between movements occurring at the midtarsal joint and movements occurring distal to this.

Despite the limitations of the foot model used within the thesis, the results have provided further insight of how the forefoot and rearfoot are coupled during gait.

10.3 Foot and Shank Kinematic Coupling

Findings indicate that during running, rearfoot frontal plane motion was proximally coupled with shank rotation and distally coupled with the forefoot sagittal and transverse plane motion. This implies the shank, rearfoot and forefoot are indeed linked together in terms of kinematic coupling. In all the gait manipulation experiments it was evident that following touchdown, the shank internally rotated, the rearfoot everted, and the forefoot dorsiflexed and abducted. The first segment to change its direction of angular rotation was the shank, which began to externally rotate. The rearfoot then began to invert after a short time lag which was then followed by forefoot adduction/plantarflexion after another short delay. Hence, it appeared that shank external rotation was driving rearfoot inversion and that this in turn was causing the forefoot to plantarflex and abduct. This suggests there is a kinetic chain evident with proximal segments driving motion of the distal segments during propulsion. This supports the findings of Bellchamber and van den Bogert (2000) who reported that during running, the power flow for transverse tibial rotation was mainly proximal to distal. Interestingly, it has been reported that during walking, the knee flexes until approximately 15% stance (Chao et al., 1983; Perry, 1992), which closely matches the instant at which the shank began to externally rotate in the findings of this thesis. In addition, Dierks et al (2004) reported that peak shank internal rotation and knee flexion occurred at a similar instant during running. This supports the concept that the knee joint may play a more important role than the

subtalar joint in determining the transverse plane rotation of the shank. The present investigations, however, only included a kinematic analysis of the foot and shank. Thus it would be of value to include the knee joint in future studies. Such work could determine the effect of altered proximal kinematics on the shank and foot to test the rigidity of the coupling between the knee and shank.

It is possible that in some subjects, excessive or prolonged pronation is a secondary response to kinematic alterations occurring further up the kinetic chain. This has important implications for the current methods that clinicians use to treat ailments caused by excessive or prolonged pronation. Typically, treatment methods have involved the insertion of foot orthoses into shoes to control the amount of pronation occurring at the subtalar joint. However, the findings of this thesis suggest that the duration of pronation is governed by the segments which are proximal (e.g the shank) to the subtalar joint. It can be speculated that the magnitude of pronation can also be controlled by the proximal segments. This implies that altering the kinematics/kinetics of the proximal joints i.e. the knee and hip, might be more effective in controlling excessive/prolonged pronation. Further research would be required to validate such a hypothesis.

10.4 Limitations and Future Directions

It was highlighted earlier in the discussion that muscular and ligament behaviour at the ankle-joint-complex may play a vital role in the mechanical coupling relationship at the subtalar joint. However, studying the influence that selected ligaments and muscles have on subtalar joint coupling presents a challenge for future researchers.

Due to the invasive procedures involved in such an experiment, this would entail studies using cadaveric models. Some studies have already attempted to study the effect of specific muscles on hindfoot kinematics using *in-vitro* methods (Niki et al., 2001). However, the *in-vitro* study conducted within the present thesis indicated a number of issues in terms of how transferable the findings from such studies are to *in-vivo* situations during gait. There is a need for future cadaver studies to examine the influence of muscular forces on subtalar joint kinematics, which incorporate physiological muscle forces similar to those found during walking and running *in-vivo*. In addition, it is essential that future research attempts to simulate the entire stance phase and not just a single instant (or selected instances) in time.

A number of limitations have already been brought up within the context of this discussion regarding the segmental model used to determine both subtalar and midtarsal joint motion. This highlighted the need to develop models which divide the foot into even smaller segments for a more precise understanding of how the many joints behave. It was also highlighted that invasive *in-vivo* studies need to be performed in order to measure the 'true' bone and joint movements during gait. Another limitation that must be recognised is that the sample sizes used in the gait manipulation studies were small and caution must be taken when extrapolating the results to be representative of a larger population. There is a strong requirement for similar gait manipulation studies to be conducted using significantly larger numbers of subjects and also on different sub-divisions of the population (e.g. age, gender, exercise activity level etc). This would be necessary to fully define what the normal kinematic coupling relationship between the foot and lower limb is. Then, once the characteristics of a normal coupling relationship have been established, it would be

possible to contrast the kinematic coupling present in groups of subjects suffering from specific chronic overuse injuries of the lower extremity. The examination of such relationships may lead to further insight into the aetiology of the injury mechanisms involved.

10.5 Summary of Findings

The overall objective of this thesis was to gain a more complete picture of how the foot was kinematically coupled with the lower limb during gait. This was undertaken with a view to investigating the association between midfoot joint motion and the kinematic coupling at the subtalar joint during gait. In order to address the objectives of the thesis a number of specific aims were formulated (section 1.2.1). The following section reminds the reader of these aims, and then goes on to highlight the outcome of each of these aims in turn.

1. Review the literature on the biomechanics of the foot and lower limb during gait with specific emphasis on the current understanding of the kinematic coupling relationship between the foot and lower limb:

A review of the literature revealed that excessive/prolonged pronation has been associated with overuse injuries of the lower extremity during running. A potential injury mechanism was attributed to kinematic coupling between the foot and shank via the action of the subtalar joint. However, this coupling relationship was unclear in the literature. It was postulated this was due to methodological limitations such as only using discrete measures of coupling and failure to include distal joints of the foot in coupling analyses. The review of the literature also highlighted a need for

experimental gait manipulations to further investigate coupling between the forefoot and shank.

2. Test the validity of using external markers to measure subtalar joint kinematics:

The results in chapter 5 suggested that external skin markers did not provide an accurate description of the kinematic motion that was occurring at the bones of the subtalar joint. However, the limitations of the *in-vitro* methods made it difficult to apply these findings to the *in vivo* studies undertaken within this thesis.

3. Develop a repeatable method to determine forefoot, rearfoot and shank 3-D angular kinematics:

A method to measure the angular kinematics of the forefoot, rearfoot and shank was developed. The findings of chapter 6 indicate this method had an acceptable level of repeatability.

4. Investigate whether forefoot, rearfoot and shank kinematic coupling is altered by step width during running:

Rearfoot eversion/inversion was found to have strong temporal coupling with the motions of shank internal/external rotation, forefoot dorsiflexion/plantarflexion and forefoot abduction/ adduction. Strong coupling for all the above planar motions was found with rearfoot eversion/inversion regardless of whether a normal, wide or cross-over running gait was used. In contrast, coupling between rearfoot frontal plane motion and forefoot frontal plane motion was poor to non-existent in all step width conditions.

5. Investigate whether forefoot, rearfoot and shank kinematic coupling differs between walking and running:

Kinematic coupling of rearfoot eversion/inversion with shank internal/external rotation was much lower in walking compared to running. In addition, slightly lower coupling was also found between rearfoot eversion/inversion and forefoot dorsiflexion/ plantarflexion during walking. There was little evidence for coupling between rearfoot eversion/inversion and forefoot eversion/inversion in either running or walking.

6. Investigate whether forefoot, rearfoot and shank kinematic coupling differs between running speeds:

Rearfoot eversion/inversion had strong temporal coupling with the motions of shank internal/external rotation, forefoot dorsiflexion/plantarflexion and forefoot abduction/ adduction regardless of running speed. Poor coupling between rearfoot frontal plane and forefoot frontal plane motions was found at all three running speeds.

7. Investigate whether forefoot, rearfoot and shank kinematic coupling is altered by foot strike pattern during running:

Rearfoot eversion/inversion was found to have strong temporal coupling with shank internal/external rotation, forefoot dorsiflexion/plantarflexion and forefoot abduction/ adduction regardless of foot strike pattern. During HFS running, however, less rearfoot eversion was transferred into shank internal rotation in the first 10-15% of stance and forefoot kinematics in all three planes were slightly altered during the same period of stance. This implies that midtarsal joint kinematics may have influenced the

coupling behaviour at the subtalar joint.

8. Determine the robustness of the kinematic coupling between rearfoot frontal plane motion and transverse plane rotation of the shank:

During running, although there were slight discrepancies in the discrete variables measured, there was strong temporal coupling between the two segments with rearfoot eversion and inversion occurring in conjunction with shank internal and external rotation respectively. This implies there was robust coupling at the subtalar joint despite alterations to the loading patterns that may have been experienced at the joint. However, walking exhibited much lower subtalar joint coupling and this was attributed to lower joint stiffness due to decreased muscular activity.

9. Determine the robustness of the kinematic coupling between rearfoot frontal plane motion and forefoot planar rotations:

There was strong coupling of rearfoot frontal plane motion with both forefoot sagittal and transverse plane motion during both walking and running. The robustness of this relationship was evident since altered loading patterns did not significantly alter midtarsal joint kinematics. There was little evidence for any coupling between rearfoot eversion/inversion and forefoot eversion/inversion regardless of the loading condition.

By satisfying aims 8 and 9 above, a further aim was to observe whether midtarsal joint function had any influence on kinematic coupling at the subtalar joint (see last point in introduction section 1.2.1). Rearfoot frontal plane motion was strongly coupled with both forefoot sagittal and transverse planar motions. This suggests that

the forefoot could alter rearfoot kinematics and thus influence the transverse kinematics of the shank via the subtalar joint. In addition, when different foot strike patterns were used (heel vs forefoot/toe strike) the amount of eversion transferred to the shank appeared to be altered. Thus the function of the midtarsal joint appeared to alter kinematic coupling at the subtalar joint.

10.6 Concluding Remarks

The kinematic coupling between the rearfoot and shank was robust during running as it did not change substantially across several gait manipulations. The lower coupling between these two segments in walking, however, implies that the relationship is not entirely rigid and thus that some degree of elasticity exists across the subtalar joint. The strong coupling of forefoot sagittal and transverse plane motions with rearfoot frontal plane motion during running and walking suggests that midtarsal joint motion is associated with subtalar joint coupling. From the timings of discrete kinematic events it appears that shank external rotation was driving rearfoot inversion, and that this in turn was causing the forefoot to plantarflex and abduct. This suggests there is a kinetic chain evident with proximal segments driving motion of the distal segments during propulsion. If the proximal segments are responsible for the kinematic behaviour of the foot then it may be argued that altering the kinematics/kinetics of the proximal joints i.e. the knee and hip, might be more effective in controlling excessive/prolonged pronation. Thus the treatment of lower extremity injuries associated with excessive/prolonged pronation may respond to rehabilitation measures that attempt to alter the kinematics of the proximal segments and joints of the leg.

References and Bibliography

Abdel-Aziz, Y. I. and Karara, H. M. (1971). In ASP Symposium on Close Range Photogrammetry, Falls Church: pp 1-18.

Andrew, G. C. (1990) The effect of running velocity on rearfoot motion and mediolateral placement of the feet: Unpublished Master's Thesis. In Cavanagh, P. R. (Ed.) Biomechanics of Distance Running. Champaign: Human Kinetics, pp 152-153.

Areblad, M., Nigg, B. M., Ekstrand, J., Olsson, K. O. and Ekstrom, H. (1990). Three-dimensional measurement of rearfoot motion during running. Journal of Biomechanics, 23, 933-940.

Arndt, A., Westblad, P., Winson, I., Hashimoto, T. and Lundberg, A. (2004). Ankle and subtalar kinematics measured with intracortical pins during the stance phase of walking. Foot & Ankle International, 25, 357-364.

Bellchamber, T. L. and van den Bogert, A. J. (2000). Contributions of proximal and distal moments to axial rotation during walking and running. Journal of Biomechanics, 33, 1397-1403.

Bland, J. M. and Altman, D. G. (1986). Statistical methods for assessing agreement between two methods of clinical measurement. The Lancet, Feb 8, 307-310.

Bryan, G. J. (1996). Skeletal Anatomy, Third Edition. New York: Churchill Livingstone.

Cappozzo, A., Catani, F., Leardini, A., Benedetti, M. G. and Della Croce, U. (1996). Position and orientation in space of bones during movement: experimental artefacts. Clinical Biomechanics, 11, 90-100.

Cappozzo, A., Catani, F., Della Croce, U. and Leardini, A. (1995). Position and orientation in space of bones during movement: anatomical frame definition and determination. Clinical Biomechanics, 10, 171-178.

Carson, M. C., Harrington, M. E., Thompson, N., O'Connor, J. J. and Theologis, T. N. (2001). Kinematic analysis of a multi-segment foot model for research and clinical applications: a repeatability analysis. Journal of Biomechanics, 34, 1299-1307.

Cavanagh, P. R. and Lafortune, M. A. (1980). Ground reaction forces in distance running. Journal of Biomechanics, 13, 397-406.

Chao, E. Y., Laughman, R. K., Schneider, E. and Stauffer, R. N. (1983). Normative data of knee joint motion and ground reaction forces in adult level walking. Journal of Biomechanics, 16, 219-233.

Chu, I., Myerson, M. S., Nyaska, M. and Parks, B. G. (2001). Experimental flatfoot model: the contribution of dynamic loading. Foot & Ankle International, 22, 220-225.

Cole, G. K., Nigg, B. M., Ronsky, J. L. and Yeadon, M. R. (1993). Application of the joint coordinate system to 3-dimensional joint attitude and movement representation - a standardization proposal. Journal of Biomechanical Engineering-Transactions of the ASME, 115, 344-349.

Cornwall, M. W. and McPoil, T. G. (1995). Comparison of 2-dimensional and 3-dimensional rearfoot motion during walking. Clinical Biomechanics, 10, 36-40.

Cornwall, M. W. and McPoil, T. G. (2002). Motion of the calcaneus, navicular, and first metatarsal during the stance phase of walking. Journal of the American Podiatric Medical Association, 92, 67-76.

De Wit, B., De Clercq, D. and Aerts, P. (2000). Biomechanical analysis of the stance phase during barefoot and shod running. Journal of Biomechanics, 33, 269-278.

DeLeo, A. T., Dierks, T. A., Ferber, R. and Davis, I. S. (2004). Lower extremity joint coupling during running: a current update. Clinical Biomechanics, 19, 983-991.

Derrick, T. R., Bates, B. T. and Dufek, J. S. (1994). Evaluation of time-series data sets using the Pearson product- moment correlation-coefficient. Medicine and Science in Sports and Exercise, 26, 919-928.

Dierks, T. A., Davis, I. S. and Hamill, J. (2004). In Proceedings of the 28th annual convention of ASB, Portland: pp 34.

Digby, C. J., Lake, M. J. and Lees, A. (2005). High-speed non-invasive measurement of tibial rotation during the impact phase of running. Ergonomics, 48, 1623-1637.

Donatelli, R. A. (1996). The Biomechanics of the Foot and Ankle, Second Edition. Philadelphia: F.A. Davis Company.

Duffey, M. J., Martin, D. F., Cannon, D. W., Craven, T. and Messier, S. P. (2000). Etiologic factors associated with anterior knee pain in distance runners. Medicine and Science in Sports and Exercise, 32, 1825-1832.

Edington, C. J., Frederick, E. C. and Cavanagh, P. R. (1990) Rearfoot motion in distance running. In Cavanagh, P. R. (Ed.) Biomechanics of Distance Running. Champaign: Human Kinetics, pp 135-164.

Elftman, H. (1960). The transverse tarsal joint and its control. Clinical Orthopaedics, 16, 41-45.

Engsberg, J. R. (1987). A biomechanical analysis of the talocalcaneal joint - in vitro. Journal of Biomechanics, 20, 429-442.

Erdemir, A., Hamel, A. J., Fauth, A. R., Piazza, S. J. and Sharkey, N. A. (2004). Dynamic loading of the plantar aponeurosis in walking. Journal of Bone and Joint Surgery-American Volume, 86A, 546-552.

Feltner, M. E., Macrea, H. S., Macrea, P. G., Turner, N. S., Hartman, C. A., Summers, M. L. and Welch, M. D. (1994). Strength training effects on rearfoot motion in running. Medicine and Science in Sports and Exercise, 26, 1021-1027.

Ferber, R., Davis, I. M. and Williams, D. S. (2005). Effect of foot orthotics on rearfoot and tibia joint coupling patterns and variability. Journal of Biomechanics, 38, 477-483.

Ferber, R., Davis, I. M., Williams, D. S. and Laughton, C. (2002). A comparison of within- and between-day reliability of discrete 3D lower extremity variables in runners. Journal of Orthopaedic Research, 20, 1139-1145.

Fioretti, S., Cappozzo, A. and Lucchetti, L. (1997) Joint Kinematics. In Allard, P., Cappozzo, A., Lundberg, A. and Vaughan, C. L. (Eds.) Three-dimensional Analysis of Human Locomotion. Chichester: John Wiley & Sons Ltd, pp 173-189.

Friederich, J. A. and Brand, R. A. (1990). Muscle-Fiber Architecture in the Human Lower-Limb. Journal of Biomechanics, 23, 91-95.

Grood, E. S. and Suntay, W. J. (1983). A joint coordinate system for the clinical description of 3- dimensional motions - application to the knee. Journal of Biomechanical Engineering-Transactions of the ASME, 105, 136-144.

Growney, E., Meglan, D., Johnson, M., Cahalan, T. and An, K.-N. (1997). Repeated measures of adult normal walking using a video tracking system. Gait and Posture, 6, 147-162.

Hall, S. J. (1999). Basic Biomechanics, Third Edition. Boston: McGraw-Hill.

Hamel, A. J., Sharkey, N. A., Buczek, F. L. and Michelson, J. (2003). Relative motions of the tibia, talus, and calcaneus during the stance phase of gait: a cadaver study. Gait and Posture, 20, 147-153.

Hamill, J., van Emmerik, R. E. A., Heiderscheit, B. C. and Li, L. (1999). A dynamical systems approach to lower extremity running injuries. Clinical Biomechanics, 14, 297-308.

Hamill, J., Bates, B. T. and Holt, K. G. (1992). Timing of lower-extremity joint actions during treadmill running. Medicine and Science in Sports and Exercise, 24, 807-813.

Hamill, J., van Emmerik, R. E. A., Heiderscheit, B. C. and Li, L. (1999). A dynamical systems approach to lower extremity running injuries. Clinical Biomechanics, 14, 297-308.

Hansen, M. L., Otis, J. C., Kenneally, S. M. and Deland, J. T. (2001). A closed-loop cadaveric foot and ankle loading model. Journal of Biomechanics, 34, 551-555.

Heiderscheit, B. C., Hamill, J. and van Emmerik, R. E. A. (2002). Variability of stride characterstics and joint coordination among individuals with unilateral patellofemoral pain. Journal of Applied Biomechanics, 18, 110-121.

Hicks, J. H. (1954). The mechanics of the foot. II. The plantar aponeurosis and the arch. Journal of Anatomy, 88, 25-31.

Hicks, J. H. (1953). The mechanics of the foot. I. The Joints. Journal of Anatomy, 87, 345-357.

Hintermann, B. and Nigg, B. M. (1998). Pronation in runners: implications for injuries. Sports Medicine, 26, 169-176.

Hintermann, B., Nigg, B., Sommer, C. and Cole, G. (1994). Transfer of movement between calcaneus and tibia in vitro. Clinical Biomechanics, 9, 349-355.

Hunt, A. E., Smith, R. M., Torode, M. and Keenan, A. M. (2001). Inter-segment foot motion and ground reaction forces over the stance phase of walking. Clinical Biomechanics, 16, 592-600.

Inman, V. T., Ralston, H. J. and Todd, F. (1981). Human Walking. Baltimore: Williams & Wilkins.

Inman, V. T. (1976). The Joints of the Ankle. Baltimore: Williams & Wilkins.

James, S. J. and Jones, D. C. (1990) Biomechanical aspects of distance running injuries. In Cavanagh, P. R. (Ed.) Biomechanics of Distance Running. Champaign: Human Kinetics, pp 249-269.

Kadaba, M. P., Ramakrishnan, H. K., Wootten, M. E., Gainey, J., Gorton, G. and Cochran, G. V. B. (1989). Repeatability of kinematic, kinetic, and electromyographic data in normal adult gait. Journal of Orthopaedic Research, 7, 849-860.

Karlsson, D. and Tranberg, R. (1999). On skin movement artefact-resonant frequencies of skin markers attached to the leg. Human Movement Science, 18, 627-635.

Kernozek, T. W. and Greer, N. L. (1993). Quadriceps angle and rearfoot motion: relationships in walking. Archives of Physical Medicine and Rehabilitation, 74, 407-410.

Kibler, W. B., Goldberg, C. and Chandler, T. J. (1991). Functional biomechanical deficits in running athletes with plantar fasciitis. The American Journal of Sports Medicine, 19, 66-71.

Kitaoka, H. B., Luo, Z. P., Kura, H. and An, K. N. (2002). Effect of foot orthoses on 3-dimensional kinematics of flatfoot: a cadaveric study. Archives of Physical Medicine and Rehabilitation, 83, 876-879.

Klenerman, L. (1991) Functional Anatomy. In Klenerman, L. (Ed.) The Foot and its Disorders, Third Edition. Oxford: Blackwell Scientific, pp 1-9.

Krivickas, L. S. (1997). Anatomical factors associated with overuse sports injuries. Sports Medicine, 24, 132-146.

Kurz, M. J. and Stergiou, N. (2002). Effect of normalization and phase angle calculations on continuous relative phase. Journal of Biomechanics, 35, 369-374.

Leardini, A., Benedetti, M. G., Catani, F., Simoncini, L. and Giannini, S. (1999). An anatomically based protocol for the description of foot segment kinematics during gait. Clinical Biomechanics, 14, 528-536.

Li, L. and Caldwell, G. E. (1999). Coefficient of cross correlation and the time domain correspondence. Journal of Electromyography and Kinesiology, 9, 385-389.

Liu, W., Siegler, S., Hillstrom, H. and Whitney, K. (1997). Three-dimensional, six-degrees-of-freedom kinematics of the human hindfoot during the stance phase of level walking. Human Movement Science, 16, 283-298.

Lundberg, A. (1989). Kinematics of the ankle and foot: in vivo roentgen stereophotogrammetry. Acta Orthopaedica Scandinavica Supplement, 233, 1-24.

Luttgens, K., Deutsch, H. and Hamilton, N. (1992). Kinesiology: Scientific Basis of Human Motion. Madison: WBC Brown & Benchmark.

Lysholm, J. and Wiklander, J. (1987). Injuries in runners. American Journal of Sports Medicine, 15, 168-171.

Manal, K., McClay, I., Stanhope, S., Richards, J. and Galinat, B. (2000). Comparison of surface mounted markers and attachment methods in estimating tibial rotations during walking: an in vivo study. Gait and Posture, 11, 38-45.

Mann, R. A. (1995) Biomechanics of running. In Nicholas, M. D. and Hersham, E. B. (Eds.) The Lower Extremity & Spine in Sports Medicine. St Louis: Mosby, pp 325-345.

Mann, R. A. and Inman, V. T. (1964). Phasic activity of intrinsic muscles of the foot. Journal of Bone and Joint Surgery-American Volume, 46, 469.

Manter, J. T. (1941). Movements of the subtalar joint and transverse tarsal joints. Anatomical Record, 80, 397-410.

McClay, I. and Manal, K. (1998a). A comparison of three-dimensional lower extremity kinematics during running between excessive pronators and normals. Clinical Biomechanics, 13, 195-203.

McClay, I. and Manal, K. (1998b). The influence of foot abduction on differences between two- dimensional and three-dimensional rearfoot motion. Foot & Ankle International, 19, 26-31.

McClay, I. and Manal, K. (1997). Coupling parameters in runners with normal and excessive pronation. Journal of Applied Biomechanics, 13, 109-124.

McClay, I. and Cavanagh, P. R. (1994). Relationship between foot placement and mediolateral ground reaction forces during running. Clinical Biomechanics, 9, 117-123.

McCormack, A. P., Niki, H., Kiser, P., Tencer, A. F. and Sangeorzan, B. J. (1998). Two reconstructive techniques for flatfoot deformity comparing contact characteristics of the hindfoot joints. Foot & Ankle International, 19, 452-461.

McIlroy, W. E. and Maki, B. E. (1997). Preferred placement of the feet during quiet stance: Development of a standardized foot placement for balance testing. Clinical Biomechanics, 12, 66-70.

McPoil, T. G. and Knecht, H. G. (1985). Biomechanics of the foot in walking: a function approach. Journal of Orthopaedic & Sports Physical Therapy, 9, 69-72.

Messier, S. P. and Pittala, K. A. (1988). Etiological factors associated with selected running injuries. Medicine and Science in Sports and Exercise, 20, 501-505.

Messier, S. P., Davis, S. E., Curl, W. W., Lowery, R. B. and Pack, R. J. (1991). Etiological factors associated with patellofemoral pain in runners. Medicine and Science in Sports and Exercise, 23, 1008-1015.

Michelson, J. D., Hamel, A. J., Buczek, F. L. and Sharkey, N. A. (2002). Kinematic behavior of the ankle following malleolar fracture repair in a high-fidelity cadaver model. Journal of Bone and Joint Surgery-American Volume, 84A, 2029-2038.

Moseley, L., Smith, R., Hunt, A. and Gant, R. (1996). Three-dimensional kinematics of the rearfoot during the stance phase of walking in normal young adult males. Clinical Biomechanics, 11, 39-45.

Murphy, D. F. (2003). Risk factors for lower extremity injury: a review of the literature. British Journal of Sports Medicine, 37, 13-29.

Myers, K. A., Wang, M., Marks, R. M. and Harris, G. F. (2004). Validation of a multisegment foot and ankle kinematic model for pediatric gait. IEEE Transactions on Neural Systems and Rehabilitation Engineering, 12, 122-130.

Nawoczenski, D. A., Saltzman, C. L. and Cook, T. M. (1998). The effect of foot structure on the three-dimensional kinematic coupling behaviour of the leg and rear foot. Physical Therapy, 78, 404-416.

Nester, C. J., Bowker, P. and Bowden, P. (2002). Kinematics of the midtarsal joint during standing leg rotation. Journal of the American Podiatric Medical Association, 92, 77-81.

Nigg, B.M., Cole, G.K. and Wright, I.C. (1999). Optical methods. In Nigg, B. M. and Herzog, W. (Eds.) Biomechanics of the Musculo-skeletal System, Second Edition. Chichester: John Wiley & Sons, pp 302-331.

Nigg, B., Khan, A., Fisher, V. and Stefanyshyn, D. (1998). Effect of shoe insert construction on foot and leg movement. Medicine and Science in Sports and Exercise, 30, 550-555.

Nigg, B. M., Cole, G. K. and Nachbauer, W. (1993). Effects of arch height of the foot on angular motion of the lower extremities in running. Journal of Biomechanics, 26, 909-916.

Niki, H., Ching, R. P., Kiser, P. and Sangeorzan, B. J. (2001). The effect of posterior tibial tendon dysfunction on hindfoot kinematics. Foot & Ankle International, 22, 292-300.

Novacheck, T. F. (1998). The biomechanics of running. Gait & Posture, 7, 77-95.

O'Connor, K. M. and Hamill, J. (2002). Does running on a cambered road predispose a runner to injury? Journal of Applied Biomechanics, 18, 3-14.

Orchard, J. W., Fricker, P. A., Abud, A. T. and Mason, B. R. (1996). Biomechanics of iliotibial band friction syndrome in runners. American Journal of Sports Medicine, 24, 375-379.

Perry, J. (1992). Gait Analysis: Normal and Pathological Function. Thorofare: SLACK Inc.

Pierrynowski, M. J., Smith, S. B. and Mlynarczyk, J. H. (1996). Proficiency of foot care specialists to place the reafoot at subtalar neutral. Journal of the American Podiatric Medical Association, 86, 217-223.

Powers, C. M., Chen, P., Reischl, S. F. and Perry, J. (2002). Comparison of foot pronation and lower extremity rotation in persons with and without patellofemoral pain. Foot & Ankle International, 23, 634-640.

Pratt, D. J. (1989). Mechanisms of shock attenuation via the lower extremity during running. Clinical Biomechanics, 4, 51-57.

Rattanaprasert, U., Smith, R., Sullivan, M. and Gilleard, W. (1999). Three-dimensional kinematics of the forefoot, rearfoot, and leg without the function of tibialis posterior in comparison with normals during stance phase of walking. Clinical Biomechanics, 14, 14-23.

Razeghi, M. and Batt, M. E. (2002). Foot type classification: a critical review of current methods. Gait & Posture, 15, 282-291.

Reeck, J., Felten, N., McCormack, A. P., Kiser, P., Tencer, A. F. and Sangeorzan, B. J. (1998). Support of the talus: A biomechanical investigation of the contributions of

the talonavicular and talocalcaneal joints, and the superomedial calcaneonavicular ligament. Foot & Ankle International, 19, 674-682.

Reinschmidt, C., van den Bogert, A. J., Lundberg, A., Nigg, B. M., Murphy, N., Stacoff, A. and Stano, A. (1997a). Tibiofemoral and tibiocalcaneal motion during walking: external vs. skeletal markers. Gait & Posture, 6, 98-109.

Reinschmidt, C., van den Bogert, A. J., Murphy, N., Lundberg, A. and Nigg, B. M. (1997b). Tibiocalcaneal motion during running, measured with external and bone markers. Clinical Biomechanics, 12, 8-16.

Reischl, S. F., Powers, C. M., Rao, S. and Perry, J. (1999). Relationship between foot pronation and rotation of the tibia and femur during walking. Foot & Ankle International, 20, 513-520.

Robbins, S. E. and Gouw, G. J. (1990). Athletic footwear and chronic overloading - a brief review. Sports Medicine, 9, 76-85.

Root, M. L., Orien, W. P. and Weed, J. H. (1977). Foot and Ankle Linkage System. Los Angeles: Clinical Biomechanics Corporation.

Scott, S. H. and Winter, D. A. (1991). Talocrural and talocalcaneal joint kinematics during the stance phase of walking. Journal of Biomechanics, 24, 743-752.

Sharkey, N. A. and Hamel, A. J. (1998). A dynamic cadaver model of the stance phase of gait: performance characteristics and kinetic validation. Clinical Biomechanics, 13, 420-433.

Sharkey, N. A., Smith, T. S. and Lundmark, D. C. (1995). Freeze clamping musculotendinous junctions for in-vitro simulation of joint mechanics. Journal of Biomechanics, 28, 631-635.

Siegler, S., Chen, J. and Schneck, C. D. (1988). The three-dimensional kinematics and flexibility characteristics of the human ankle and subtalar joints - part I: kinematics. Journal of Biomechanical Engineering, 110, 364-373.

Solomon, E. P. (2003). Introduction to Human Anatomy and Physiology, 2nd Edition. Philadelphia: W.B.Saunders.

Spoor, C. W. and Veldpaus, F. E. (1980). Rigid body motion calculated from spatial co-ordinates of markers. Journal of Biomechanics, 13, 391-393.

Stackhouse, C. L., Davis, I. M. and Hamill, J. (2004). Orthotic intervention in forefoot and rearfoot strike running patterns. Clinical Biomechanics, 19, 64-70.

Stacoff, A., Reinschmidt, C., Nigg, B., van den Bogert, A., Lundberg, A., Denoth, J. and Stussi, E. (2001). Effects of shoe sole construction on skeletal motion during running. Medicine and Science in Sports and Exercise, 33, 311-319.

Stacoff, A., Nigg, B. M., Reinschmidt, C., van den Bogert, A. J. and Lundberg, A. (2000a). Tibiocalcaneal kinematics of barefoot versus shod running. Journal of Biomechanics, 33, 1387-1395.

Stacoff, A., Reinschmidt, C., Nigg, B. M., van den Bogert, A. J., Lundberg, A., Denoth, J. and Stussi, E. (2000b). Effects of foot orthoses on skeletal motion during running. Clinical Biomechanics, 15, 54-64.

Stacoff, A., Reinschmidt, C. and Stussi, E. (1992). The movement of the heel within a running shoe. Medicine and Science in Sports and Exercise, 24, 695-701.

Stacoff, A., Kaelin, X. and Stuessi, E. (1991). The effects of shoes on the torsion and rearfoot motion in running. Medicine and Science in Sports and Exercise, 23, 482-490.

Stacoff, A., Kaelin, X., Stuessi, E. and Segesser, B. (1989). The torsion of the foot in running. International Journal of Sport Biomechanics, 5, 375-389.

Stahelin, T., Nigg, B. M., Stefanyshyn, D., van den Bogert, A. J. and Kim, S. (1997). A method to determine bone movement in the ankle joint complex in vitro. Journal of Biomechanics, 30, 513-516.

Stergiou, N., Bates, B. T. and Kurz, M. J. (2003). Subtalar and knee joint interaction during running at various stride lengths. Journal of Sports Medicine and Physical Fitness, 43, 319-326.

Stergiou, N. and Bates, B. T. (1997). The relationship between subtalar and knee joint function as a possible mechanism for running injuries. Gait & Posture, 6, 177-185.

Stergiou, N., Bates, B. and James, S. (1999). Asynchrony between subtalar and knee joint function during running. Medicine and Science in Sports and Exercise, 31, 1645-1655.

Sutlive, T. G., Mitchell, S. D., Maxfield, S. N., McLean, C. L., Neumann, J. C., Swiecki, C. R., Hall, R. C., Bare, A. C. and Flynn, T. W. (2004). Identification of individuals with patellofemoral pain whose symptoms improved after a combined program of foot orthosis use and modified activity: a preliminary investigation. Physical Therapy, 84, 49-61.

Tiberio, D. (1987). The effect of excessive subtalar joint pronation on patellofemoral mechanics: a theoretical model. Journal of Orthopaedic & Sports Physical Therapy, 9, 160-165.

Tranberg, R. and Karlsson, D. (1998). The relative skin movement of the foot: a 2-D roentgen photogrammetry study. Clinical Biomechanics, 13, 71-76.

van Gheluwe, B., Kerwin, D., Roosen, P. and Tielemans, R. (1999). The influence of heel fit on rearfoot motion in running shoes. Journal of Applied Biomechanics, 15, 361-372.

van Gheluwe, B., Tielemans, R. and Roosen, P. (1995). The influence of heel counter rigidity on rearfoot motion during running. Journal of Applied Biomechanics, 11, 47-67.

van Langelaan, E. J. (1983). Kinematic analysis of the tarsal joints. Acta Orthopaedica Scandinavica Supplement, 204.

van Mechelen, W. (1992). Running injuries: a review of the epidemiological literature. Sports Medicine, 14, 320-335.

Waller, J. F. and Maddalo, A. V. (1995). Foot and ankle linkage system. In Nicholas, M. D. and Hersham, E. B. (Eds.) The Lower Extemity & Spine in Sports Medicine. St Louis: Mosby, pp 347-351.

Wen, D. Y., Puffer, J. C. and Schmalzried, T. P. (1997). Lower extremity alignment and risk of overuse injuries in runners. Medicine and Science in Sports and Exercise, 29, 1291-1298.

Whittle, M. W. (1996). Gait Analysis: An Introduction, Second Edition. Oxford: Butterworth Heinemann.

Wickiewicz, T. L., Roy, R. R., Powell, P. L. and Edgerton, V. R. (1983). Muscle Architecture of the Human Lower-Limb. Clinical Orthopaedics and Related Research, 275-283.

Williams, D. S., Davis, I. M. and Baitch, S. P. (2003). Effect of inverted orthoses on lower-extremity mechanics in runners. Medicine and Science in Sports and Exercise, 35, 2060-2068.

Williams, D. S., McClay, I. S., Hamill, J. and Buchanan, T. S. (2001a). Lower extremity kinematic and kinetic differences in runners with high and low arches. Journal of Applied Biomechanics, 17, 153-163.

Williams, D. S., McClay-Davis, I. and Hamill, J. (2001b). Arch structure and injury patterns in runners. Clinical Biomechanics, 16, 341-347.

Williams, D. S., McClay, I. S. and Manal, K. T. (2000). Lower extremity mechanics in runners with a converted forefoot strike pattern. Journal of Applied Biomechanics, 16, 210-218.

Williams, K. R. and Ziff, J. L. (1991). Changes in Distance Running Mechanics Due to Systematic Variations in Running Style. International Journal of Sport Biomechanics, 7, 76-90.

Winter, D. A. (1991). The Biomechanics and Motor Control of Human Gait: Normal, Elderly and Pathological, Second Edition. Waterloo: University of Waterloo Press.

Winter, D. A. (2005). Biomechanics and Motor Control of Human Movement, Third Edition. New York: John Wiley & Sons.

Woodburn, J., Nelson, K. M., Siegel, K. L., Kepple, T. M. and Gerber, L. H. (2004). Multisegment foot motion during gait: proof of concept in rheumatoid arthritis. Journal of Rheumatology, 31, 1918-1927.

Woodburn, J., Helliwell, P. S. and Barker, S. (2002). Three-dimensional kinematics at the ankle joint complex in rheumatoid arthritis patients with painful valgus deformity of the rearfoot. Rheumatology, 41, 1406-1412.

Wu, G. and Cavanagh, P. R. (1995). ISB recommendations for standardization in the reporting of kinematic data. Journal of Biomechanics, 28, 1257-1261.

Yates, B. and White, S. (2004). The incidence and risk factors in the development of medial tibial stress syndrome among naval recruits. American Journal of Sports Medicine, 32, 772-780.

Zatsiorsky, V. M. (1999). Kinematics of Human Motion. Champaign: Human Kinetics.

Appendix A – Anatomical Terminology

In order to communicate specific information concerning human movement, specialised terminology is required to precisely identify body position and direction. It is important to define the terminology used to avoid any confusion in the interpretation of the information within this thesis. All position and movement terms are described relative to the universally accepted anatomical reference position. This is an erect standing position with all body parts, including the palms of the hand facing forward. The arms hang at the side of the body and the feet are placed slightly apart.

Positional Terms

In describing the relative position of body parts the use of directional terms is necessary. The following are commonly used directional terms:

Superior: Closer to the head.

Inferior: Further away from the head.

Proximal: Closer to the trunk.

Distal: Further away from the trunk.

Anterior: Toward the front of the body.

Posterior: Toward the back of the body.

Medial: Toward the midline of the body.

Lateral: Away from the midline of the body.

Plantar: On the sole of the foot.

Superficial: Toward the surface of the body.

Deep: Inside the body and away from the body surface.

Anatomical Reference Planes

Three conceptual cardinal planes bisect the body commonly known as the sagittal, frontal and transverse planes:

Sagittal plane: An imaginary plane that divides the body vertically into left and right halves of equal mass. Sometimes referred to as the anteroposterior plane. Rotary motions in this plane take place about the medio-lateral axis. In three dimensional position data this corresponds to the *x* and *y* co-ordinates.

Frontal plane: An imaginary plane that splits the body vertically into front and back halves of equal mass. Sometimes referred to as the coronal plane. Rotary motions in this plane take place about the antero-posterior axis. In three dimensional position data this corresponds to the *x* and *z* co-ordinate.

Transverse plane: An imaginary plane that separates the body into top and bottom halves of equal mass. Also referred to as the horizontal plane. Rotary motions in this plane take place about the longitudinal axis. In three dimensional position data this corresponds to the *y* and *z* co-ordinates.

Although many human movements are not strictly planar, the cardinal planes provide a useful way to describe movements that are primarily planar. Complex composite movements can also be broken down to describe the contribution of each cardinal plane to the final movement.

Joint Motion Terminology

While not necessarily accurate, most joint motions are described as if they were pure rotary movements. Angular motion is rotation around a central imaginary line known as the axis of rotation, which is oriented perpendicular to the plane in which the rotation is occurring. The following are commonly used terms to describe the angular motion (displacement) occurring at the joints:

Flexion: the bending of adjacent body segments in the sagittal plane so that their two anterior/posterior surfaces are brought together.

Extension: the moving apart or straightening of two opposing surfaces in the sagittal plane.

Plantarflexion: moving the dorsal surface of the foot away from the anterior surface of the leg i.e. pointing the toes downwards.

Dorsiflexion: moving the dorsal surface of the foot towards the anterior surface of the leg i.e. pulling the toes upwards.

Abduction: the motion of a body segment in the frontal plane toward the midline of the body. However, in the case of the foot, this is motion of the segment in the transverse plane towards the midline of the body (similar to internal rotation).

Adduction: the motion of a body segment in the frontal plane away from the midline of the body. However, in the case of the foot, this is motion of the segment in the transverse plane away from the midline of the body (similar to external rotation).

Internal rotation: rotation of a body segment in the transverse plane towards the midline of the body.

External rotation: rotation of a body segment in the transverse plane away from the midline of the body.

Eversion: tilting of the foot in the frontal plane so that the plantar aspect of the foot is facing towards the midline.

Inversion: tilting of the foot in the frontal plane so that the plantar aspect of the foot is facing away from the midline.

Pronation: a triplanar movement of the foot which is a combination of plantarflexion, eversion and abduction of the calcaneus relative to a fixed talus and lower limb.

Supination: a triplanar movement of the foot which is a combination of dorsiflexion, inversion and adduction of the calcaneus relative to a fixed talus and lower limb.

Appendix B – Subject Information Sheet and Consent Form

SUBJECT INFORMATION SHEET

TITLE OF INVESTIGATION: Changes in Rearfoot and Lower Leg Kinematics Due to Systematic Variations in Step Width During Barefoot Running.

You have been invited to take part in a research study investigating possible mechanisms that may cause chronic overuse injuries in activities involving running. In addition to increasing knowledge in this area, this study is also designed to provide data to fulfil the requirements of a Research Degree for the principle investigator. If there are any points that need further explanation, please ask a member of the research team. It is important that you understand what you are volunteering to do and are completely happy with all the information before you sign this form.

Why have I been chosen? You have been selected as a possible participant in this investigation because you are currently participating for more than one hour per week in exercise that involves running. Before you become a participant, you will complete a medical questionnaire. People who have asthma, heart-related and/or circulatory problems, hypertension or any other potentially problematic condition will not be allowed to take part in the study. If you are suffering from or recovering from a musculoskeletal injury you will also be excluded from the participation in the study.

Do I have to take part? It is up to you to decide whether or not to take part. If you decide to take part, you will be given this information sheet to keep and will be asked to sign a consent form. If you decide to take part, you are still free to withdraw at any time and without giving a reason.

What will happen to me if I take part? As a subject you will be asked to perform a number of barefoot running trials along a ten metre long walkway in a laboratory whilst being recorded using an optoelectronic camera system.

You will be asked to visit the laboratory on one occasion. This visit should last less than 1½ hours. When you arrive for the testing session you will first be introduced to the laboratory staff and shown all the equipment that will be used in the study. You will then be asked to complete two confidential questionnaires to obtain information related to your general health and any musculoskeletal injuries you have suffered.

For the testing you will be required to wear shorts and also to remove your shoes and socks. Reflective spherical markers will be attached to a number of bony anatomical landmarks on your foot and lower leg using double sided sticky tape. If you have any skin allergies, particularly relating to glue, please inform the researcher immediately. Once the markers have been applied you will be asked to stand stationary in the middle of the walkway while a static standing trial is recorded using the cameras. You will then be asked to perform barefoot running trials (maximum of ten metres) along the laboratory walkway using three different step widths. Five running trials will be recorded for each of the three step widths leading to a total of 15 trials. Information regarding the step width will be given by the researcher just prior to the running trials. You will be given time to practise running using each of the three different step widths. The running trials are to be conducted at your self-selected pace and you make take as much rest as you require between trials. However, the same running speed must be used for all 15 trials and if there any trials where the speed differs by ± 5% then the

trial will not count and must be repeated. You are allowed an external observer during your visit to the lab if this makes you feel more comfortable.

What are the side effects of taking part? The running tests may leave the soles of your feet a little sore but there should be no long-term discomfort.

What are the possible disadvantages and risks of taking part? Exercise has a negligible risk in healthy adults. Occasionally people with previously unknown heart disease may develop chest pain due to myocardial ischaemia on exertion. If you experience any unusual sensations in your chest during the experiment, you should cease exercising immediately. In the unlikely event you experience serious problems during the exercise, personnel with life-support training are within one minute of the laboratory at all times during the test and approved emergency procedures are in place.

As with any exercise involving exertion, there is a slight risk of musculoskeletal injury. To minimise this risk you will allowed a period to warm-up prior to the testing and then a period to warm-down afterwards. Injury could also be suffered through a trip or fall, or by stepping on an object whilst barefoot. The walkway area where testing is conducted will be cleared of any objects and you are asked to stay within this designated area once you have removed your shoes.

What are the possible benefits of taking part? At the end of the study, the researchers will take the time to explain the results to you from an injury biomechanics perspective. It may be possible to learn if your foot structure means you are at an increased risk of obtaining a chronic overuse injury.

What if something goes wrong? If you are harmed by taking part in this research project, there are no compensation arrangements. If you are harmed due to someone's negligence, then you may have grounds for a legal action but you may have to pay for it. There will always be a trained first-aider at hand. In the event of an untoward incident, he/she will provide appropriate first aid until emergency medical staff arrive on site.

Will my taking part in this study be kept confidential? All information which is collected about you during the course of the research will be kept strictly confidential.

What will happen to the results of the research study?
This research is being conducted as part of a doctoral dissertation, and it is likely that the results will be published in a peer-reviewed scientific journal once the study is completed. You will not be identified in any publication. If you would like a copy of the full publication, please contact the primary researcher (Mike Pohl - see contact details below).

If you are worried about any unwanted side effects from any of the above procedures, or want to know more about the study you should contact one of the researchers named below:

Mike Pohl (Primary researcher)
School of Sport and Exercise Sciences
University of Leeds,
Leeds LS2 9JT
Phone: 0113-343-1669
e-mail: bmsmbp@leeds.ac.uk

Dr. Neil Messenger
School of Sport and Exercise Sciences
University of Leeds
Leeds LS2 9JT
Phone: 0113-343-5084
n.messenger@leeds.ac.uk

Project Title: Changes in Rearfoot and Lower Leg Kinematics Due to Systematic Variations in Step Width During Barefoot Running.

Consent Form

I ..... (Print name)

give my consent to the research procedures which are outlined above, the aim, procedures and possible consequences of which have been outlined to me.

Signature .....

Date .....

Appendix C – Subject Medical Questionnaire

MEDICAL QUESTIONNAIRE

If you feel unwell on the day of a proposed test, or have been feeling poorly within the last two weeks, you are excluded from taking part in an exercise test. The considerations that follow apply to people who have been feeling well for the preceding two weeks.

NAME: .....

SEX: M/F AGE: ..... (yr) HEIGHT: ..... (m) WEIGHT: ..... (kg)

Details of last medical examination (in the last six months):

Date: ..... Location:
.....
(*day/mo/yr*)

Exercise lifestyle:
What kind of exercise(s) do you participate in that involves running and how long do you spend participating in that exercise per week? (*Please circle the length of duration per average week*):

Running	<30min	30-60min	1-2hrs	>2hrs
Field Athletics	<30min	30-60min	1-2hrs	>2hrs
Racket Sports	<30min	30-60min	1-2hrs	>2hrs
Field Sports (i.e soccer)	<30min	30-60min	1-2hrs	>2hrs
Court Sports (i.e. netball)	<30min	30-60min	1-2hrs	>2hrs
Others*				

*(*Please specify*) .....

Illnesses: *Have you ever had any of the following?* (Please circle NO or YES)

Anaemia	NO/YES	Asthma	NO/YES
Diabetes	NO/YES	Epilepsy	NO/YES
Heart Disease	NO/YES	High Blood Pressure	NO/YES
Other*	NO/YES		

*(*Please specify*) .....

Symptoms:
Have you ever had any of the following symptoms to a significant degree at rest or during exercise? That is, have you had to consult a physician relating to any of the following?

	Rest	*Exercise*
Breathlessness	NO/YES	NO/YES
Chest Pain	NO/YES	NO/YES
Dizzy Fits/Fainting	NO/YES	NO/YES
Heart Murmurs	NO/YES	NO/YES
Palpitations	NO/YES	NO/YES
Tightness in chest, jaw or arm	NO/YES	NO/YES
Other*	NO/YES	

*(*Please specify*) .....

Muscle or joint injury:
Do you have/or have had any muscle or joint injury which could affect your safety in performing exercise (*e.g.* cycling or running)? NO/YES*

*(*Please specify*) .....

Medication:
Are you currently taking any medication? NO/YES*

*(*Please specify*) .....

Family History of Sudden Death:
Is there a history of sudden death in people under 40 years in your family? NO/YES*

*(*Please specify*) .....

Skin Allergies:
Do you have any known skin allergies? NO/YES*

*(*Please specify*).....

The following exclusion and inclusion criteria will apply to this study:
Exclusion criteria: If you have any of the following, you will be excluded from the study:

(a) Asthma, diabetes, epilepsy, heart disease, a family history of unexplained or cardiac sudden death at a young age, fainting bouts, high blood pressure or anaemia.
(b) Have a current muscle/bone/joint injury or are in the process of recovering from such an injury.
(c) A recent illness or viral infection (including an upper respiratory tract infection) within two weeks of the experiment.
(d) Taking any medication that may adversely affect health or exercise performance.
(e) Deemed to be under the influence of recreational/ performance enhancing drugs or alcohol at the time of testing.

Inclusion criteria:

(a) Male or female subject aged at least 18 years and no more than 35 years.
(b) In good health at the time of testing.
(c) Participate for at least two hours per week in any form of exercise that involves running.

If you are involved in more than one visit to the laboratory, you will be asked to complete the medical and physical activity questionnaire on each subsequent visit, to establish whether or not your health status has changed. If the investigator has any concern in this regard (see Exclusion criteria above), you will be excluded.

Signature ..... Date .....

Appendix D – Chapters Published in Peer Reviewed Journals

Pohl, M.B., Messenger, N. and Buckley, J.G. (2006). Changes in foot and lower limb coupling due to systematic changes in step width. *Clinical Biomechanics*, **21**, 175-183.

Pohl, M.B., Messenger, N. and Buckley, J.G. (2005). Changes in foot and lower limb coupling due to systematic changes in step width. In proceedings of the Third Conference on Biomechanics of the Lower Limb in Health, Disease and Rehabilitation, Salford, pp 178-179.

Pohl, M.B., Messenger, N. and Buckley, J.G. (in review). Rearfoot, forefoot and shank coupling: effect of variations in speed and mode of gait. *Gait and Posture*, **x**, **xxx-xxx.**